SLOPE STABILITY AND WATER TIGHTNESS ASSESSMENT OF GOLOLCHA DAM SITE, WEST HARARGHE ZONE, EASTERN ETHIOPIA.

SISHAW MERDASSA ERENA

A THESIS SUBMITTED TO THE DEPARTMENT OF APPLIED GEOLOGY

SCHOOL OF APPLIED NATURAL SCIENCE

PRESENTED IN PARTIAL FULFILLMENT OF THE REQUIREMENT FOR THE DEGREE OF MASTER'S IN ENGINEERING GEOLOGY

OFFICE OF GRADUATE STUDIES

ADAMA SCIENCE AND TECHNOLOGY UNIVERSITY

JUNE, 2022

ADAMA, ETHIOPIA

Slope Stability and Water Tightness Assessment of Gololcha Dam site, West Hararghe Zone, Eastern Ethiopia

Sishaw Merdassa Erena

Major advisor
Yadeta Chemdesa (PhD.)

Co-advisor
Tola Garo (MSc)

A thesis submitted to the department of applied geology

School of applied natural science

Presented in partial fulfillment of the requirement for the degree of master's in engineering geology

Office of Graduate Studies
Adama Science and Technology University

June, 2022

Adama, Ethiopia

Declaration

I hereby declare that this Master Thesis entitled "**Slope Stability and Water Tightness Assessment of Gololcha Dam site, West Hararghe Zone, Eastern Ethiopia**" is my original work. That is, it has not been submitted for the award of any academic degree, diploma or certificate in any other university. All sources of materials that are used for this thesis have been duly acknowledged through citation

Name of student	Signature	Date

Recommendation

I/we, the advisor(s) of this thesis, hereby certify that I/we have read the revised version of the thesis entitled "**Slope Stability and Water Tightness Assessment of Gololcha Dam site, West Hararghe Zone, Eastern Ethiopia"** prepared under my/our guidance by **Sishaw Merdassa** submitted in partial fulfillment of the requirements for the degree of Mater's of Science in **Engineering Geology**. Therefore, I/we recommend the submission of revised version of the thesis to the department following the applicable procedures.

___________________________	________________________	________________
Major Advisor	Signature	Date
___________________________	________________________	________________
Co-advisor	Signature	Date

Approval Page

I/we, the advisors of the thesis entitled "**Slope Stability and Water Tightness Assessment of Gololcha Dam site, West Hararghe Zone, Eastern Ethiopia**" and developed by **Sishaw Merdassa**, hereby certify that the recommendation and suggestions made by the board of examiners are appropriately incorporated into the final version of the thesis.

______________________	______________________	______________
Major Advisor	Signature	Date
______________________	______________________	______________
Co-advisor	Signature	Date

We, the undersigned, members of the Board of Examiners of the thesis by **Sishaw Merdassa** have read and evaluated the thesis entitled "**Slope Stability and Water Tightness Assessment of Gololcha Dam site, West Hararghe Zone, Eastern Ethiopia**" and examined the candidate during open defense. This is, therefore, to certify that the thesis is accepted for partial fulfillment of the requirement of the degree of Master of Science in Engineering Geology.

______________________	______________	______________
Chairperson	Signature	Date
______________________	______________	______________
Internal Examiner	Signature	Date
______________________	______________	______________
External Examiner	Signature	Date

Final approval and acceptance of the thesis is contingent upon submission of its final copy to the Office of Postgraduate Studies (OPGS) through the Department Graduate Council (DGC) and School Graduate Committee (SGC).

______________________	______________	______________
Department Head	Signature	Date
______________________	______________	______________
School Dean	Signature	Date
______________________	______________	______________
Office of Postgraduate Studies, Dean	Signature	Date

Acknowledgement

First and foremost, I want to thank the almighty God for helping me in completing my thesis despite my difficult circumstances. I would like to thank my advisers, Dr. Yadeta Chemedesa and Mr. Tola Garo, for their constructive feedback, encouragement, and follow-up in assisting me in completing this thesis. Especially without Mr. Tola Garo this mission would not have been completed for his tireless efforts and helpful recommendations on subject matter. I would also like to express my gratitude to Oromia Water Works Design and Supervision Enterprise for offering data and enabling me to stay at the camp site. Finally, I would want to convey my appreciation for Adama Science and Technology University's financial assistance. In addition I want to thanks pervious head of department, Dr. Muhamed Raji for his encouragement and supporting me by writing letter when I need his help. Furthermore I would want to thanks my friends for their supportive advises and praying for me when I get tired and getting difficulty situation.

Contents

List of figure

List of table

List of Acronyms

ASTU	Adama Science and Technology University
DEM	Digital Elevation Model
FOS	Factor of safety
FSL	Full Supply Level
GPS	Global Positioning System
GSI	Geological Strength Index
HEP	Horizontal Electrical Profiling
LEM	Limit Equilibrium Method
M a.s.l	meter above sea level
LL	Liquid Limit
OIDA	Oromia Irrigation Development Authority
OWWDSE	Oromia Water Works Design and Supervision Enterprise
PhD	Doctor of Philosophy
PI	Plastic index
PL	Plastic Limit
RAS 1	Right abutment slope section 1
RAS 2	Right abutment slope section 2
RMR	Rock Mass Rating
SR	Seismic Refraction
RQD	Rock Quality Designation
UCS	Uniaxial Compression Strength
UCS	Uniaxial Compressive Strength
URRAP	Universal Rural Road Access Program
USCS	Unified Soil Classification System

Abstract

The economy of Ethiopia is mainly dependent on agriculture. Water is very essential for agriculture that sustains the development of the country. Gololcha dam is an earth and rock fill dam, which is under construction on Kurkura River in Eastern Ethiopia for the purpose of irrigation. For the dam to meet the intended primary purpose, its safety must be determined and the reservoir must store enough amount of water for the long period of time. This study aimed to conduct detailed geological, geophysical, surface and subsurface geotechnical investigation to characterize the engineering geological properties in the view of slope stability and water tightness. To achieve the objective of the study, geological and engineering geological mapping, discontinuity surveying, digging test-pit, permeability testing, sampling and laboratory testing have been carried out. A critical slope stability analysis on the right abutment (RAS 1 and RAS 2) was also carried out. The area is covered with volcanic rock (Basalt) and soil deposit (alluvial and residual) both at the dam site and reservoir area. The exposed basaltic rock is highly fractured and fragmented, which falls into very poor to good rock quality according RQD value obtained from boreholes. RMR and GSI were used to identify the quality of rock mass and the result revealed that the rock in the study area is classified as fair. The strength of the rock of the study area ranges from medium to high strength. The soil found in the study area was dominated by sandy and silty soil of low to high plasticity with plastic index ranges from 9.72% to 20.95%. The right abutment RAS 1 slope section is non-structural controlled failure which is unstable during saturated condition with FOS = 0.85 and stable during dry condition. Whereas RAS 2 slope section is structurally controlled with one planar mode of failure and two wedge mode of failure. The analysis for RAS2 slope section was conducted by Rocplane and Swedge software for planar and wedge mode of failure respectively. From analysis result RAS2 is unstable under saturate conditions and stable under dry condition. The permeability of surface rock ranges from $4.08*10^{-3}$m/s to 1m/s and permeability from boreholes ranges from $4.68*10^{-5}$cm/s to $1.29*10^{-2}$cm/s. Based on permeability result, excessive seepage problem was expected from abutments and reservoir rim. Whereas, the reservoir area covered by soil is almost watertight. Finally, this study recommended proper remedial measures such as provides sufficient drain hole, remove loose material from the slope, rock bolt and anchor for stabilization of structural controlled slope section, shotcrete and reducing slope angle for stabilization of non-structural controlled slope section and grouting and clay blankets to control leakage problems.

Key words: Ethiopia, Gololcha, slope stability, Water tightness, Hydraulic conductivity and leakage problem.

CHAPTER ONE

1. INTRODUCTION

1.1 Background

The dam is among water harvesting structures constructed across the river to store water for different purposes such as irrigation, domestic water supply, and flood control. The construction of dams was recognized by the country since the drought of the early 1980s and there were some efforts still going on (MOA, 2011). These activities are even more critical in arid and semi-arid areas, including the study area, where there is a limited supply of rainfall for agriculture or other purposes.

However, the dam's construction requires a proper understanding of the site because the dam's failure can lead to loss of investment, income, property, and life. Failure of achieving the primary purposes for which it is constructed is also considered as failure of dam. Engineering geological investigation of dam sites plays a significant role in the design and execution of the project. The investigation is conducted pre-construction, during construction as well as after construction. According to Fookes (1966), site investigation can be divided into two approaches: surface investigation (geological mapping, engineering geological mapping, discontinuity survey, etc.) and sub-surface site investigation (drilling, boring, geophysical, etc.). The investigations allow identifying in advance problems that endanger the safety of the dam and taking the necessary remedial measures.

The common engineering geological problems that lead to dam projects failure without giving their desired purposes are leakage and reservoir siltation. For example, the failure of more than 60% of earth-fill dams constructed in Northern Ethiopia, Tigray region, is related to excessive leakage (Abdulkadir, 2009; Haregeweyn et al., 2006) via the reservoir bottom and/or via the dam foundation. Excessive seepage beneath a dam in highly permeable rock masses may damage the foundation. Therefore, it is important to consider the geological and geotechnical conditions of the reservoir and foundation site of the dam for water tightness assessments. Similarly, slope stability problems are another hazards that can lead to the destruction of dams and flooding of a downstream area like the case of the Vaiont dam. Hence, slope stability analysis is becoming an important part of dam site investigation. The presence of a discontinuity in dam abutments may trigger slope instability problems if its orientation is favorable for the movement of rock. Similarly, excessive leakage may occur following the discontinuity orientation.

In the case of the study area, the geologic formation is different from the dam constructed in Northern Ethiopia mentioned above. The geology of the study area is volcanic and found in the Main Ethiopian Rift (MER). The geology is highly discontinuous geology due to tectonic activities in the area. Therefore the slope instability and excessive seepage problem are highly abundant problems of the dam in this area.

The primary objective of this study is, therefore, to determine geotechnical properties of soil and rock that affect water tightness and slope stability problems in the study area. It will be achieved by geological and engineering geological mapping, discontinuity surveying, packer permeability test, sampling, and laboratory testing which helps to evaluate the conditions of materials along the dam abutments and reservoir area. For slope stability analyses of the dam abutments kinematic and deterministic methods was applied. Scientific information obtained from such investigations is then qualitatively and quantitatively interpreted to produce a geomechanical model used for designing the dam. Hence, this study is aimed at addressing such activities for the Gololcha dam site.

1.2 Location and Accessibility

The study area, the Gololcha dam site, is located in the Bordede District of West Hararghe Zone, Oromia Regional State, and Eastern Ethiopia (Figure 1. 1). This area is situated around 300km from the capital, Addis Ababa, in the eastern direction. It is bounded by geographic coordinates of 40^0 10' 0'' to 40^0 40' 0'' E longitude and 8^0 50' 0'' to 9^0 20' 0''N latitude in the UTM Zone of 37. Topographically, it is characterized by flat to rugged topography with altitudes ranging from 845 to 2487 m a.s.l. It is usually accessible via 400km Addis –Awash-Bordede-Chiro asphalt road. At Bordede station, there is an east junction non-asphalt all weathered Bordede to Micheta gravel road for a distance of 6km after which there is a SE junction through a 15km road constructed by URAP.

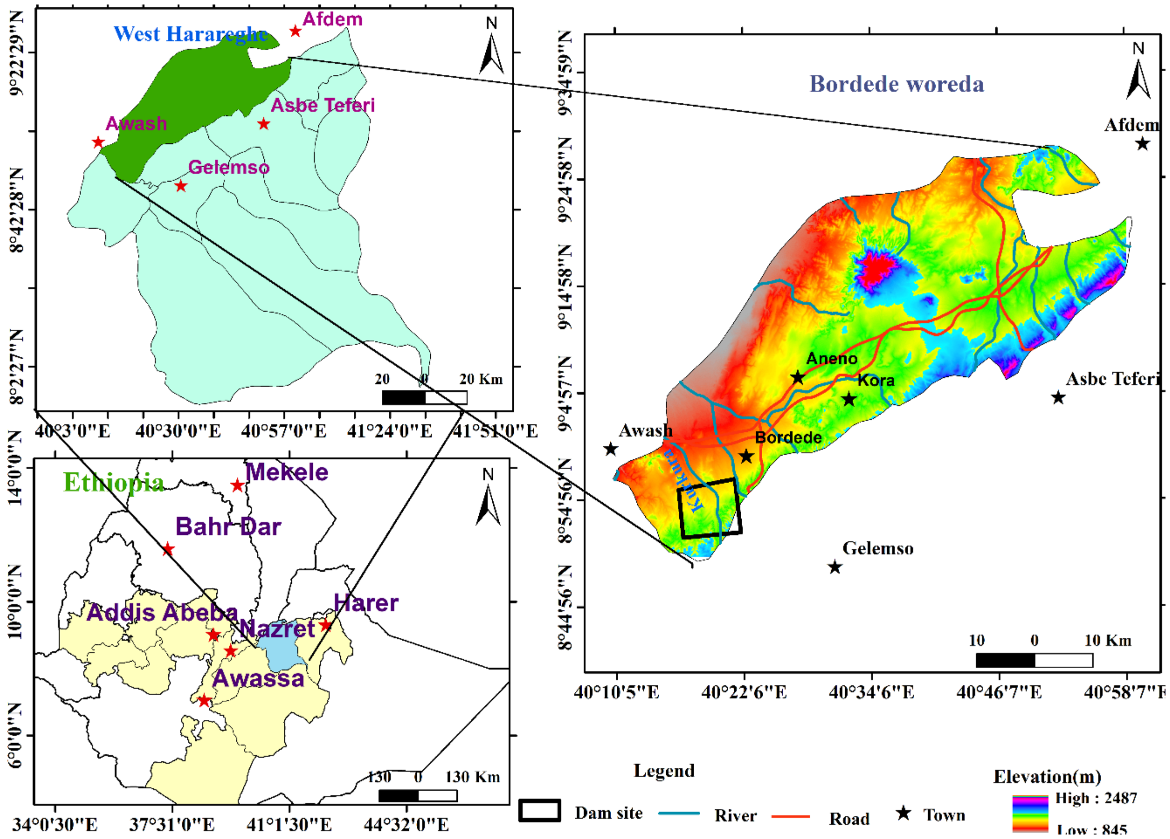

Figure 1. 1 Location Map of Project area

1.3. Physiography

Gololcha dam site is characterized by rugged landscape, cut by shallow to moderately deep valleys and punctuated by volcanic ridges. The maximum elevation is 2350 m a.s.l., and the minimum elevation is 900 m a.s.l (Figure 1. 2).

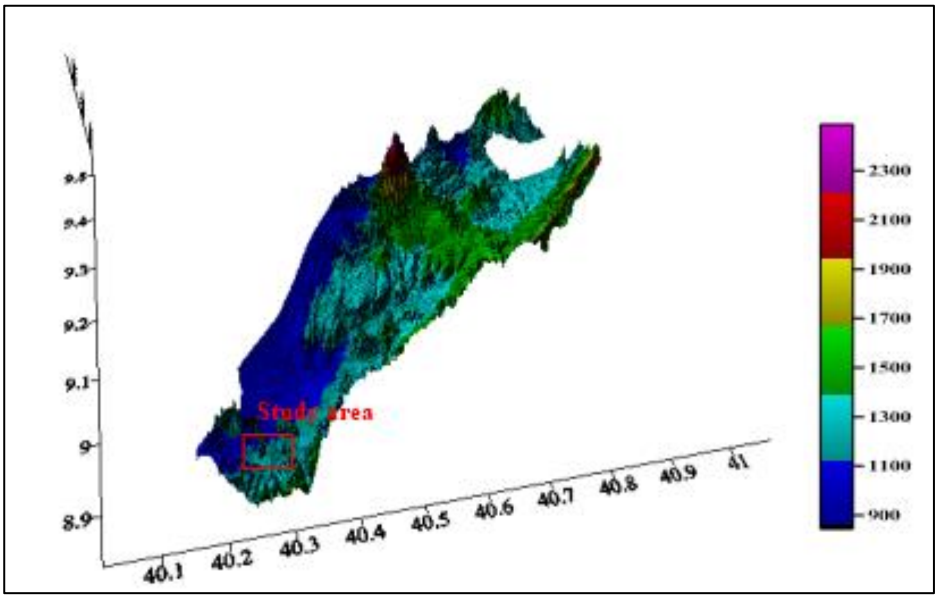

Figure 1. 2 Physiographic map of the study area

1.4. Climate

1.4.1 Temperature

Climate is one of the most important factors to consider while planning and using a water impoundment. The temperature of the project region is associated to an altitude range of 500m a.s.l to 1500m a.s.l, which is the Kola climatic zone categorization (OWWDSE, 2021).

1.4.2 Rainfall

The rainy season in the project area's environs lasts from July to September (Figure1.3). The average annual rainfall is 874.1mm, which is far less than the demand. In terms of intensity, volume, and distribution, there are also considerable variations in the rainfall pattern.

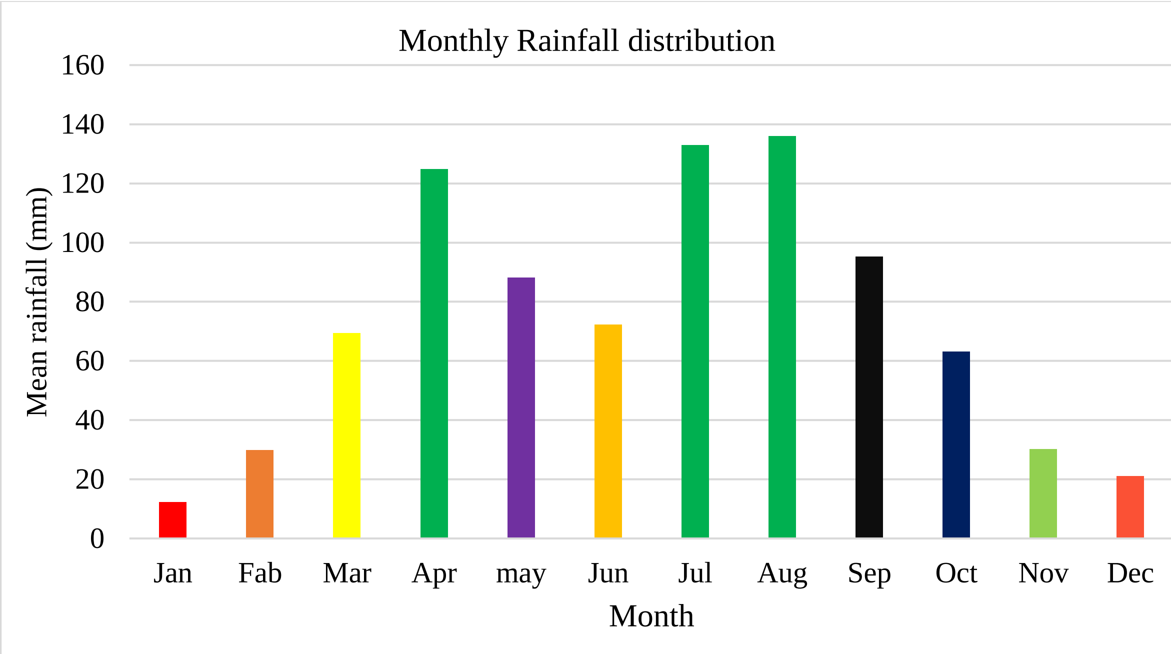

Figure 1. 3 Monthly rainfall distribution of the study area (by permission from OWWDSE 2021).

1.5. Seismicity of the area

In active seismic zones, faults and accompanying earthquakes are one of the most common causes of numerous hazards, especially where there are potentially active faults and inadequate earth materials. As a result, seismic loading should be included during slope stability analyses to reduce the effects of earthquake shaking on structural safety (ICOLD, 1998). One of the most common causes of earthquakes is faults and their accompanying earthquakes. The project area is in the eastern section of the Ethiopian Rift System. The project area is located on the border of zone 4 on Ethiopia's seismic zonal categorization map

(Figure 1. 4 and Table 1. 1). According to Ethiopia's seismic hazard map (Ayele, 2017), α_0 is the site's bedrock acceleration ratio, which varies depending on the seismic zone. Zones 1 to 4 are assigned a constant bedrock acceleration ratio of 0.03, 0.05, 0.07, or 0.1, whilst Zone 0 is considered seismic free. The project area in this scenario is around where α_0 = 0.1.

Table 1. 1 Seismic zone and its corresponds of bedrock acceleration (Worku, 2011)

Zone	4	3	2	1
α_o	0.1	0.07	0.05	0.03

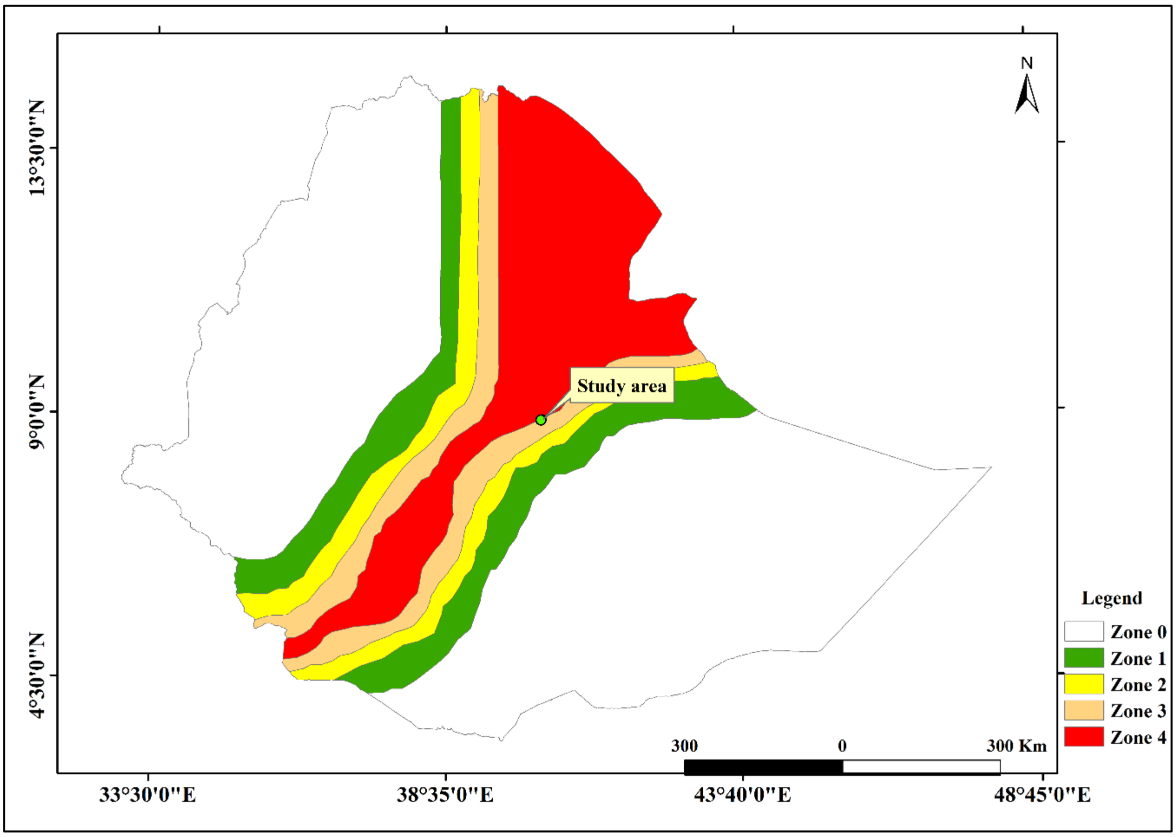

Figure 1. 4 Seismic hazard map of Ethiopia for the 100-year return period as per Ethiopian Building Code Standards (EBCS) (Worku, 2011).

1.6. Statement of the problem

The problem with the dam is due to the geology, geological structure, and seismicity of the area. The geology of the dam site (study area) is volcanic (Kazmin, 1975; Kazmin & Seifemichael, 1978; Zanettin et al., 1979) the problem is due to its geological structure, and nature of lithologies. As the dam site is at the Main Ethiopian Rift (MER) the lithology found in the area is highly fractured and it have been highly weathered. Therefore, the dam will face slope instability and excessive water seepage problems if the rock is highly weathered.

Highly fractured rock possesses abundant problems in the dam axis and reservoir area. During the construction of the dam and reservoir, the most technical difficulties posed by the presence of highly fractured are excessive water seepage. Seepage problems encountered in fractured volcanic rock and slope instability problems would be significant. The highly fractured natural slope of the reservoir would promote the probability of a major landslide (instability of the slope). The geological structure such as fault, joint, shear zone and fold were weakening the rock formation and the area may adversely for dam construction.

The study area is in the Main Ethiopian Rift (MER), hence tectonic activity is another challengeable to the dam site and reservoir. Preexisting fracture (microstructure) of the rock widens due to tectonic activity. In the MER area, there would be secondary structures (discontinuity) formed due to tectonic activity. The discontinuity in the rock mass is a frequent problem in the construction of dams and reservoirs. The stability of the abutment is also mainly dependent on the seismicity of the site. The slope stability of dam abutment is also dependent on the direction of discontinuity. Even if the dam remains stable after a seismic event, it is highly plausible that spring, leaks, and seepage developing in the adjacent rock abutments could cause a dam failure.

In general, in the study area, the expected problem is excessive seepage and instability of slope in the case of the degree of fractured and also due to tectonic activity (seismicity related problem). Therefore, a detailed geotechnical and engineering geological investigation of the proposed site is very crucial for planning, designing, and construction. This research will assess the problem that affects the dam safety and stability to achieve the primary purpose and recommend the appropriate mitigation method to increase the life span of the dam.

1.7 Research questions

This research work is expected to answer the following questions:

- What are the geology and geological structure of the site?
- What are the geotechnical properties of the soil and rocks of the study area?
- What is the water tightness condition of the site?
- What is the stability of the slope of the dam axis?
- What are the most effective remedial measures for the engineering problems based on site-specific parameters?

1.8 Objectives of the research

1.8.1 General objective

The main objective of the study is to determine the engineering geological properties of rocks and soils of the Gololcha dam site with the main emphasis on slope stability and water-tightness analysis.

1.8.2 Specific objectives

- To prepare a geological and engineering geological map of the study area
- To determine geotechnical properties of rocks and soils of the study area.
- To evaluate the water-tightness condition of the dam site.
- To conduct slope stability analysis of the dam abutments and reservoir rims.
- To recommend effective remedial measures based on the findings of the study.

1.9 Significance of the research

A dam is vital for the storage of water that in turn is useful for irrigation, hydropower, water supply, etc. However, the failure of such a structure may cause damage and endanger the life and properties located downstream of the dam. Therefore, detailed engineering geological investigations of the site of the proposed project must be conducted to ensure the safety of the dam for a longer period. This research work will come up with h detailed engineering geological characterization of the site on matters associated with seepage, foundation, and slope stability problem of the dam site. This in turn will allow us to identify in advance the possible problems, such as slope instability and excessive leakage, and take the necessary remedial measures. In general, it is significantly important to provide information on the type, depth, direction, and amount of grouting required during the construction of the dam.

Chapter Two

2. Literature Review

Dams have been constructed for various beneficial purposes. Nowadays, modern design technology is used for construction techniques and maintenance, however, the failure of the dam still occurs due to unpredicted adverse loading induced by natural forces and other factors. Despite the increasing safety of dams due to improved engineering knowledge and better construction quality, it is impossible to guarantee the absolute safety of the dams(Ge et al., 2021). A dam failure is the uncontrolled release of water from the reservoir, due to structural failure, geological defects, and deficiency of the dam. According to ICOLD (1974), the dam failure is categorized as a major failure that involves the complete forsaking of the dam and a failure that at the time may have been severe but has since been successfully repaired and the dam has again brought into use. The knowledge of the cause and condition that contributed to the dam's failure is essential to developing methods and measures to reduce dam accidents. Dam failure is mainly caused by improper design, lack of thorough investigation, inadequate care in construction, and poor maintenance. The embankment dam failure can be grouped into three according to Jandora and Riha (2009) such as hydraulic failures, seepage failures, and structural failures. In general, the factor that triggers the failure of embankment dams are overtopping, piping, seepage/leakage, and settlement problem failures.

2.1. Factor causing embankment failure

2.1.1. Overtopping failures

Particularly for an embankment dam, overtopping is one of the most frequent causes of dam failure. It may happen as a disaster when overtopping hits an embankment dam. Statistics established by the International Commission on Large Dams (ICOLD, 1974) show that embankment dams are among the most sensitive to problems arising from flood management, which may cause the watertight core or the crest level to overtop and create erosion leading to failure. According to Ehsan et al., (2016) overtopping can be prevented by slope pitching or a riprap up to a height above the tail water level.

2.1.2. Piping or internal erosion

When water penetrates through poor soils into the dam's interior body, small channels are formed that transport materials downstream (Ehsan et al., 2016; Zumrawi, 2015). As

Zumrawi (2015) stated that piping and internal erosion occur when the seepage is concentrated within the dam body. As more materials are transported downstream, the channel becomes widened, which could lead to washing out of the dam ((Ehsan et al., 2016). If the initial piping can be detected before it reaches critical condition, the remedial measure might be possible to prevent dam failure (Zumrawi, 2015).

2.1.3. Embankment Dam Settlement Failures

Dams are massive structures that constructed on the geology that have path to the movement of water and seepage. When the dam is in the construction phase even the rate of occurrence of consolidation is rapid and after construction, the rate becomes lesser. During impounding and operation, the dam body withstands all internal and external loads. This often causes horizontal and vertical displacements, called settlement locations (Beiranvand & Komasi, 2021 reference within it). When building the body of an embankment dam, the weight of the material and its gradual increase (with increasing the height of the dam) causes the settlement of the body. If the dam rests on sediments, the settlements of the crest and slopes are increased by the compression of the foundation materials produced by the weight of the dam and the impounded water at a later stage (Terzaghi et al., 1996). In addition, Avella (1993) described that the deformation of an embankment dam is permanent. Permanent vertical settlement of the fill material continues at a decreasing rate for decades after construction, while permanent horizontal deformation of the embankment is caused by the reservoir water pressure. Although major displacement occurs during the dam construction, the investigation of the earth dam's settlement sometimes leads to the dam assessment in its midpoints and gradually decreasing until it reaches zero. Because of the settlement, the structure of the dam gradually stretched and the distance between the tiller's slope along the base slightly increases (Beiranvand & Komasi, 2021 reference within it).

2.1.4. Leakage and Seepage problems of dams

A reservoir has suffered from increasing water loss or leakage by the gradual development of channels and openings formerly filled with fine sediments. Leakage is the water loss associated with the presence of major geological defects, conditions such as solution channels, fault zones, or buried channels through which large amounts and essentially localized flows can occur and these water losses create streams downstream, while seepage is a more discreet flow, which takes place over a larger area and the seepage failure occurs due to the saturation of the foundation materials or a weakening of the rock towards a sliding failure (Zumrawi, 2015).

A certain degree of leakage or seepage is accepted if it does not affect the safety of the dam and surrounding the infrastructures. However, if it becomes excessive, it is very difficult to assess their risk and consequences because it results in other geological and geotechnical problems that could threaten the normal operation of the reservoirs and dams. Seepage and leakage can be assessed and evaluated by investigating the permeability of the dam foundation, dam abutments, reservoir area, and geological condition in its surrounding area (Gurocak & Alemdag, 2012; Öge, 2017). The presence and frequency of discontinuities alter the permeability of the intact rock and rock masses. Discontinuity within the rock mass and its engineering properties (such as orientation, aperture, spacing, roughness, and infilling) are important parameters affecting the permeability (Gurocak & Alemdag, 2012; Öge, 2017). The permeability value is affected by the discontinuity orientation as the water in the rock mass travels along the discontinuity surface and also compactness/opening and roughness, as well as the type of infilling also affect the permeability (Gurocak & Alemdag, 2012).

Many seepage problems and failures of the dams have occurred because of inadequate seepage control measures or incomplete cleanup and preparation of the cores, foundation, and abutments which can result in dam failure (National Research Council, 1983). Excessive seepage through sinkholes, rock formation, or any previous soil formation is a principal type of defect in reservoirs. The effect of this defect is normally obvious in that the reservoir will lose water (National Research Council, 1983). According to Bell (2008) when assessing the seepage and leakage problems from the reservoir; two main factors have to be taken into consideration i.e. the water tightness of the basin and bank stability. Accordingly, an assessment of water tightness can be made once the groundwater conditions and geological features have been investigated, and then any necessary groundwater control measures can be planned.

As National Research Council (1983) stated that excessive seepage may be controlled by using one or more of the following remedial measures: such as grouting, installation of clay layer or impervious soil over the problem area, use of bentonite, mixing soda ash with the previous soil in the problem area, use of liquid chemical soil sealants and installation of polyvinylchloride (PVC) liners. However, some researchers frequently utilized the foundation treatment using cut-off systems or rock mass grouting to control excessive seepage problems (Mozafari et al., 2012; Turkmen, 2003; Uromeihy & Barzegari, 2007; Warner, 2004).

2.2. Rock Mass Characterization

Rock mass classification is the process of grouping a rock mass into classes on defined relationships and assigning a unique number or description to it based on similar properties such that the behavior of rock mass can be predicted (Zdzisław Tadeusz Bieniawski, 1989). Classification of rock mass improves the quality of site investigation by calling for systematic identification and quantification of input data. Results of classification in quantitative information for design purpose enable better engineering judgment more effective communication on a project (Bieniawski, 1993). A quantified classification assists proper and effective communication as a foundation for sound engineering judgment on a given project (Hoek, 2007). According to Goodman (1989), rock mass can be classified based on the parameters such as strength, discontinuity condition, weathering condition and structural orientation, which can be obtained qualitatively will be converted into rated parameters that provide a basis for estimating the deformability and strength properties which provide measurable data for support estimation and present platform for communication between researches, designers, engineers and construction groups (Bieniawski, 1989).

Most of the multi-parameter classification systems (Bdearton et al., 1974; Bieniawski, 1968, 1973; Bieniawski, 1989; Wickham et al., 1972) were developed from civil engineering case histories (Evert Hoek, 2007). Among the classification system that is often used in rock, engineering are Rock Mass Rating (RMR), Rock Quality Designation (RQD), Rock Mass Quality (Q), and Geological Strength Index (GSI) system (Barton et al., 1974; Bieniawski, 1973; Deere et al., 1966; Hoek & Brown, 1997).

2.2.1 Rock Quality Designation (RQD) Classification Method

To quantify the quality of the rock from drill cores, Deer et al. (1966) developed the concept of RQD. In addition, this classification system plays an important role in characterizing a rock mass (Bieniawski, 1989) as the quality of rocks is one of the major parameters in characterizing the rock mass. RQD can be obtained by a direct or indirect method. RQD can be obtained by a direct (core drilling) or indirect method (volumetric). Rock Quality Designation is defined as the percentage of intact core pieces longer than 10cm in the total length of a core having a core diameter of 54.7 inches (Hoek, 2007). Artificial fractures can be identified by the close-fitting of cores and unstained surfaces. All the artificial fractures should be ignored while counting the core length for RQD. A slow rate of drilling will also give better RQD.

$$\text{RQD} = \frac{\sum \text{Length of core pieces} > 10\text{cm}}{\text{Total length of the core}} * 100\% \qquad (1)$$

Palmstrom (1982) demonstrated that the RQD may be obtained from the numbers of discontinuities per unit volume, which are exposed on the outcrops or exploration adits, using the following relationship for clay-free rock masses:

$$\text{RQD} = 115 - 3.3J_v \qquad (2)$$

Where; J_v, known as the volumetric joint count, is the sum of the number of joints per cubic meter or volumetric joint counts.

The equation 2 may yield the RQD values greater than 100, which is not persuasive (Şen & Eissa, 1991). For example, if $J_v = 3$ equation (2) yield an RQD value of 105.1, however the RQD value of that rock is less than or equal to 100. As a result, the volumetric joint counts (J_v) can be calculated from joint spacing which is described by Palmstrom (1982, 1985, 1986); and Şen & Eissa (1991).

$$J_v = \sum_{i=1}^{J} \left(\frac{1}{Si}\right) \qquad (3)$$

Where; Si is the average joint spacing in meters for the i^{th} joint set and J is the total number of joint sets except for the random joint set.

RQD is a measure of the degree of fracturing of the rock mass and is aimed to represent the in-situ rock mass quality. The relationship between RQD value and rock mass quality is given in Table 2. 1 below. As indicated in table 1 the greater the RQD value the better the rock mass quality.

Table 2. 1 Rock mass quality classification according to RQD (Deere et al. 1966)

No	RQD (%)	Rock Quality
1	<25	Very poor
2	25 – 50	Poor
3	50 – 75	Fair
4	75 – 90	Good
5	90 - 100	Excellent

2.2.2. Rock Mass Rating (RMR) Classification Method

Rock Mass Rating (RMR) system was developed by Bieniawski during 1972–1973 in South Africa to assess the stability and support requirements of underground structures. Since then the classification has undergone several significant evolutions: In 1974, the classification parameters have reduced from 8 to 6; in 1975, rating adjustment and reduction of recommended support requirements; in 1976, modification of class boundaries to even multiples of 20; in 1979, adoption of ISRM (1978) rock mass description and then it has been modified and improved as more case histories became examined, the latest version of the system was published in 1979 (Bieniawski, 1989).

The importance of this classification system is that only a few basic parameters relating to the geometry and mechanical condition of rock mass are used. To classify a rock mass, the RMR system incorporates the six parameters, from which the five parameters are known as ‘basic parameters’ and the rest is a correction factor (discontinuity orientation). The ‘basic parameters’ are; (1) UCS of intact rock, (2) RQD, (3) spacing between discontinuity, (4) discontinuity condition, and (5) groundwater condition. For each parameter, there is a given weight (Rating) and the rating of each parameter are summed to yield the RMR basic which ranges between “0 to 100” (Bieniawski, 1989).

2.2.2.1. Uniaxial Compressive Strength (UCS) of Intact Rock

Uniaxial Compressive Strength (UCS) is a mechanical property of intact rocks that is important in civil and mining engineering works (Aladejare & Idris, 2020). The input of data like UCS on the geomechanical behavior of rocks is required to design and stability analysis of underground excavation and other geotechnical structures (Ulusay et al., 1994). From surface to underground engineering construction, UCS is a key parameter and it is required to be known with certainty to a great extent for engineering analysis (Aladejare et al., 2021). The uniaxial compressive strength of the intact rock material can be obtained from rock cores in the laboratory test. However, direct determination of the UCS is relatively expensive and it can be estimated from point load strength index Is(50) using empirical formula (Broch & Franklin, 1972), and Schmidt hammer rebound hardness value (R) measurements both in the laboratory and in situ tests (Aydin, 2009).

2.2.2.1.1 Point Load Strength

The point load strength is often used to estimate (approximate) the strength of the rock. The point load strength is usually determined by a test given by Broch and Franklin (1972), and they have given empirical formula to calculate the point load strength or point load index (I_s).

$$I_s = \frac{P}{D^2} \qquad (4)$$

Where; P is the load at rupture and D is the distance between the point loads.

The point load strength varies with the variation of the diameter of the core specimen. The relationship between uniaxial compressive strength and point load was described by Broch and Franklin (1972).

$$UCS = 23 * Is(50) \qquad (5)$$

Where Is(50) is the size corrected point load strength.

2.2.2.1.2 The Schmidt Hammer Rebound Hardness Value (R)

The Schmidt hammer is a perfect index instrument because of its portability, simplicity, and low cost, which explains its growing popularity and wide range of applications. The Schmidt hammer rebound hardness value (R) is likely the most widely used index in rock mechanics for evaluating the uniaxial compressive strength (UCS) and modulus of elasticity (E) of undamaged rock in both laboratory and field circumstances. The instrument is also commonly used to calculate the UCS of discontinuity walls and to analyze the mechanical workability, excavatability, and boreability of rocks (cutting, polishing, milling, crushing, and fragmentation processes in quarrying, drilling, and tunneling) (Adnan Aydin, 2015). Schmidt hammers are divided into two types: L and N, which have impact energies of 0.735 and 2.207 Nm, respectively (Aydin & Basu, 2005). When the UCS of the rock material or discontinuity wall is outside the range of 20–150MPa, sensitivity drops, and data scatter increases, both types of hammers should be used with caution. The N-type hammer is less sensitive to surface defects and should be used in field applications; however, the L-type hammer has more sensitivity in the lower range and performs better when testing weak, porous, and worn rocks (Aydin and Basu, 2005). The Schmidt hammer rebound value can be affected by the type of hammer used, the direction of hammer impact, weathering, moisture content, specimen requirements (no visible cracks) and testing, data gathering/reduction, and analysis procedures (Aydin and Basu, 2005), and all of these factors should be taken into account during the test. Surface imperfections of the rock, test specimen size, impact spacing, hammer direction, weathering state of the rock, and the test process used are all major elements that influence the hardness values of rocks (Karaman & Kesimal, 2015).

Miller (1965) as cited in Barton & Choubey (1977) found a reasonable relationship between the rock's uniaxial compressive strength (σ_c) and the rebound number (range 10 to 60). When he multiplied the rebound number by the dry density of the rock, he got a stronger correlation.

$$\log_{10}(\sigma c) = 0.00088\gamma R + 1.01 \qquad (6)$$

Where; σ_c is the uniaxial compressive strength in MN/m2, γ is the dry rock densities in KN/m3 and R are the average Schmidt rebound value.

2.2.3. Geological Strength Index (GSI)

The geological strength index (GSI) is a system of rock-mass characterization developed in engineering rock mechanics to meet the need for reliable input data, particularly those related to rock-mass properties, as inputs into numerical analysis or closed-form solutions for designing tunnels, slopes, or foundations in rocks. The geological characteristics of rock material, as well as a visual assessment of the mass it forms, are used as direct inputs to the parameter selection for predicting rock-mass strength and deformability (Marinos et al., 2005).

The value of GSI was obtained from the last form of the quantitative GSI chart (Figure 2. 1). The original Geological Strength Index chart was based on the notion that competent and experienced geologists or engineering geologists would observe the rock mass. With the growing use of the GSI chart as the basis for selecting input parameters for numerical analysis, often by people who lack the geologic understanding of rock mass variability required to properly interpret the graphical GSI chart, some uniformity, and quantification of the chart appears to be required (Hoek et al., 2013). Also, GSI values were estimated from RMR using empirical equation 7 (Hoek & Brown, 1997)). The GSI value of each weathered rock mass was used for the estimation of rock mass properties (i.e. equivalent rock mass properties) for the analysis and design of slopes.

$$GSI = RMR_{89} - 5 \tag{7}$$

Where; RMR_{89} is the basic Rock Mass Rating value and GSI is Geological Strength Index.

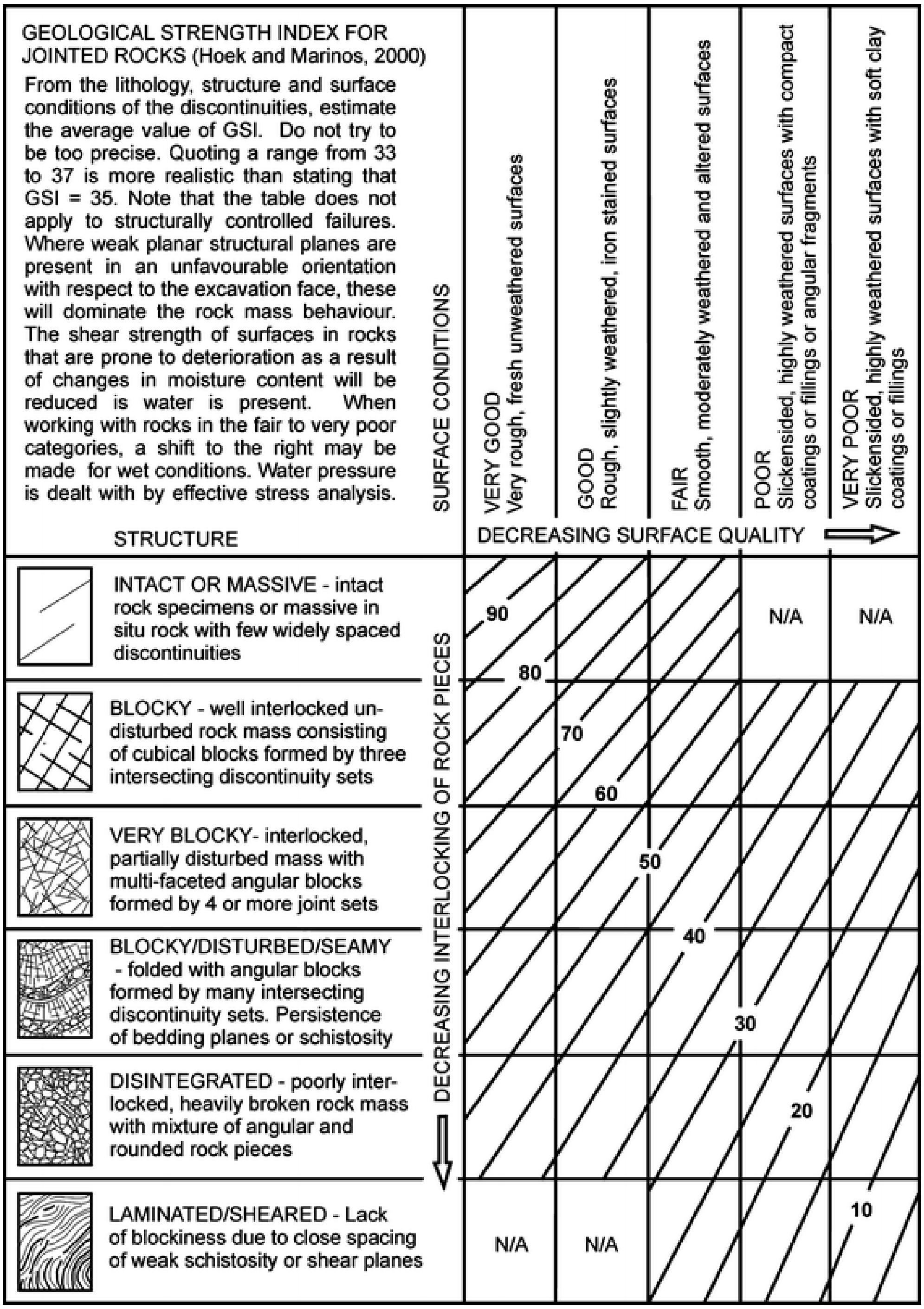

Figure 2. 1 General chart for GSI estimates from the geological observations (after Marinos et al., 2005)

2.3. Water tightness assessment

There is no absolute water tightness achieved in the reservoir of the dam, however, it is usually recommendable that the rate of any leakage is minimized because the water loss cost can be unacceptable large and in some situations, leakage may cause a raising of the water table (Fell et al., 2005). The water losses could occur through the dam body, foundation, abutments, and geological structure located near the dam site and reservoir beds and rims. However, water losses become excessive due to various factors such as seepages and leakages and it could also result in other geological and geotechnical problems which could threaten the normal operation of the reservoirs and dams. Excessive seepage and/or leakage may lead to a problem with the safety of the dam. The water tightness of the dam foundation and reservoir area mainly depends on the factor such as permeability of the underlying rock and soil masses, the permeability of rock and soils that surrounding it, the level of the groundwater table, and the length and gradient of potential leakage paths (Fell et al., 2005). Therefore, for dam and reservoir site investigation is important to consider factors such as the geological condition of the area, topographical condition, land use, and land cover and hydrological records (amount of rainfall, run-off, infiltration, and evapotranspiration) that occurs in the catchment area to minimize the failures and water tightness problems (Bell, 2007).

2.3.1. Water tightness Models for Non-soluble rocks

The model is used to evaluate site characteristics and factors to draw an inference on potential leakage and identify potential areas of leakage (Fell et al., 2005 & Bell, 2007). Most non-soluble rock substances are effectively impermeable, and rock masses formed by them are only pervious if sufficient numbers of interconnected open joints are present (Fell et al., 2005). As stated by Fell et al. (2005) with increasing depth the joint becomes more tightly closed, so most rock masses of non-soluble become less permeable with increasing depth. There are five models of water tightness as described in the schematic diagram in Figure 2. 2, it shows the effect of creating storage in such non-soluble rock, in five relatively common topographic and groundwater situations (Fell et al., 2005).

These models are assumed that the rock becomes less permeable with increasing depth, across the floor of the storage area, the water table lies close to the ground, and the water table shown represent the end of dry season conditions, groundwater pressures measured below the water table as shown will all confirm it as the piezometric surface and flow beneath the high ground or ridges forming the rims will be essentially laterally from the storage (Fell et al., 2005). The following explanations on models of water tightness of non-soluble rocks are illustrated by Fell et al. (2005).

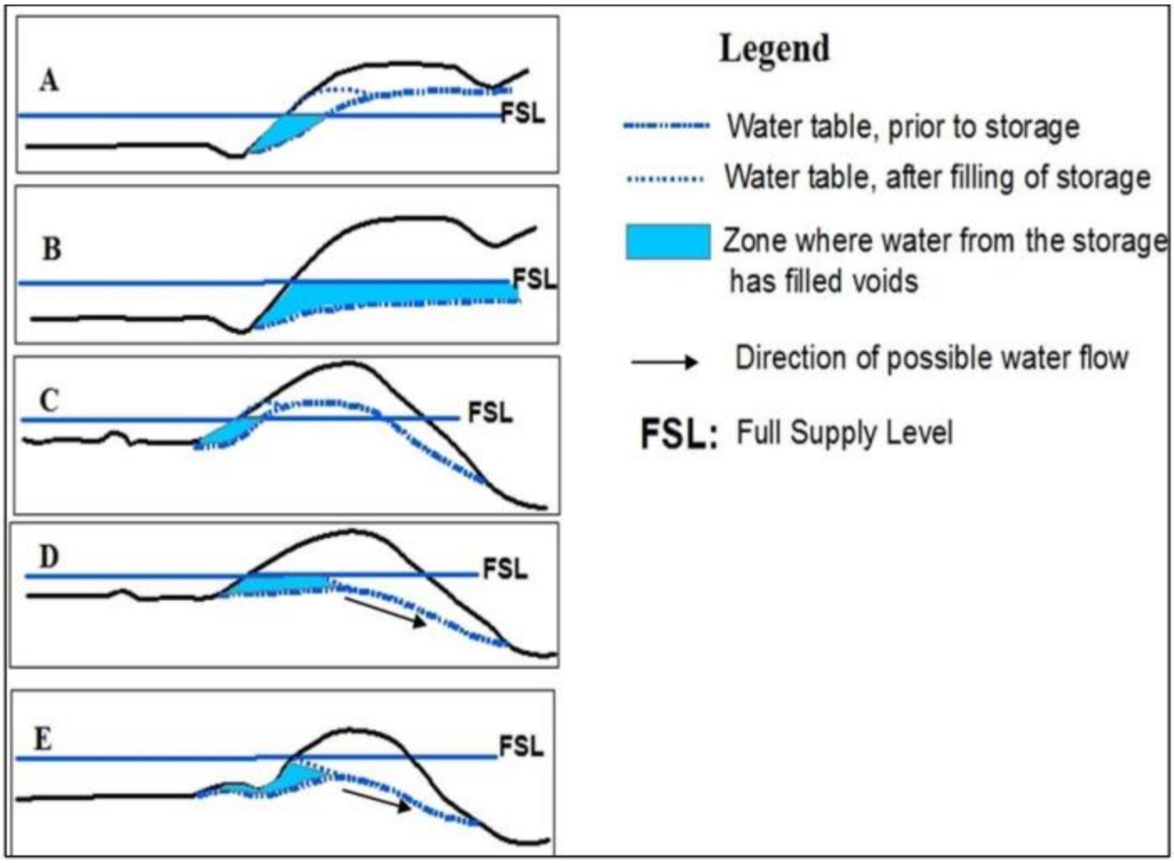

Figure 2. 2 Storages formed by non-soluble rocks-water tightness models (after Fell et. al., 2005)

Model A

This model is characterized by high rainfall and the storage is in an ingrained valley underlain by rock and surrounded by a wide area of high ground underlain by rock. The rock on the floor of the valley covered by soils of alluvial or glacial origin partially or wholly Figure 2. 2A. There is no potential leakage as the water table rises above the proposed Full Supply Level (FSL) of the reservoir on high ground and it will be partly fed by groundwater. Therefore, the storage should be essentially watertight and when the reservoir fills a very small amount of water will fill the voids in the adjacent rock mass (shaded).

Model B

The topographic and geological conditions of this model are similar to model (A), but the groundwater table lied beneath the proposed FSL due to a drier climate, greater surface runoff, and permeable subsurface formation. In this condition, there is potential leakage, however the leakage paths would be so long and at such a low gradient, the loss of water from the reservoir would be probably negligible. The shaded area shown in Figure 2. 2B indicates the water table rises locally where a small amount of water enters, fills the voids.

This model likely represents a storage in non-soluble rock areas with low to moderate rainfall.

Model C

This model involves when the river valley is bounded by subsequent high and wide ground, followed by a gradual decrease in topography resulting in another valley as shown in Figure 2. 2 (C). This model also assumes that the proposed FSL is below the groundwater table in high ground areas which follows the topography. Therefore, in this condition apart from the initial loss of a small amount of water from the storage to fill voids of rocks on the side of the valley (shaded zone in Figure 2. 2C), there is no potential for leakage as the water table is already above the proposed FSL in high ground areas.

Model D

This model assumes similar preconditions to Model C but with the groundwater table to be below FSL. In this scenario, a drier climate, greater surface runoff, and the presence of permeable rocks may act as causative factors for lower groundwater table assumptions than Model C. In this model, significant leakage is not expected as the leakage path is long in high ground areas adjacent to the valley Figure 2. 2D.

Model E

This model assumes conditions in which the groundwater table is soundly below FSL compared to Model C and D. Furthermore, the ridge forming the rim of the valley for storage is considered to be narrow and low. As a result, the rock beneath the ridge and below FSL is likely to be affected by the release of stress and hence more permeable than that at Models (C) and (D). In this model, the groundwater is unlikely to rise significantly to meet with FSL even if the area is located in the high rainfall region. Therefore, significant potential for leakage is expected, owing to the above-mentioned permeable rocks and the high hydraulic gradient between FSL and the actual groundwater table Figure 2. 2E.

2.4. Permeability of Rock Mass

Hydraulic conductivity of rock masses is highly affected by geometric properties or fracture characteristics (aperture, frequency, length, orientation, interconnectivity network of fracture, infilling materials, and fracture plane paths) and degree of weathering (Foyo et al., 2005; Hamm et al., 2007; Karagüzel & Kilic, 2000). Understanding the relationship between hydraulic conductivity and fracture characteristics is very important to determine the permeability of the rock mass. The intact rock is very well cemented mineral grains that contain tiny pores. The pores or voids are not interconnected however, may represent at least very low permeability if the rock is not fractured. As shown in Figure 2. 33 the fractured/jointed basalt has a hydraulic conductivity ranges from 10^{-5}cm/s to 1cm/s, which means moderately to highly hydraulic conductivity.

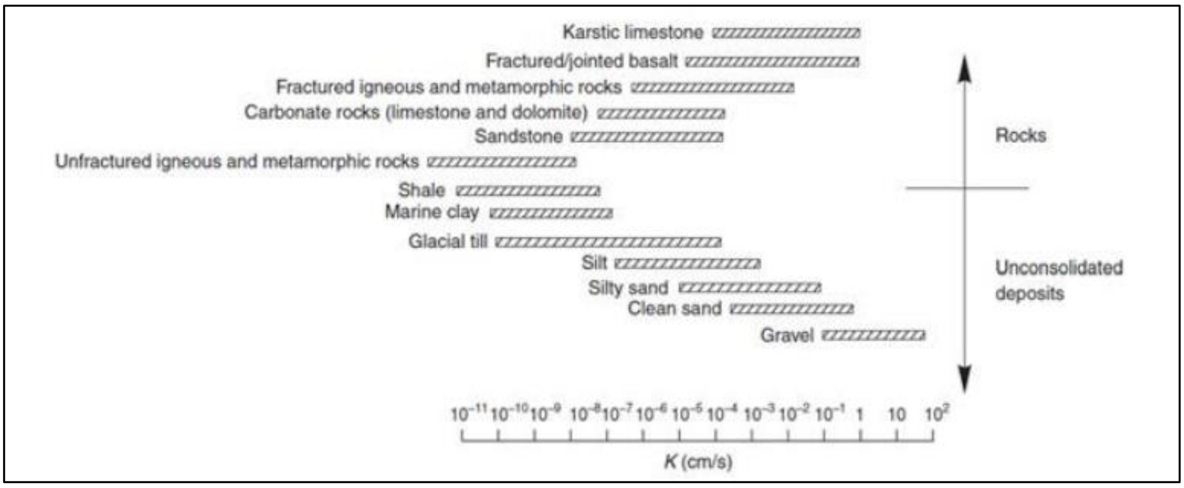

Figure 2. 3 Hydraulic conductivity of various geological units (after Atkinson, 2000)

Hydraulic information can get from field measurements (core log, geophysical log, pumping tests, and water pressure tests) and laboratory tests (Hamm et al., 2007). Therefore, hydraulic conductivity of rock mass can determine from field measurements and laboratory tests. As El-Naqa (2001) also discussed that the hydraulic conductivity of rock mass was determined for subsurface by using packer test (water pressure tests) and for surface by using fracture properties. Even though field test to determine the hydraulic conductivity of rock masses is very difficult due to complex field conditions, it is considered to be more useful than the laboratory hydraulic test because the in-situ test represents the real stress condition of the site on a larger scale than the laboratory test(Hamm et al., 2007).

2.4.1. Permeability of Rock Mass Determination from Packer Test

One of the hydraulic test methods conducted in-situ to get the hydraulic characteristics of rock mass is the packer test (Tesema & Ekmekci, 2019). It is used to determine the hydraulic conductivity of fractured rock mass (Tesema & Ekmekci, 2019). They also stated that the test is performed by measuring the flow rate of water into an isolated test section of the borehole at a given pressure head. The test is conducted in five stages with a particular water pressure magnitude associated with each stage. A single-stage consists of keeping a constant water pressure at the test interval for 10 minutes by pumping as much water as required. The first stage is held at a low water pressure, increasing the pressure in each subsequent stage until reaching maximum pressure. Once maximum pressure is reached, pressures are decreased following the same pressure stages used on the way up, thus describing a “pressure loop”. During the execution of each stage, both water pressure (P) and flow rate (q) values are recorded every minute. Subsequently, average values for P and q are then used to compute the hydraulic conductivity for each stage. The hydraulic conductivity is given in terms of Lugeon value, which is empirically defined as the hydraulic conductivity required to achieve a flow rate of 1 liter per minute per meter of test interval under a reference water pressure equal to 10 bar (Quiñones-Rozo, 2010).

$$\text{Lugeon} = \text{uL} = \frac{q}{L} * \frac{P_0}{P} \tag{8}$$

Where q is water loss (Lt/min), L is testing length (m), P_0 is a reference pressure (1MPa) and P is applied pressure at a test stage (MPa).

As stated by Ajalloeian & Azimian (2013) the result of the Lugeon value was then used to express the characteristics of discontinuities and types of rock mass in the dam foundation and reservoir area as well as to determine the water/cement ratio and grout injection pressure used during grouting. In Table 2. 2, Lugeon values and corresponding classification values are given.

Table 2. 2 Condition of rock mass discontinuities associated with different Lugeon values (after Quiñones-Rozo, 2010)

Lugeon range	classification	Hydraulic conductivity range (cm/sec)	Condition of rock mass discontinuities	Reporting precession (Lugeons)
<1	Very low	<1 x 10^{-5}	Very tight	<1
1-5	Low	1x 10^{-5} – 6 x 10^{-5}	Tight	±0
5-15	Moderate	6 x 10^{-5} – 2 x 10^{-4}	Few partly open	±1
15-50	Medium	2 x10^{-4} – 6 x 10^{-4}	Some open	±5
50-100	High	6 x 10^{-4} – 1 x 10^{-3}	Many open	±10
>100	Very high	>1 x 10^{-3}	Spaced or voids	>100

2.4.2. Permeability of Rock Mass Determination from Fracture Characteristics

Permeability of rock mass alters due to the presence and frequency of discontinuities. Discontinuity properties such as persistence, tightness, aperture, roughness, type of infill material, filling thickness of the discontinuities also govern the flow rate of water through the rock mass (Öge, 2017). The permeability of fractured (jointed) rocks depends on the dimensions and nature of the joints. The closer the spacing and the wider the opening, the higher the permeability. From the fracture aperture and spacing, it is possible to calculate the hydraulic conductivity of the rock mass. With the assumption of parallel flow within smooth fractures, Louis Louis (1967) and Snow (1965) derived the relationship between hydraulic conductivity (K) and fracture characteristics. However, the hydraulic conductivity in a rough fracture is 25% of that in smooth fractures (El-Naqa, 2001).

$$K = \frac{ge^3}{12\mu S} \quad (9)$$

Where; g is the gravitational acceleration (9.81 m/s^2), e is the average aperture of fracture (m), μ is the coefficient of kinematic of the fluid (1 x 10^{-6} m^2/s for water at 20^0c) and S is the average spacing of fracture (m). However, the fracture frequency (λ) is equal to the reciprocal of fracture spacing. So the above equation can be written as follows;

$$K = \frac{\lambda ge^3}{12\mu} \quad (10)$$

2.5. Permeability of Soil Mass

Permeability is a very important engineering property of soil. Permeability of soil is defined as the property of soil that allows the water to move through its interconnected void spaces (Arora, 2003). Hydraulic conductivity of soil is controlled by different factors such as particle size, shape, texture, mineralogical composition, soil fabric, degree of saturation, void ratio, and arrangement of its voids (Terzaghi et al., 1996). Arora (2003) stated that knowledge of permeability is very essential in different soil engineering applications, especially in the stability of dam foundations, seepage loss below and through embankments of reservoirs, for the design of filters to prevent piping and settlement of buildings. The coefficient of permeability of soils can be determined in the laboratory (constant head and falling head permeability tests), in-situ field test (packer test), and from empirical correlations (Arora, 2003). The soil samples used in laboratory tests are either disturbed or undisturbed.

2.5.1. Constant Head Permeability Test Method

Constant – head permeability test is a laboratory method to determine the hydraulic conductivity (coefficient of permeability) of cohesionless or relatively more permeable soil ($K>10^{-4}$cm/s) by using the equipment of constant – head permeameter (Arora, 2003). According to Arora (2003), hydraulic conductivity (K) is determined by using Darcy's law, for the soil sample length, L, and cross-sectional area, A, is subject to a head, h, which is constant during the progress of a test. Constant–head permeability test methods are performed by water flowing through the sample and measuring the quantity of discharge, Q, in time, t, and the value of k can be determined by Darcy's law which expresses as follows;

$$K = \frac{QL}{hAt} \tag{11}$$

2.5.2. Falling Head Permeability Test Method

Falling – head permeability test is also known as the variable – head permeability test, which is used to determine the coefficient of permeability for cohesive (clayey) or less permeable soils ($K<10^{-4}$ cm/s) (Arora, 2003). The soil sample remolded system is the same as that used in the constant head permeability test, but the hydraulic conductivity k can be determined based on the drop in the head (h0 – h1) and the elapsed time (t1 – t0) required for the drop of the head and the quantity of water flowing through the sample in a given time using Darcy's law which can be expressed as follows in equation xx

$$K = \frac{2.3aL}{A(t_1-t_0)} log_{10}(\frac{h_0}{h_1}) \tag{12}$$

Where; A is a cross-sectional area of the vertical cylinder in which the sample is kept, a is a cross-sectional area of the transparent standpipe, L is the length of the sample, h0 and h1 are initial head and final head drop respectively, and t0 is the initial time at h0 and t1 is a final time when the water level drops from h0 to h1.

2.6. Slope stability analysis

Slope stability analysis is one of the oldest histories in geotechnical engineering and recently it is one of the most active areas in both practice and academic (Griffiths & Marquez, 2007). Rock slope stability analyses are routinely performed and directed towards assessing the safe and functional design of excavated slopes (for example; open-pit mining, road cuts, dam site slopes, etc.) and the equilibrium conditions of natural slopes (Eberhardt, 2013). The instability of a rock slope may be influenced by the material characteristics of the rock slope, height, face angle, and the joint orientation (Evert Hoek & Bray, 1981). Slope instability may also occur due to internal and external factors. An internal factor includes adverse slope geometries, geological discontinuities, weak or weathered slope materials as well as severe weather conditions while external factors like human activity, heavy precipitation, and seismicity could play a significant role in slope failures (Basahel & Mitri, 2017). The stability of jointed rock slopes is mainly controlled by the discontinuities because failure is expected on these planes of weakness. The relative orientation of discontinuity concerning the slope face and the shear strength parameters of the weakness planes and pore water pressure in the tension crack will determine how blocks fail (Özsan et al., 2007).

Slope stability problems attract major concerns of researchers, and consequently, several techniques and methods for slope stability evaluation have been proposed. These methods are grouped into four categories, such as kinematic analysis, limit equilibrium, numerical modeling and empirical methods (R E Goodman, 1976; Evert Hoek & Bray, 1981; Jaeger, 1971; Kutter, 1972). Slope stability analysis consists of two steps (Park & West, 2001). The first step is to conduct kinematic analysis, by using stereographic analysis to determine the possible mode of failure. On the other hand to determine if the orientation of the discontinuities could result in instability for the slope define by those discontinuities. The second step (limit equilibrium) proceeds, if the first step (kinematic analysis) indicates that the structural condition is potentially unstable (i.e. if there is an instability problem). The chosen slope stability analysis technique depends on the site condition and potential mode of failure and also careful consideration of the strength, weaknesses, and limitations of each methodology (Eberhardt, 2013).

2.6.1. Kinematic analysis

Kinematic analysis is a method used to identify the various modes of failure (planar, wedge, and toppling failure) that can occur for existing rock slopes and formed in the presence of unfavorable oriented discontinuities along the road, hilly, and pit slope (Evert Hoek & Bray, 1981). It is purely geometric, examining which mode of slope failure is possible in jointed rock mass (Yoon et al., 2002). The angular relationship between discontinuities and slope surface is applied to determine the possible mode of failure (Kliche, 1999). Numerous researchers ((R E Goodman, 1976; Evert Hoek & Bray, 1981; Markland, 1972) have been performed failure modes by utilizing stereographic projection technique since Panet et al., (1969).

The parameters used in kinematic analysis method are friction angle (friction cone), dip amount, and dip direction of discontinuities, and slope face. These parameters are import into dip software (Dips 6.0; Rocscience, 2004) and the software undergo that kinematic analysis by identifying the main joint, daylight envelope, lateral limit, and mode of rock slope failure (Goodman, 1989; Hudson & Harrison, 1997).

2.6.1.1. Kinematic Check for Plane sliding modes of Failures

To consider the kinematic admissibility of the planar mode of failure the following criteria must be satisfied (Goodman, 1989; Hoek & Bray, 1981; Wyllie & Mah, 2004).

- The plane on which sliding occurs must strike near parallel to the slope face (within approx. ±20°).
- Release surfaces (that provide negligible resistance to sliding) must be present to define the lateral slide boundaries.
- The sliding plane must have "daylight" on the slope face.
- The dip of the sliding plane must be greater than the angle of friction.
- The upper end of the sliding surface either intersects the upper slope or terminates in a tension crack.

2.6.1.2. Kinematic Check for Wedge sliding modes of Failures

The wedge failure occurs when movement takes place by sliding along both planes in the direction of the intersection line; the following basic conditions must be satisfied for wedge failure to be kinematically possible (Markland, 1972).

- The dip of the slope must exceed the dip of the line of intersection of the two wedges forming discontinuity planes.
- The line of intersection must be "daylight" on the slope face.
- The dip of the line of intersection must be such that the strength of the two planes is reached.
- The upper end of the line of intersection either intersects the upper slope or terminates in a tension crack.

2.6.1.3. Kinematic Check for toppling failure

Toppling mode of failure may occur when the two criteria are satisfied; such as the direction of slope face dip toward the opposite direction of the orientation of discontinuity plane and the difference between the strike of slope face and discontinuities is less than 20^0 (Evert Hoek & Bray, 1981; Wyllie & Mah, 2004). Kinematic analysis can be carried out using stereographic projection and identifying the mode of failure by using dips software (Dips 6.0; Rocscience, 2004).

2.6.2. Limit Equilibrium Method

The limit equilibrium method is the most common approach for analyzing slope stability in both two and three dimensions (hung, 2014). It is the method of analysis in terms of evaluating factors of safety for slope instability of rock and soil where the translation or rotational movements occur on the distinct failure surfaces (Eberhardt, 2013; Lin et al., 2014). The factor of safety is the ratio of resisting (strength) to deriving force (loading) along a potential failure surface in which a factor of safety equal to one represent critically or limit equilibrium implies that the slope is on the verge of sliding while the factor of safety greater and less than one shows that stable and unstable slope respectively (Christian, 2004; Steffen et al., 2008). To undergo limit equilibrium analyses of rock slope, a representative of the joint set (mean value) should be first selected from kinematic analysis and then the shear strength parameter for that joint will be used to determination factor of safety (Park & West, 2001). If the driving force and resisting force were equal, the stability is independent of any deformation and size of the sliding block and indicates a factor of safety (FOS) of 1.0. Is assumed that a FOS of 1.0 is the “threshold” where the slope goes from stable to unstable. If FOS is less than 1.0, the driving forces overcome the resisting forces causing slope movement (Ureel & Momayez, 2014), the slope is stable if FOS is greater than 1.0.

In limit equilibrium analysis, the sliding mass is separated into several slices and the shear and normal inter-slice force is determined considering the force and moment equilibrium acting on each slice (Memon, 2018). Limit equilibrium methods calculate the factor of safety based on the inter-slice of normal and shear forces. However, the basic difference is how these forces are determined and FOS calculations depend on the shape of the critical slip surface (Memon, 2018). However, the LEM is not considered the stress and deformation in the rock mass and also the displacement and velocities of the failure surface are not calculated movement (Ureel & Momayez, 2014).

Currently limit equilibrium slope stability analysis software such as Slide software, Swedge software, and Rocplane software are widely used in engineering practices developed in the Rocscience computer program (Rocscience, 2004). This computer program is used for slope stability analysis for both rock and soil slopes. The Slide computer software is a 2D slope stability program for evaluating the stability of circular or non-circular failure surfaces in soil or highly weathered and fractured rock slopes (Rocscience, 2004). The factor of safety was calculated by Slide software based on the Mohr-Coulomb failure criterion without tension cracks (Rocscience, 2004). Similarly, Swedge and RocPlane software are used to analyze the stability of the wedge and planar mode of failure respectively in two dimensions.

2.6.3. Numerical Method

Many slope stability problems involve complex due to the complexities relating to geometry, material anisotropy, non-linear behavior, in situ stresses, and presence of several factors such as pore pressure and seismic loading (Eberhardt, 2013). Conventional types of slope stability analyses are limited to the simplistic problem in their scope of application encompassing simple slope geometries and basic loading conditions and provide limited analyses regarding the mechanism of slope failure (Abramson et al., 2002). Kinematical analysis refers to the motion of bodies without considering the force that causes them to move, whereas the limit equilibrium considers the shear strength along the failure surface, the effects of pore water pressure, and the influence of reinforcing elements or seismic acceleration which is external forces. On the other hand, numerical methods such as finite element and distinct element methods are performed to confirm results occurred from kinematical and equilibrium analysis and also they are used in more complex slope geometries and failure mechanisms and provide possible solutions to such problems that could not be possibly solved using kinematic and limit equilibrium methods (Gurocak et al., 2008). Furthermore, kinematical analysis sometimes does not work when the rock has close-very close-spaced low persistent joints and for the rotational mode of failures.The finitee element method (FEM) is increasingly being applied to slope stability analysis by performing the shear strength reduction (SSR) approach (Hammah et al., 2005). The concept of shear strength reduction systematically redu the shear strength envelop of material by factor of safety and compute FEM models of the slope until deformations are unacceptably large or solution do not converge (Hammah et al., 2005).

The numerical method is one of the typical slope stability analyses approach which solves slope stability in the form of mathematical calculation by taking deformation into account(Abramson et al., 2002). Finite element analysis can be carried out using Phase2 software. Phase2 software is a powerful 2D Elasto-plastic finite element stress analysis program for underground and surface excavations in rock or soil. Besides for the user it gives an idea of the general outline of the rock slope and predicted failures. The method uses some geotechnical parameters such as slope height, slope angle, uniaxial compressive strength, Poisson's ratio, unit weight of the rock, geological strength index (GSI), Hoek-Brown parameters, deformation modulus of rock mass, friction angle, cohesion and direction of the discontinuities and groundwater condition (Gurocak et al., 2008). There are three types of numerical slope stability analyses approach which are a continuum, discontinuum and hybrid modeling approach (Abramson et al., 2002; Eberhardt, 2013).

2.6.3.1. Continuum approach

Continuum approaches used in slope stability analysis include the finite-difference and finite element methods. In both these methods, the problem domain is divided into a set of sub-domains or elements (Eberhardt, 2013). In the case of the Finite Difference Methods (FDM) solution procedure based on the differential equations of equilibrium, the strain-displacement relations and the stress-strain equations can be applied. Alternatively, the procedure may exploit approximations to the connectivity of elements and continuity of displacements and stresses between elements, as in the Finite Element Method (FEM). The continuum method is best suited and widely used in stability analysis of rock slopes that are comprised of massive rock, intact rock, weak rock, and highly jointed rock masses (Eberhardt and Vancouver, 2003). Shear strength parameters along the failure plane, surface and groundwater conditions, and in-situ stress are the main input parameter in continuum modeling (Abramson et al., 2002).

2.6.3.2. Discontinuum Approach

The discontinuum method is more appropriate for a rock slope comprising multiple joint sets, which control the mechanism of failure. The methods treat the problem domain as an assemblage of distinct, interacting bodies or blocks that are subjected to external loads and are expected to undergo significant motion with time (Eberhardt, 2013). This method is collectively referred to as the discrete element method (DEM). The input parameters used for the discontinuum method are shear strength parameter, the geometry of the slope, and groundwater conditions.

2.6.3.3. Hybrid Approach

A hybrid approach of the numerical method involves the coupling of the two continuum and discontinuum to maximize their key advantages (Eberhardt, 2013). Hybrid approaches are increasingly being adopted in the rock slope analysis and this may include combined analyses using limit equilibrium, stability analysis and finite element groundwater flow and stress analysis (Eberhardt, 2013). Although separately continuum and discontinuum analyses provide a useful means to analyze rock slope stability problems, complex failures often involve mechanisms related to both preexisting discontinuity and the brittle fracturing of intact rock. The hybrid analysis allows for the modeling of both intact rock behavior and the development and behavior of fractures. These methods use a finite element mesh to represent either the rock slope or joint bounded blocks coupled together with discrete elements able to model deformation involving joints. If the stresses within the rock slope exceed the failure criteria within the finite-element continuum a discrete fracture is initiated (Eberhardt, 2013).

2.7. Stabilization methods of slopes

In the mountainous area where there are numerous slope stability problems may result in a significant cost and loss of life and properties, stabilization methods are very necessary. Slopes in most dam abutments, tunnel, mines, and road cuts in mountainous areas are prone to instability problems due to variation in the rock mass conditions and factors induced by the environment such as seismic activities and water in the slope (Pantelidis, 2009). The slope instability problem of the road cut, mining pit, and dam abutments are influenced by the material characteristics of the slope, height of slope, angle of slope face, and orientation of joints (Basahel & Mitri, 2017).

From the slope stability analyses approach to first identify the point where the instability problem occurs; the possible mode of failure and the factor that causes the problem, afterward the stabilization method undertake to stable the slope. There are various stabilization methods used for stabilizing rock slopes some of which are; removal of unstable rock, surface protection, reinforcement, and drainage (Abramson et al., 2002). The most appropriate remedial measures used to stabilize rock slope at the dam site are the installation of rock reinforcement (such as rock bolts, rock anchors, and shotcrete), modifying the geometry of the slope, and providing drainage holes (Evert Hoek & Bray, 1981).

Removal and protection: Removing the unstable material that usually lies on the upper layer of the slope and placing protection means, (e.g., nets).

Rock bolts: is the systematic reinforcement of rock slopes by the insertion and grouting of steel bars (usually about 3m long) into holes predrilled into the more or less fractured rock mass, improving its stability and often fully grouted. Rock bolts can hold the loosened rock mass in place and adopted to strengthen and stabilize the rock mass (Hoek and Bray, 1981).

Rock anchors: the stability of a slope can be increased to good effect by anchoring them into the bedrock below the probable shear surface. The pre-stressing of the anchor increases the effect of friction on this surface and creates forces that directly act against possible movement of the slope (Hobst & Zajíc, 1983).

Shotcrete: is chosen when the slope is discontinuous, and many fissures appear, under high pressure, the shotcrete will be penalized into these fissures and adhere rocks into a whole. Moreover, the shotcrete can help to adhere to rock bolts and soil nails, improving stability and anchor-ability. Shotcrete is used frequently to preserve the integrity of a rock face by sealing the surface and inhibiting the action of weathering (Bell, 2007). It is a mixture of cement, water, and aggregate, and is mainly applied to the surface of highly weathered and fractured rocks. For the shotcrete surface, it is essential to provide sufficient drain holes to remove pore pressure that is built up underneath the shotcrete surface. The adhesion of the shotcrete rock surface, together with the shear strength of the shotcrete layer, provides resistance to the failure of loose rock blocks as well as confinement of the rock mass. It will also seal rock that is prone to weathering due to exposure to the elements of nature (Abramson et al., 2002).

Drainage: The water enters along tension cracks, builds up hydrostatic pressure and freeze during winter, which causes displacement of rock blocks. The drainage system is used to limit the amount of water that accumulates along the rock mass discontinuities, to prevent rock blocks from failure to the effect of water pressure. There are two general drainage systems, such as surface drainage and subsurface drainage. Surface drainage refers to the diversion of surface runoff away from tension cracks or open rock mass discontinuities near the slope face. Whereas, subsurface drainage includes horizontal drains, tunnels, and other methods (Abramson et al., 2002).

Modifying the slope geometry: is often done by reducing the slope angle, reducing the weight at the head of the slope, increasing weight at the toe ("heels" or rip-rap), or constructing benches (Hoek and Bray, 1981).

2.8. Remedial Measure to Control Leakage

Seepage is a common problem in almost all dam sites. All embankment dams are subject to thorough foundation, dam body, and abutments. Seepage control is very necessary to prevent the effects of seepage (excessive uplift pressures, instability of the downstream slope, piping through the embankment and/or foundation, and erosion of material by migration into open joints in the foundation and abutments). Controlling the quantity of seepage that occurs after construction is difficult and quite expensive. There are different methods to control or prevent leakage of water from reservoirs of dams which can be employed based on the geological conditions of the dam site, economical studies, and available material in the region (Shehata, 2006).

Grouting: is a process of injecting under pressure a fluid sealing material into the underlying formations through specially drilled holes to seal off or fill joints, fractures, fissures, bedding, cavities, permeable strata, or other openings. It is the most effective method to control the percolation of water through geological defects (Bell, 2007). In addition, grouting is used to consolidate/strengthen the foundations below dams and minimize settlements, minimize leakage below dams, and control seepage/pore pressures in rock abutments of dams (Fell et al., 2005). There are two types of grouting are widely used at the dam site i.e. curtain grouting and consolidation grouting.

Curtain grouting is designed to create a narrow barrier (or curtain) through an area of high permeability (Houlsby, 1991). It usually consists of a single row of grout holes which are drilled and grouted to the base of the permeable rock, or to such depths that acceptable hydraulic gradients are achieved. For large dams on rock foundations, 3, 5 or even more lines of grout holes may be adopted. The holes are drilled and grouted in sequence to allow testing of the permeability of the foundation (by packer testing) before grouting and to allow a later check on the effectiveness of grouting from the amount of grout accepted by the foundation (grout take).

Consolidation grouting for embankment dams is designed to give intensive grouting of the upper layer of more fractured rock in the vicinity of the dam core, or in regions of "high" hydraulic seepage gradient to control seepage/leakage and to improve bearing capacity. It is usually restricted to the upper 5m to 15m and is carried out in sequence but commonly to a predetermined whole spacing and depth (Houlsby, 1991). In addition, consolidation grouting is adopted to fill the fractures and joints and strengthen the rock mass. This grouting method is adopted for sealing water passages into the foundation excavation or under the dams and also to fill/treat cavities under dams, abutments, and reservoirs.

Cut-off Walls are uniquely suited to remedy seepage through an existing embankment. The cutoff can be extended to remedy foundation and abutment seepage problems as well (Sherard, 1968). As Nusier et al., (2002) discussed the cut-off was constructed to prevent seepage problem in the Kafrein dam through foundation below dam and the abutment or the reservoir side away from the dam.

Upstream Impervious Blankets: is an impervious layer the upstream of a dam to control the seepage from the dam foundation (Jour et al., 2015). Replacing the top layer of a river bed with higher permeability is the most economical way of controlling the seepage/leakage. In addition, clay blanketing is used particularly in alluvial soil when cement grouts are not applicable (Fell et al., 2005). An impervious blanket immediately upstream of a dam can be used to seal the reservoir bottom and sides and thereby reduce seepage quantities and pressures beneath a dam. If the dam contains a permeable shell, the impervious blanket must be extended up the embankment slope to effectively control the seepage problem.

Drainage: can also be used as a treatment to control seepage. Generally, the work can be performed from the downstream side of the dam. Expedient installation of filter materials and a toe drain can help prevent piping of embankment and foundation materials and may increase embankment stability but will not normally reduce seepage quantities. Horizontal drains of slotted pipe normally do not have a filter envelope and would generally be used for seepage or as an expedient measure until a more permanent solution could be installed (ACE, 1986).

2.9. Case study of dams constructed on volcanic rock in Ethiopia

Primary and secondary porosity, joints, and cracks define volcanic rock, creating a favorable environment for reservoir water loss. A significant degree of weathering is also characteristic of volcanic basalt to have an impact on the rock's bearing ability Mechanical qualities degrades due to weathering. In numerous rock-engineering structures, producing failure or significant settlements (Chala & Rao, 2017). There is some study conducted on a dam project in Ethiopia that underlie on volcanic rock units.

The Koga dam was built on the Koga River, a tributary of the Blue Nile flowing into Lake Tana in Northern Ethiopia. The study was aimed to slope stability analysis of the Koga main dam. The Koga watershed have regional geology of the site, with dominated by tertiary volcanic rock and quaternary basalt (Zewdu, 2020).

The slope stability analysis of the dam was carried out by using PLAXIS 2D software of finite element model. Based on the analysis the factor of safety value resulting during end of construction is 1.6221 and 1.3592, for both static and dynamic conditions, respectively. And also the analysis results the factor of safety varies for steady-state condition (2015.25m) to rapid drawdown (from 2015.25m to 2008.5m) from 1.6136 to 1.2199 for static analysis and from 1.3157 to 1.0353 for dynamic analysis, respectively. Based on the result of the analysis Zewdu (2020) concluded that Koga earth dam is safe at all critical loading conditions.

Engineering geological characterization of rock for dam in Gullel Botanic Garden dam found in central Ethiopia specifically in Addis Ababa was conducted by Moges & Meten (2019). They conducted through the method of integrated geophysical method and packer test to evaluate water tightness of the dam project. The geology of the area is volcanic rock includes Ignimbrite, Rhyolite, Tuff and Basalt and Residual soils. The rocks are affected moderately to highly weathered and fractured according to the authors. As the result of packer test revealed that the area ranges from low permeable to high permeable. Hence excessive seepage problem is a critical issue from the site. According to the authors the dam is affected by water tightness problem evaluated by water pressure test. Accordingly, grout with variable depth depending upon Lugeon values were recommended for the left abutment and the riverbed of the dam as remedial measures for anticipated problems.

Asfaw & Meten (2021) conduct a geological and geotechnical investigation of the Arjo Didesa dam site to determine water tightness and stability using a discontinuity survey, engineering geology mapping, core drilling and accompanying in-situ testing, and seismic refraction Tomography investigations. The dam site's geology is dominated by quaternary alluvial soil deposits, colluvial and residual soils, all of which are underlain by porphyritic Rhyolite rock and aphanitic basalt rocks, some of which are jointed, faulted, Lineaments, and weathered (on the surface). The analysis also revealed that leakage issues are likely to occur in both the dam's left and right abutments, as well as structural and nonstructural slope stability issues in dam abutments. According to the authors, Grouting, rock bolts, anchors, shotcrete surface, and appropriate drain holes to reduce pore water pressure were the recommendations for the Arjo Didesa site's engineering problems.

CHAPTER THREE

3. MATERIALS AND METHODS

The approach utilized in this study to meet the research objectives can be divided into three parts: pre-field office work, detailed fieldwork (discontinuity surveying, in-situ testing, mapping, and sampling), and post-field work (laboratory testing and data processing). The primary and secondary data were used to evaluate, summarize, and present the findings.

3.1 Office Works

Pre-field office work included obtaining a topographic map, regional geology map, and reports from the Ethiopian Geospatial Information Agency and the Geological Survey of Ethiopia, as well as various field equipment from Adama Science and Technology University. A base map was created, and a survey of published journals and unpublished publications was conducted. Furthermore, past works and design reports from OWWDSE were obtained, including geotechnical data, in-situ permeability tests, hydrogeological and geophysical data from the Gololcha dam site. To understand the water tightness evaluation methods, slope instability failure mechanisms, and select acceptable methods of analyses for this project, a literature review on dam failure mechanisms, soil and rock mass characterization, slope stability, and water tightness analyses was conducted.

3.2 Primary Data Collection

During the fieldwork, the primary data were acquired from the Gololcha dam site. Detailed geological and engineering geology assessments were performed at the dam site and reservoir area during the field survey. Detailed discontinuity surveys (including discontinuity characteristics such as spacing, roughness, orientation, aperture, persistency, degree of weathering, and infilling materials), digging test pits, field description of soils and rocks, mapping, and sample for laboratory examination are among these. Mapping was done at the reservoir and dam site using representative traverse lines that intersected numerous lithological units and important geological formations. In general, each of these data points was briefly detailed in the parts that follow.

3.2.2 Discontinuity survey

Discontinuity survey was carried out mainly from the abutment of the dam and reservoir area where there is rock exposure. During discontinuity survey slope section for stability analysis were identified based on the degree of weathering and fracturing; the slope section with a highly degree of weathering and highly fractured are considered as non-structural control of slope instability, whereas the discontinuity orientation of the rock mass plays a significant role in slope instability it considered as structural control.

A numerical description of discontinuity characteristics like orientation, roughness, spacing, persistence, continuity, aperture (openness), filling material, groundwater condition, and joint set number was collected from exposed rocks at the abutment and reservoir. The orientation of the discontinuity was taken into account for rock slope instability and leakage potential during the discontinuity data collection. Also measured were slope geometry properties like dip and dip direction. A Brunton compass was used to measure joint orientations such as strike, dip, and dip direction, while a meter was used to measure spacing, continuity, and aperture (Figure 3.1).

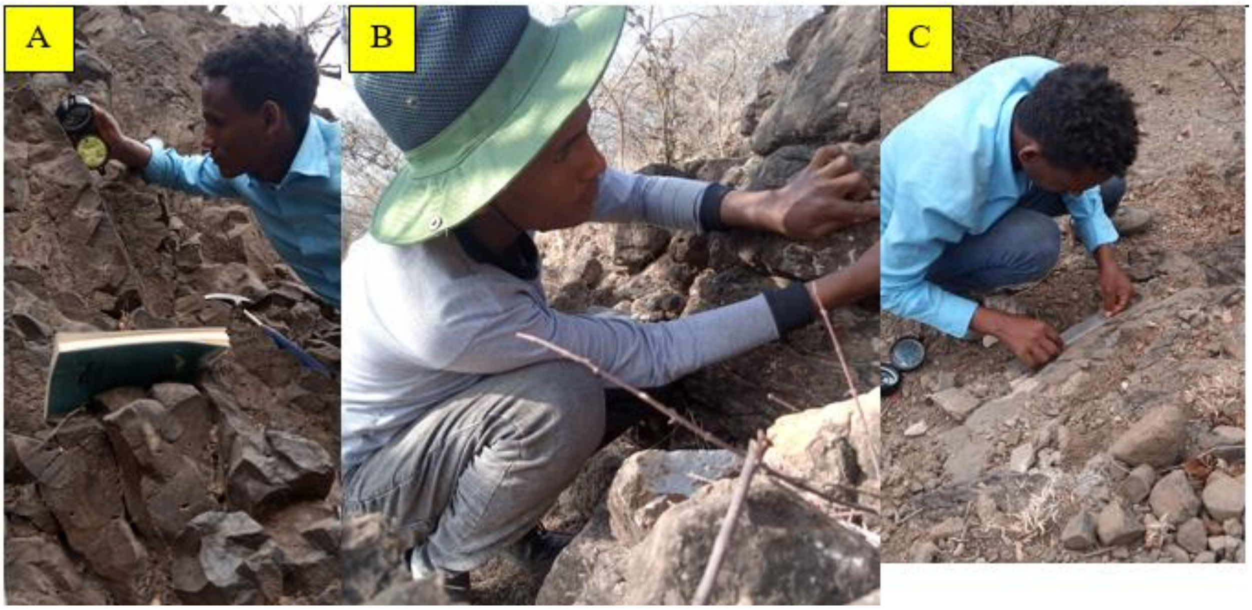

Figure 3. 1 Discontinuity survey from abutments and reservoir: A) Measuring dip direction and dip amount using Brunton compass, B & C Measuring discontinuity characteristics using ruler.

3.2.1 Sampling

For various laboratory tests, disturbed soil samples and rock samples were taken from the test pit and exposure, respectively (Figure 3. 2 and Appendix 1). Four test pits with a maximum depth of 2.5 meters were dug (TP-1, TP-2, Tp-3 and TP-4), which were discovered in the study area. To preserve the soil samples' natural moisture content, they were collected and placed in a plastic bag. In addition rock sample were collected from dam axis and reservoir area. Furthermore, engineering properties were used to describe the rocks that make up the dam site and reservoir area. Following that, rock samples were taken for laboratory testing from the surface exposure.

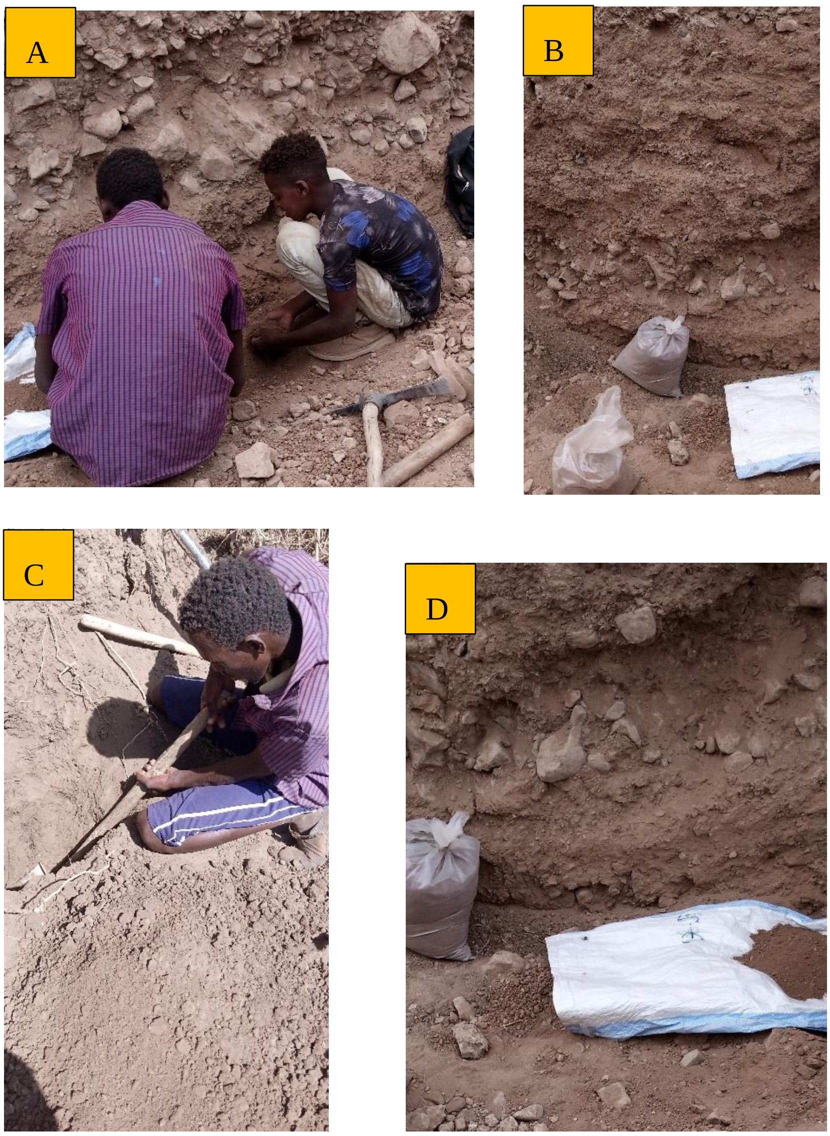

Figure 3. 2 Soil sample from test pit A) TP-1, B) TP-2, C) TP-3 and D) TP-4

3.3. Laboratory Testing

3.3.1 Laboratory Test for Soil

Natural moisture content, particle size analysis (sieve and hydrometer analysis), specific gravity, Atterberg limit (liquid and plastic limit), and permeability are a few of the laboratory tests performed on soil samples. The tests were carried out in the Geotechnical Laboratory of Ethiopian Construction Design and Supervision Works Corporation.

3.3.1.1. Grain Size Analysis Test

The grain size analysis for each soil sample was carried out according to the ASTM D 422 (1998) standard. This test method is used to determine the quantitative distribution of particle sizes in soils. Sieving determines the distribution of particle sizes bigger than 75µm (retained on the No. 200 sieve), while sedimentation and hydrometer analyses determine the distribution of particle sizes lower than 75µm. Accordingly, the test was performed in the laboratory using the following procedure: Using a hammer and pestle crushing apparatus, dry soil samples were prepared and crushed into appropriate small sizes. The pan was placed at the bottom of all sieves after a stack of sieves was cleaned with a brush and a set of sieves was positioned gradually with the narrower aperture from the top to the bottom. The test was then conducted for 15 minutes, with the soil retained on each sieve and pan measured using a balance. A hydrometer was used to evaluate the soil sample left on the pan. Finally, the recorded data were analyzed on an excel spreadsheet, and the grain size distribution curve was drawn as a result of the analysis (Figure 5. 12).

3.3.1.2. Atterberg Limit Test

To assess the plastic limit (PL) and liquid limit (LL) of fine-grained soil and to classify fine-grained soil, according to the Unified Soil Classification system, an Atterberg limit test is used. The test was carried out in accordance with ASTM D 4318 (1998). The test was conducted in the laboratory as follows. Part of the soil sample that passed through sieve #40 (0.425mm aperture size) was placed in an evaporating dish for the liquid limit test. Distilled water was added to the soil sample and mixed to form a uniform paste with the help of a spatula,, which was then applied to the cup of the liquid limit device to make a smooth surface paste of soil and divide it into two halves, which was then done by rotating the handle at a rate of 2 revolutions per second in range of 15 to 35 number of blow until the soil cake came into contact with the bottom of the groove over a distance of approximately 13mm. The number of blows required to close the two halves of soil specimen by 13mm was recorded. The representative sample was collected from the flow part and placed in moisture Cans, measured the mass and oven dried for 16 hours at 105°C for calculating water content. Finally, each soil sample data were recorded and examined.

Similarly, a portion of the wet sample of liquid limit testing was taken, and the sample was placed on the glass plate and rolled with the finger to form a uniform diameter thread. The thread was crumbled after being rolled to a diameter of 3mm. The crumbled soil sample was collected in cans, weighed using a mass balance, and then baked for 16 hours at 105°C. Finally, the moisture cans were removed and each sample data were recorded and examined. The plasticity index (PI) was calculated using equation 13 once the liquid and plastic limits were obtained.

3.3.1.3. Moisture Content Test

A moisture content test was conducted according to ASTM D 2216 (1998) standard by oven drying method. Accordingly mass of the wet soil sample was weighted and put in oven-dried for 24 hours at 105$_0$C and then the weight of oven-dried soil samples was recorded. Finally, natural moisture content was determined using equation 14.

$$w = \frac{M1 - M2}{M2} * 100\% \qquad (14)$$

Where w is natural moisture content (%), M1 is the mass of wet soil sample and M2 is the mass of soil after oven dried.

3.3.1.4. Specific Gravity Test

Using a pycnometer, the test was carried out according to (ASTM D 854 (1992). Accordingly, the following procedure was followed in the laboratory. Before beginning the test, weigh the empty, clean and dry pycnometer (WP) with a digital balance, then add 10g of oven dried soil sample that passed through sieve #10 in the pycnometer, then weigh the pycnometer containing the dry soil sample again (WPS). Add distilled water to the pycnometer water to the level somewhat above the soil sample and soak the sample for 10 minutes and the entrapped air was removed by boiling technique. After that, fill the pycnometer with distilled water to the mark and then determine the weight of the pycnometer that contained soil and water (W_B). Then the pycnometer was emptied and cleaned and fill it with distilled water only to mark and measure the weight of the pycnometer and distilled water (W_A). Finally, specific gravity (Gs) was determined using equation 15 as follows;

$$Gs = \frac{W0}{W0 + (WA - WB)} \qquad (15)$$

Where W_0 is the weight of the sample of oven dry soil.

3.3.1.5. Permeability Test

The test was carried out in accordance with ASTM D 2434 (1994). The constant head approach is used to determine the coefficient of permeability in this test procedure. The soil sample was compacted in a typical mold and totally saturated with 2000kpa pressure, which was utilized to pump water into all regions of the soil sample and fully saturated the soil. After that, collect the water that has passed through the soil sample and keep track of the time. Using Darcy's Law, calculate the coefficient of permeability of the soils using equations 11 for the length, L, and cross-sectional area, A, in time, t, and a head, h which remains constant throughout the test.

***3.3.1.6*. Direct Shear Test**

The resistance of soil to shearing stress determines its strength. It is primarily caused by two factors: friction between individual particles and particle adhesion (cohesion). At optimum moisture level, the test was conducted using an ASTM D 3080 compacted soil sample in a 60*60*20mm mold. After placing the specimens in the shear box, the shear force loading system was attached to them and configured to measure horizontal and vertical displacement. The shear stresses for various normal stresses were recorded, and the shear strength parameters were calculated from the plot of shear stress vs. normal stress (Appendix 10).

3.4. Laboratory Test on Rock

The laboratory tests on rock were carried out in the Geotechnical Laboratory of the Ethiopian Construction Design and Supervision Works Corporation. The laboratory tests on rock samples conducted were point load tests and unit weight tests.

3.4.1. Point Load Test

The intact rock's uniaxial compressive strength was determined by point load strength tests. The test is also used as an index for determining rock strength classification. To measure the strength of irregular rock samples, the test was conducted according to ASTM D 5731 (1995) standards. The test was carried out on uneven rock samples with natural moisture content. Irregular rock samples were processed into the appropriate size using a geological hammer. The point load strength is defined as the peak pressure at failure. Finally, using equation 5, the average value of corrected point load strength was converted to the rock's uniaxial compressive strength.

3.4.2. Unit Weight Test

The unit weight was calculated on irregular rock samples using buoyancy techniques according to the standard proposed by ASTM D7263 standard. The test was carried out on a total of 4 irregular rock samples collected from both dam abutments, with the average used for slope stability analysis and rock strength determination. The following are the test procedures used during the unit weight test.

- The rock samples were oven-dried for 24 hours at 105°C and then the dry weight (M) was recorded.
- The rock samples were then immersed in water for 24 hours to saturate with water and the saturated weight recorded.
- The saturated samples immersed in water and volume of displaced water recorded, which is equal to the volume (V) of the rock sample.

The density of the rock sample was calculated from the ratio of mass to volume as follows: $\rho = \frac{M}{V}$ and $\gamma = \rho g$. Where ρ is density of rock sample (gm/cm^3), M is the mass of rock sample (g), V volume of rock sample (cm^3), γ is the unit weight of rock sample (KN/m^3) and g is the acceleration due to gravity ($9.81 m/s^2$).

3.5. Data Analysis and Processing

3.5.1. Rock mass classification

In this study, rock mass rating system (RMR) proposed by Bieniawiski (1989) and Geological Strength Index (GSI) (Marinos and Hoek (2000) has been utilized to work out the shear strength parameters. To determine RMR value five basic parameters were used. These are Uniaxial Compressive Strength of the rock (UCS), Rock Quality Designation (RQD), the condition of discontinuities, the spacing of discontinuities and groundwater condition. For rock mass classification, the Uniaxial Compressive Strength of the Intact Rock (UCS) determined from the point load test is chosen. In addition, RQD calculated in the field was utilized to classify the rock quality discovered at the dam site.

Selecting a representative slope segment and measuring the area with one square meter of rock mass is the first step in determining RQD. The number of joint sets in the chosen area, as well as the number of joints in the joint sets, were then determined. Finally, equation 4 was used to calculate Jv values, while equation 2 was used to calculate RQD values. Finally, descriptively obtained rock mass classification parameters were transformed into rated parameters, and the RMR value was determined.

The Geological Strength Index (GSI) was calculated using equation 7 and a visual assessment of the rock mass to characterize the rock mass condition according to the Hoek and Marinos (2000) GSI basic charts. The result of GSI values was used in the RocData software for determination of shear strength parameters.

3.5.2. Estimation of Rock Mass Shear Strength and Deformation Parameters

RocData software was used to calculate the shear strength parameters (cohesion and friction angle) and modulus of deformation of the dam site rocks using Generalized Hoek-Brown Failure criteria (Hoek et al., 2002). To evaluate the Geo-mechanical properties of rock masses, this software uses GSI, the material constant of intact rock (mi), UCS of intact rock, and disturbance of factor (D). In addition, unit weight of rock (γ) and slope height (H) were also required in the RocData software for application of slopes. Finally, the software expressed the shear strength parameters in terms of the cohesion (c) and friction angle (ϕ). The result (output) from RocData software was used for input parameters to slope stability analysis.

3.6. Slope stability Analysis Method

The critical slope section of this study is structural controlled and non-structural controlled. Hence, kinematic analyses were carried out for the structurally controlled slope sections. Limit equilibrium method was used to slope analysis for non-structural control and structural control which is for planar and wedge mode of failure.

3.6.1 Kinematic Method

These methods rely on the detailed evaluation of rock mass structure and the geometry of existing discontinuity sets that may contribute to block instability. This technique uses the dominant discontinuity planes within slope mass to forecast the probability of failures. This assessment was carried out by using stereonet plots or Dips software (Rocscience, 2004). The dips software allows for the visualization and determination of the kinematic feasibility of rock slopes using friction cones and daylight envelopes and also graphical and statistical analysis of the discontinuity properties (Eberhardt and Vancouver, 2003). In this study kinematic analysis of rock slopes was conducted for structurally controlled failure using Dips 6.0 software (Rocscience, 2004). From kinematic analysis mode of failure was identified for further analysis by limit equilibrium methods.

3.6.1. Limit Equilibrium Method

In this study, LEM was used to stability analysis for both structurally and non-structurally controlled slope section by using RocPlane, Sewdge and Slide software (Rocscience, 2004). Accordingly, stability analysis for the structurally controlled slope sections RAS2 was undertaken by using RocPlane and sewdge software where the possibility of kinematic instability had been identified.

The failure surface tends to follow a circular route when rock slopes are highly weathered and soil mass deposits (Norrish & Wyllie, 1996). In this study, the LEM was used for stability analysis by using Slide software (Rocscience, 2004). In slide software to conduct slope stability analysis first created the external boundary using slope geometry from the field, then created the material boundary.

The slide software takes input parameters such as shear strength parameters (cohesion and friction angle) that were estimated in the RocData software. In addition, the unit weight of rock which determined in the laboratory, slope geometry which determined in the field, and external forces (groundwater and seismic load) were considered as input parameters for slide software. The factor of safety was determined by Spencer method.

3.7. Water Tightness Evaluation Method

Laboratory permeability testing of the soil sample, surface hydraulic conductivity estimation from discontinuity aperture and spacing, water tightness model, and in-situ permeability tests were used in the water tightness analysis.

To determine the coefficient of permeability of the soil deposits in the reservoir area, a laboratory permeability test was carried out on four representative soil samples collected from the test pits. Equation 9 is used by Snow (1965) and Louis (1974) to determine the hydraulic conductivity of exposed rock mass in dam abutments and reservoir areas. During the data collection for the discontinuity survey, special attention was given to the orientation of joints that were favorable to leakages. Furthermore, based on factors such as topography, geology, groundwater condition, rainfall/climate condition, hydraulic conductivity of lithological units, and reservoir design of maximum full supply level, the water tightness model was used to evaluate and confirm the area of potential water leakage after impoundment. Furthermore, the water tightness of dam abutments was assessed by OWWDSE (2021) utilizing a water pressure test.

In addition the water tightness model is used to evaluate site characteristics and factors to draw an inference on potential leakage and identify potential areas of leakage. The model was drawn at left and right abutments and reservoir area. As Fell et.al. (2005) stated the model is considering non-soluble rock of the study area. Based on the constructed model the water tightness of the area was evaluated.

The detailed methodological approach used in this study is indicated in the following flow chart (Figure 3. 3).

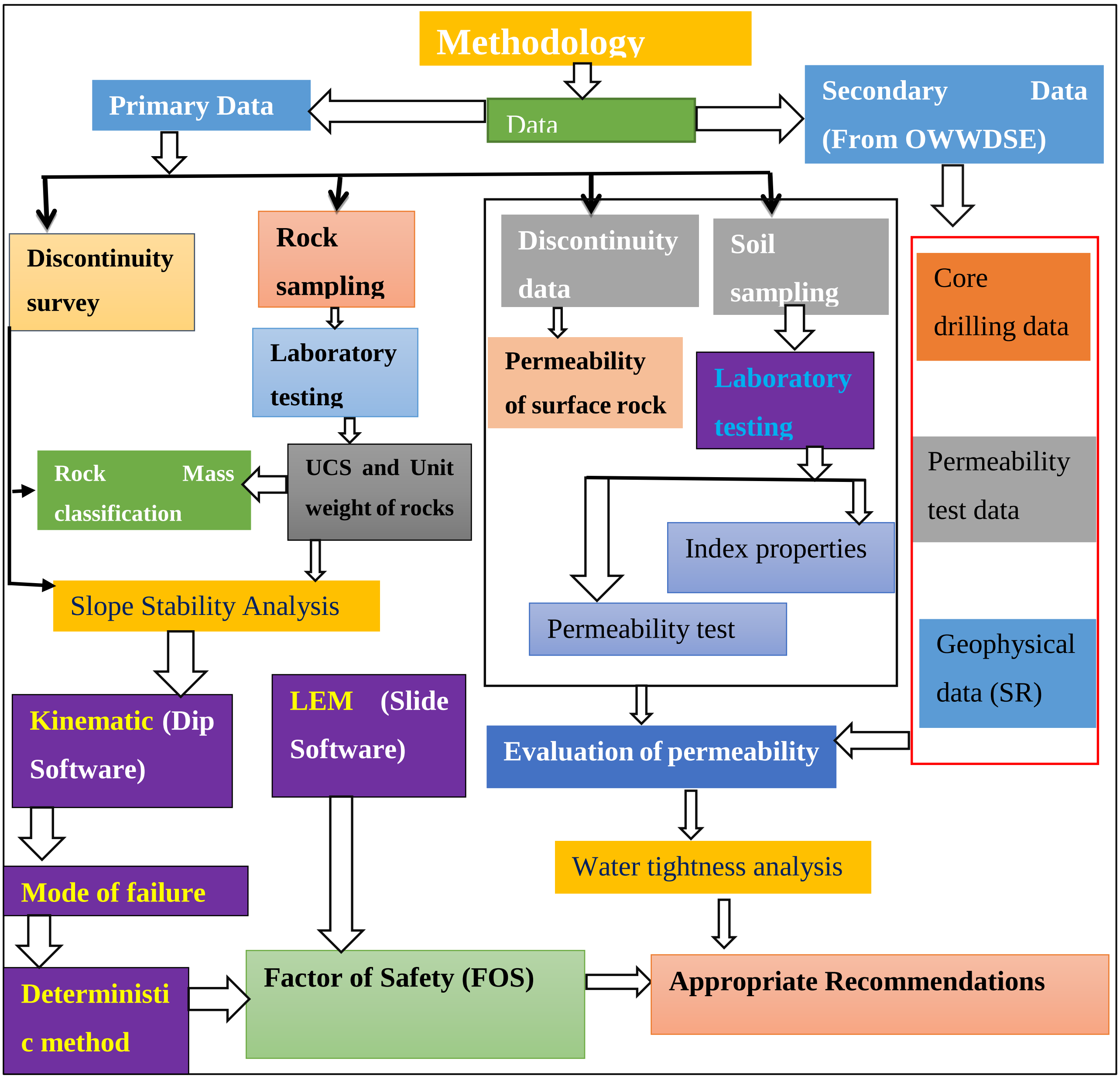

Figure 3. 3 The general Flowchart showing a methodological framework of the study

3.8. Material Used

Both laboratory and field equipment were used in this research project. GPS, compass, geological hammer, chisel, sample bag and tape meter were among the field equipment used for data collection, measurement, and testing. The index and engineering properties of soils were determined using soil mechanics laboratory equipment. The strength of intact rock was determined using a rock laboratory analysis (point load) instrument. For mapping and processing different Geotechnical data, multiple softwares such as Arc GIS 10.4, Strater 5, Surfer,Dips 6, RocData, Rocplane, Sewdge and Slide 6.0 software were used.

CHAPTER FOUR

4. GEOLOGY OF THE STUDY AREA

4.1 Regional geology

The location is situated in the rift, and the geology is complex on a regional scale. Tertiary volcanic rock groups and Quaternary to Recent sediments characterize the majority of the area's highlands (Zanettin et al., 1979) (Figure 4. 1). Pliocene and Pleistocene volcanic rocks, such as Rhyolite, trachytes, and ignimbrites, are prevalent in the rift floor and adjacent plateau (Kazmin, 1975).

The eruption of the Oligocene - lower Miocene Alaji volcanic pre-dates the opening of the northern part of the Ethiopian rift and Afar, according to the regional geological map (Kazmin & Seifemichael, 1978). The Miocene basalts form the upper section of the Ethiopian traps' general succession, with the oldest being Eocene in age. It was deduced that the thickness of Miocene basalt increases toward the rifts since it is thicker in Ethiopia than on the southeastern plateau. The Alaji basalts are conformably overlain by a unit of flood basalts and siliceous rocks along the rift's eastern margin, which is in turn overlain with slight unconformity by silicic volcanic of the Nazret Group. Nazret Group (Ignimbrites, unwelded tuffs, ash-flows, rhyolites, and trachytes) make up the majority of the rift floor, as well as the rift escarpments and surrounding plateau borders (Kazmin & Seifemichael, 1978). The rift floor has a thicker layer of its formation than the escarpment. According to Kazmin & Seifemichael, (1978) the formation of the shield volcanoes on the rift's eastern shoulder coincided with the accumulation of the Nazret Group.

The Anchor Basalt and Arba Guracha silicic (14-10myrs) began accumulating within the area bounded by rift escarpments 14myrs ago, resulting in the formation of these rifts (Kazmin & Seifemichael, 1978). The unit is characterized in the Anchar area by around 400m of basalts with multiple intercalations of ignimbrites, the oldest of which is 12.4 Myr old (Kazmin & Seifemichael, 1978). The basalt is laterally replaced by welded and unwelded ash flows to the south and northeast, and the section is essentially or entirely silicic in a Guracha valley in the vicinity of Asabe Teferi (Kazmin & Seifemichael, 1978).

The oldest Ignimbrite from the Wonji group, a volcanic assemblage associated with the axial zone, is 1.5 million years old (Kazmin, 1975). The Dino ignimbrite covers a large area of the rift floor and consists of several flows of compact Fiamme ignimbrites intercalated with aphyric basalt and pyroclastic in some locations. It is 1.5 million years old and lies atop Bofa Basalts with a paleosol horizon at the base.

According to the regional geological map (Nathret sheet NC37-15, 1:250,000, 1978) the geological unit includes volcanic unit (Alaji Basalt, Anchar Basalt, Arba Guracha silicic, Arba Gugu Basalt, Bofaa Basalt, and Wonji group). As shown in Figure 4. 1 the geologic unit of the study area most dominated by Anchar Basalt.

4.2 Regional Geological Structures

The project region is located on the Main Ethiopian Rift (MER), which is part of the East African Rift System. It runs over around 500 kilometers in a NE-SW direction through Ethiopia, serving as a link between the Afar triple junction to the north and the East to the south, as well as the extensively rifted zone in southern Ethiopia. The MER exhibits a wide range of fault architecture, volcanism, deformation timing, crustal and lithospheric structures along its axis. Many scholars as cited in Kazmin & Seifemichael (1978) divided the MER into three segments, the Northern, Central, and Southern MERs, each with its own structural pattern.

The Northern MER extends from the southern Afar depression in the northeast to the region of Lake Koka and Gedemsa caldera showing a roughly NE-SW trend (Boccaletti et al., 1998 as cited in Kazmin & Seifemichael, 1978). Two different normal fault systems (Mohr, 1962; Mohr and Wood, 1967; Gibson, 1969; Boccaletti et al., 1998; cited in Kazmin, 1975) characterize the structural development and thus evolution of MER. They differ in terms of orientation, structural characteristics (length, vertical throw), timing of activation, and relationship with magmatism (Mohr, 1962; 1967; cited in Kazmin, 1975). These are the border fault system and the Wonji fault Belt, a system of faults that affects the rift floor (WFB). Fault slip data from border faults reveals a stress field with an extension direction around ESE-WNW and local variation between E-W and NW-SE (Boccaletti et al, 1992, 1998; cited in Kazmin & Seifemichael, 1978).

The Ethiopian rift's eastern boundary occurs at a latitude of 8^0 20^0 N and has a smaller displacement. These faults run parallel to the Arsi plateau's northern boundary, swinging gradually from east to west to northeast and southeast (Kazmin & Seifemichael, 1978). As they discussed the rift escarpment runs northeast (045^0) and forms obtuse angles with sub latitudinal lineaments. Easterly or east-northeasterly winds are well-known in the eastern African basement, and it's conceivable that these lineaments shaped the rift system's form, such as the southern escarpment of Afar and the Gulf of Aden. Also, they have said northerly and northeasterly strikes, on the other hand, are hallmarks of Ethiopia's Precambrian basement, and it has been proved that the rift escarpment there follows major Precambrian faults in some cases.

Plate tectonic reconstructions demonstrate that the relative Africa-Somalia motion is north west-southeast, which is almost right angles to the rift's north easterly portions and at a sharp angle to the easterly section, which produces smaller extension. In the northern half of the Ethiopian rift, many zones of significant quaternary volcano-tectonic activity can be identified (Kazmin & Seifemichael, 1978). The rift escarpment has a number of tiny northwesterly trending transverse faults and fractures (Kazmin & Seifemichael, 1978).

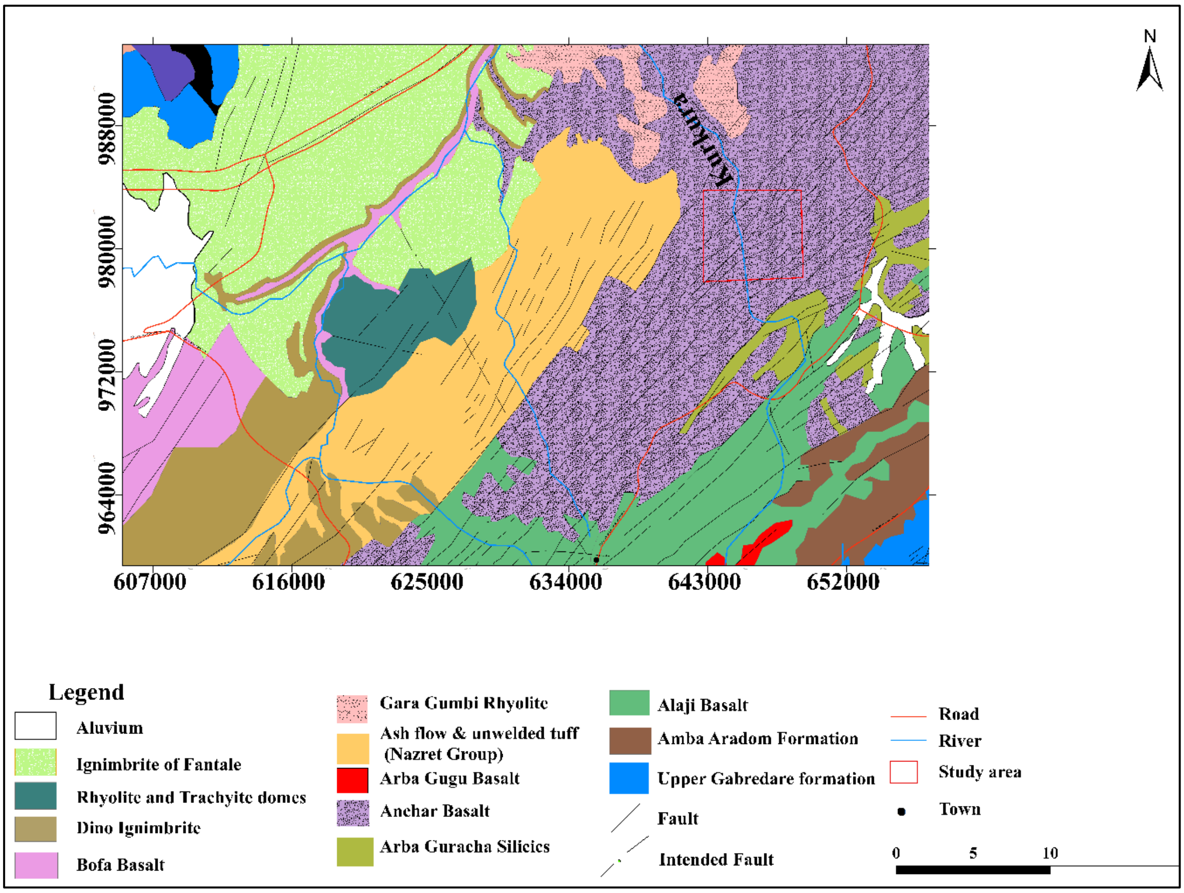

Figure 4. 1 Regional geology of the study area (after EGS 1978)

4.3 Local geology

The geology of the study area and its surrounding is dominantly covered with tertiary volcanic rock (Basalt and Rhyolite) and quaternary soil deposits such as alluvial, fluvial (Figure 4. 5) and colluvial soil. The tertiary volcanic rocks are exclusively exposed at both right and left of the river. Soil deposits are covering the slopes of the abutments and reservoir rims. The lithological units that exposed in the study area are described below:

4.3.1 Alluvial soil

These deposits are dispersed in the study area following the intermittent rivers. They are mainly represented by sand, silt, gravels and cobbles. The major components of the gravel and cobble grains are basalts with few felsic rocks. This deposits display rounded to sub-rounded fragments of parent rocks indicating abrasion during transportation. These deposits also extensively exposed on the upstream and downstream of dam axis on the both right and left bank of the river (Figure 4. 5). It is unconsolidated sediment and very fine. It is light brown to dark brown in color and consists of fine grain size.

4.3.2 Colluvial deposit

The colluvial deposit covers the slopes and feet of the slopes of the ridges bounding the river valley. It is formed by erosion of slopes and deposited by the action of gravity to the base of abutments. The sediments are scattered all over the feet of the ridges. It consists of variable grain of soil particle which range from fine (clay/silt) to coarse (gravel/boulder). The deposit occurs at the foot of the ridge forming the abutment of the dam site and also at the foot of the ridge forming landscape in the reservoir area from the right side of the river.

4.3.3 Residual Soils

These soils covers a large area of the study area and exclusively found on the left abutment of the dam site (Figure 4. 5). The wide area of the farmland at the side of left abutment is covered by the residual type of soil. It consists of variable grain size particles ranges from fine to coarse with a mixture of cobbles of basalt. It is characterized by brown to whitish brown color. From the borehole data obtained (OWWDSE, 2021) the thickness of the soil range from 10 – 15m. These soils are formed by weathering (chemical and physical) of the parent basaltic rock at its origin and it forms gentle slope that used to farm.

4.3.4 Basalt

This rock unit is exposed in the study area on both right and left sides of Kurkura River. It is highly exposed in the spillway due to excavation of up to 10m by contractors of the Gololcha dam project. This geological unit forms the right-side bounding ridge (right abutment and right reservoir rim) of the gorge and appears forming a small ridge at the left abutment of the dam site (Figure 4. 5). It is highly fragmented and fractured at the exposed site in the reservoir area as well as on both right and left abutments of the dam. The unit is affected by pervasive jointing and fracturing. It is characterized by dark grey fresh colour and reddish to brownish weathered colour, moderate degree of weathering, aphanitic texture and highly fractured Figure 4. 2.

Figure 4. 2 Basalt exposure (A) exposure from the spillway and (B) exposure from the right abutment of dam axis moderately to highly weathered

4.3.5 Rhyolite

This rock unit is exposed at the left abutment on downstream of the dam axis (Figure 4. 5). It forms typically cliff and rugged topography as compared to the underlying sedimentary unit. It is characterized by high degree of weathering. The unit is frequently affected by intense vertical jointing (Figure 4. 3). It is fine grained and characterized by light creamy to grey colour, darkish brown colour on weathered surfaces. It can be a potential source of construction material for the dam as it is located closer to dame site.

Figure 4. 3 Rhyolite exposure from downstream of left abutment

4.4 Geological structures

The major geological structures observed in the area include lineaments, faults, fractures, and joints.

4.4.1 Faults

As discussed in literature review the study area is located in Ethiopian rift system and the major fault strike to NE- SW direction, which is parallel to dam axis. In the study area the valley and ridges aligned in NNE- SSW direction parallel to the rift orientation. There is also additional fault which orient in NW- SE direction (Figure 4. 5), which is perpendicular to dam axis.

4.4.2 Lineaments

Fault-controlled valleys, mountain or hill ranges, ridges, and isolated hill lines are examples of large-scale topographic features. In the examined region, several lineaments influence stream and river flows, as well as the alignment of ridges. They are typically straight to curved with varied lengths and have general NNW and infrequently N-S tendencies (Figure 4. 5).

4.4.3 Joints

In the study area, the joints are observed on exposed rock mass in dam abutments, reservoir rims and in excavated spillway area. The strike orientation and properties (persistence and spacing) of the joints are very complex, since the rock masses are highly fractured as shown in Figure 4. 4B, C&D. whereas, at excavated spillway area there is horizontal and vertical joint set as shown Figure 4. 4A.

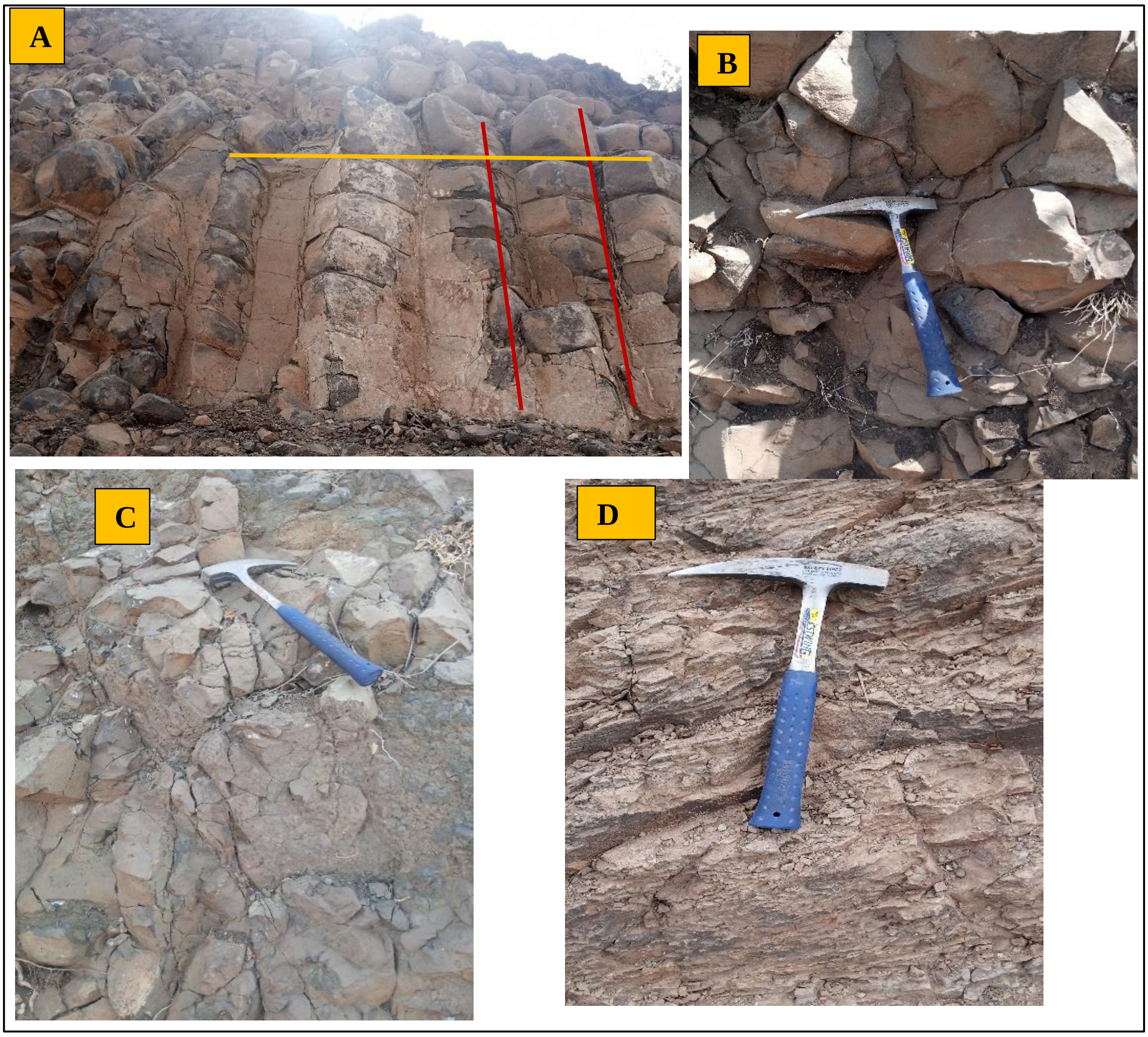

Figure 4. 4 Different joints at (A) Spill way, (B & C) right abutment and (D) left reservoir rim

From the field, observed joints have different strike orientation, closely spaced and open to fill by fine material. The major joints strike orientation are NE – SW, NW – SE, and there is also some strike orientation NNE – SSW and ENE – WSW (Figure 4. 5A).

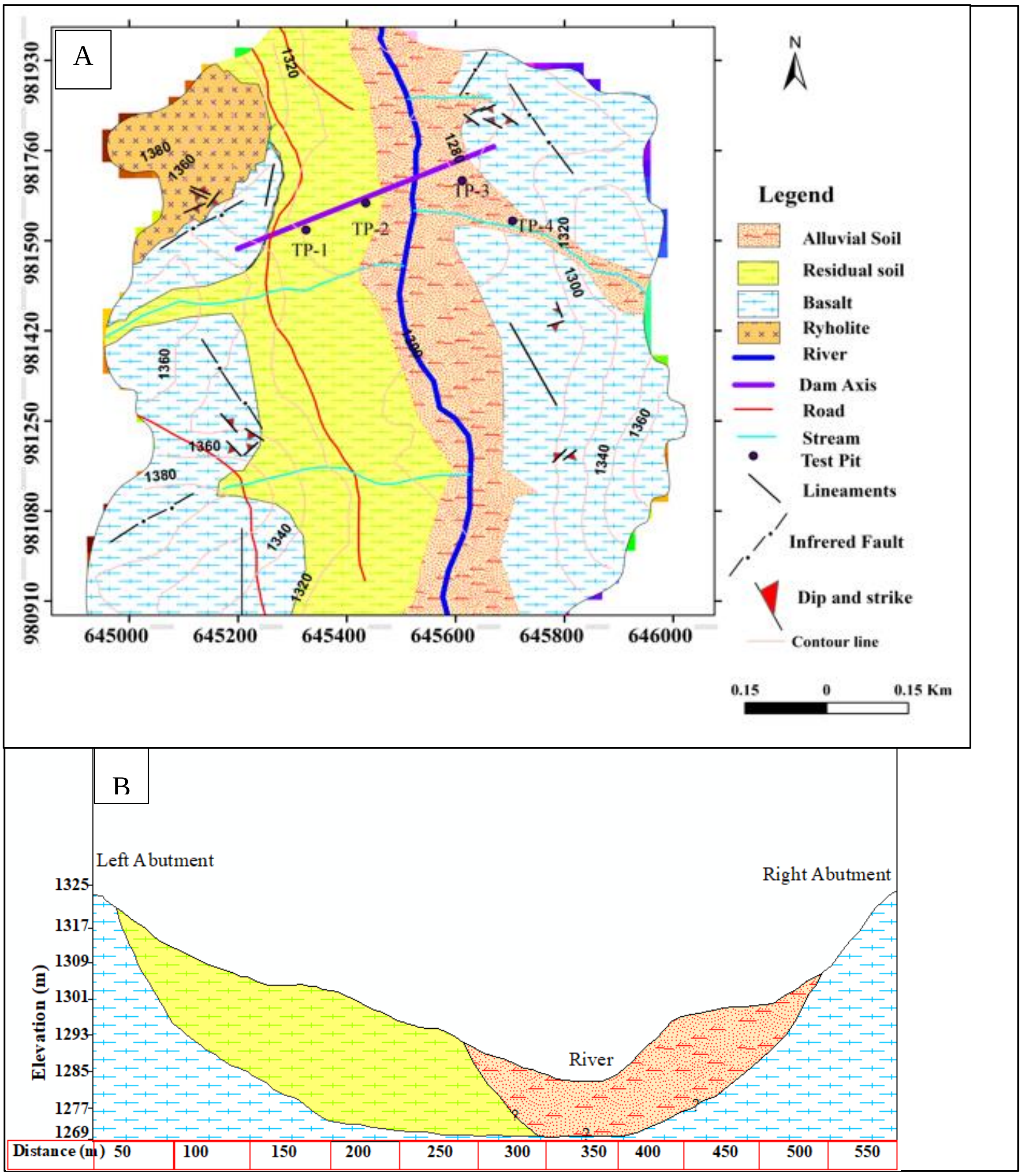

Figure 4. 5 A) Geological map of the study area at scale of 1:8000 and B) geological cross-section along the dam axis.

CHAPTER FIVE

5. RESULTS AND DISCUSSIONS

5.1. Description and Characterization of Geology of the Area

The project area is characterized by a wide river valley bounded by ridge and partially elevated ground. The elevation of the ground is moderately steep to highly steep on the right side of the Kurkura River and gentle to less steep on the left side of the river. These gently to steep ground of the study area is composed of different types of lithology; volcanic rock and recent sediment deposits. The volcanic rock observed in the area is basaltic and rhyolite. The basaltic rock, which is exposed in the area is highly fractured, jointed, and weathered. In addition to basalt, the rhyolite that is exposed in the study area from downstream of the dam axis and adjacent to the ridge from upstream is highly weathered and jointed. The joint in rhyolite rock is open without filling with secondary material.

The safety of a hydraulic structure such as a dam is dependent on the behavior of rock mass exposed in the area. To assess the suitability of the area for intended purpose, a detailed investigation was conducted in the area of dam axis and reservoir area. Field work and laboratory test were carried out for surface rock mass characterization. Accordingly, the rock exposed in the area were identified through detailed investigation. From the discontinuity survey, the result obtained is used to determine the RQD of surface rock mass and permeability of rock mass. The area that covered by rock is characterized by highly discontinuous with high degree of fractures and slightly - highly weathered. Furthermore most joints of rock in the dam site and reservoir area is closely spaced, moderately tight and partially filled of fine materials. In addition gently slope of the dam axis of the area is covered by soil, which contains the cobble of basalt and rarely rhyolite.

5.1.1. Characterization of surface rock mass

Characterization of rock mass from surface exposure has been carried out through field data collection, laboratory test on collected representative samples and interpretation of field data and laboratory test result. The characterization is mainly based on physical and engineering properties of the rocks, discontinuity properties/characteristic, laboratory test result of representative rock sample, estimation of deformability parameters and strength of rocks, determination of RQD, hydraulic conductivity and engineering classification of rock mass.

5.1.1.1. Discontinuity survey

During fieldwork discontinuity data has been collected, in the outcrops of dam axis and reservoir area to characterize the rock mass condition and to determine hydraulic conductivity of rock masses. The discontinuity data collection was undertaken according to International Society of Rock Mechanics (ISRM, 1978) standards. The collected data include orientation, spacing, aperture, opening, infilling material and roughness. The data were interpreted with respect to determination of engineering properties of rock and water tightness of the study area.

The discontinuity survey was carried out on both left and right abutment of dam axis and its respective adjacent of reservoir rims. Nearly three discontinuity sets were identified on right abutment and four sets were observed on left abutment. The discontinuities on the right abutment and its adjacent reservoir rim dominantly orient NNE – SSW(J1), NE – SW(J2) and WNW – ESE(J3) (Figure 5. 1A), while on strike direction on left abutment of dam axis and its adjacent reservoir rim orient NW-SE (J1), NE – SW(J2), NNW-SSE (J3)and E – W(J4) (Figure 5. 1A). The orientation of the discontinuity is one factor of causing leakage problem in the dam project. From this study some discontinuity orientation have strike direction parallel (NNW – SSE) and nearly parallel (NNE – SSW) to the direction of water flow on the left abutment and right abutment of dam, that may highly favorable for leakage of water.

Furthermore, the characteristics of discontinuity are also the major factors that control leakage of impounded water in the reservoir area. As observed from the field, the discontinuity of rock mass of the study area is characterized by its low aperture, closed spacing, slightly to highly rough surface, empty (clean) to fine soil infilling materials, moderate to high degree of weathering, and moderate to long persistent (Table 5. 1). In addition to measurable discontinuity sets, there is also fractured characteristics of rock mass that cannot be measured in its orientation and other properties. The highly fractured and fragmented characteristics of rock mass is due to the intersecting of discontinuities. The intersecting properties of discontinuity and a high degree of weathering may increase the probability of leakage of water from a reservoir.

Table 5. 1 Summary of discontinuity characteristics

Discontinuity characteristics							
Location	Strike	Aperture(cm)	Spacing(cm)	Persistence(m)	Infilling material	roughness	Degree of weathering
Right abutment	NNE–SSW (J1)	0.8-3	15-24	0.5-1.5	clean	Rough	Highly weathered
	NE-SW (J2)	1-1.5	20-30	0.5 – 3	Fine soil	Rough	Moderately to highly weathered
	WNW-ESE (J3)	0.5-1.5	33-74	>3	Fine soil	Moderately rough	Moderately weathered
Left abutment	NW-SE (J1)	0.5-3	10-30	>1	Fine soil	Slightly – moderately rough	Highly weathered
	NE-SW (J2)	0.7-2	10-15	0.75 - 5	Clean	Moderately rough	Highly weathered
	NNW-SSE (J3)	0.5-1	15-40	>1	Fine material	Slightly rough	Highly weathered
	E-W (J4)	1-4	20-30	1 - 2	Clean	Rough	Highly weathered

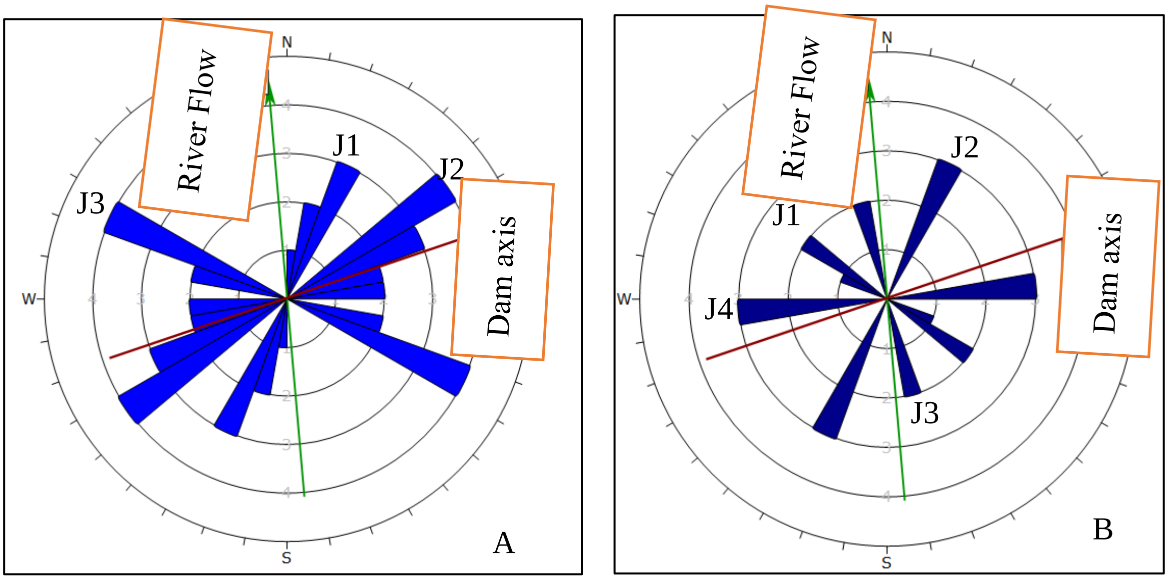

Figure 5. 1 Rosette diagram of discontinuity: A) Right abutment, and B) left abutment

5.1.1.2. Rock Quality Designation (RQD)

The surface rock mass quality was estimated from discontinuity frequency of exposed rock at dam abutment and reservoir area through volumetric joint count method (Equation 2) as proposed by Palmstrom (1982). The volumetric joint count (Jv) measurement has been calculated from joint spacing as described by Palmstrom (1982, 1985, 1986); and Şen & Eissa (1991). The measurement of Jv has taken place from total of 4 section, 2 from right side and 2 from left side; at the abutments and reservoir area. The result of average Jv value revealed that the area is characterized as high degree of jointing surface rock (Palmstrom, 2005). The average estimated RQD value on right (Abutment and reservoir rim) range from 31.55% to 45.22% (Table 5. 2). Similarly it range from 30.50% to 38.97% on the left (Abutment and reservoir rim) (Table 5. 2). Based on this, the rock exposed on abutments and reservoir slopes have poor qualities according to Deere (1968). This result indicates that the rock mass exposed in the study area are affected by numerous joints and fractures. In other words the rock exposed are highly fractured and jointed, that makes the rock falls in poor quality.

Table 5. 2 Estimated RQD value from volumetric joint count (Jv).

Observation location	**Jv and RQD%**		**Average Jv**	**Average RQD%**	**Rock quality According to Deere (1968)**
	Jv	**RQD%**			
Right abutment	24.74	33.36	25.29	31.55	Poor
	22.40	41.08			
	28.73	20.20			
Right side reservoir rim	24.20	35.14	21.15	45.22	Poor
	18.09	55.30			
Left abutment	25.14	32.04	23.04	38.97	Poor
	20.93	45.93			
Left reservoir rim	31.34	11.58	25.61	30.50	Poor
	19.88	49.40			

5.1.2. Laboratory Results for Rock Samples

A total of 6 irregular rock samples were collected from the dam's abutments and the reservoir area to determine point load strength and unit weight in laboratory. The point load test was performed on irregular rock samples in accordance with ASTM D 5731 (1995) guidelines to evaluate the uniaxial compressive strength of entire rocks using equation 5. As shown in

Table 5. *3*, the obtained UCS values of the rocks of the area vary from 69.46MPa to 146.97MPa, which are classed as medium strength to high strength (Deere and Miller, 1966).

Table 5. 3 Point load test results and the estimated UCS values

Rock Unit	Location	Sample code	$I_{(50)}$ (MPa)	UCS (MPa)	Classification based on (Deere and Miller, 1966)
Aphanitic basalt	Right abutment	RDA1	4.67	107.41	Medium strength
Aphanitic basalt	Right abutment	RDA2	3.02	69.46	Medium strength
Rhyolite	Left abutment	LDA1	3.67	84.41	Medium strength
Aphanitic basalt	Right abutment	RRA1	5.53	127.19	High strength
Aphanitic basalt	Reservoir area	RRA2	6.39	146.97	High strength
Aphanitic basalt	Right abutment	RRA3	4.46	102.58	Medium strength

The unit weight test was carried out on four irregular rock samples gathered from both dam abutment and reservoir area, and the test was carried out utilizing buoyancy techniques according to an ISRM (1978) standard. As shown in Table 5. 4, the unit weights range from 24.03KN/m^3 to 26.78KN/m^3, with the average value being 25.73KN/m^3. The unit weight results were used as input parameters for the rock slope stability analysis.

Table 5. 4 The result of laboratory measurements of rock unit weights

Rock unit	Sample code	Dry density (gm/cc)	Unit weight (KN/m^3)
Aphanitic basalt	RDA1	2.63	25.80
Aphanitic basalt	RDA2	2.45	24.03
Aphanitic basalt	RRA1	2.68	26.29
Aphanitic basalt	RRA2	2.73	26.78

5.2. Engineering Classification of the Rock Mass

To classify and identify the quality of the rock mass, engineers employ engineering classification. For rock mass characterization and to estimate the rock mass quality at the dam abutments, the two most extensively used rock mass classification methods, Rock Mass Rating (RMR) (Bieniawski, 1989) and Geological Strength Index (GSI) (Marinos and Hoek, 2000), were utilized. As we discussed in detail under section 3.5.1, the RMR system is made up of five basic factors that reflect various rock mass and discontinuity situations.

Based on the above mentioned basic discontinuity parameters and laboratory results, basic rock mass rating (RMR_{basic}) was conducted. As a result, the rock mass quality result from the dam site falls under fair rock, with rock mass rating values ranging from 44 to 55 (

Table 5. *5*).

Furthermore, GSI values were calculated from RMR using empirical equation 7 (Hoek and Brown, 1997), and the findings were compared to GSI values calculated from the field observation using (Marinos and Hoek's, 2000) quantitative GSI chart (Figure 2. 1). The value of the GSI of the rock mass was evaluated based on the condition of discontinuity surfaces and structures in the rock masses and was assessed at surface outcrops and excavated slope faces on the abutments. Accordingly, with GSI values ranging from 30 to 45, the rock mass on the right abutment can be characterized as blocky/disturbed/seamy and also with GSI value ranging from 40 to 55, while the rock mass on the right reservoir can be characterized as very blocky rock with moderately weathered. On the other hand, the rock mass on the left abutment can be classified as disintegrated to blocky/disturbed/seamy with GSI value of ranging from 25 to 35. The GSI value determined from RMR and estimated from field observation are summarized in Figure 5.6.

Table 5. 5 the dam site's rock mass rating (RMR) values and classification

Location		Right abutment		Reservoir area Following Right Abutment		Left abutment	
Discontinuity Parameters		Condition	Ra	Condition	Ra	Condition	Ra
USC(MPa)[a]		88.43	7	125.58	12	84.41	7
RQD(%)[a]		31.55	8	45.22	8	38.97	8
Spacing(cm)		23 – 43	10	20 – 28	10	14 - 20	8
Discontinuity condition	Aperture(cm)	1 – 2	0	0.93 -2.5	0	0.5 – 4	0
	Persistence(m)	1.5 - 3	4	1 – 1.75	4	3 – 4	2
	Roughness	Slightly rough	3	Slightly rough	3	Slightly rough	3
	Filling	Fine material	0	Fine material	0	Fine soil	0
	Degree of weathering	Highly weathered	1	Moderately weathered	3	Highly weathered	1
Groundwater cond.		Dry	15	Dry	15	dry	15
RMR rating values		48		55		44	
Class		III		III		III	
Description		Fair rock		Fair rock		Fair rock	
Where; Ra is Rating value, a is average value							

Table 5. 6Estimated GSI values of dam site.

Location	Rock units	RMR_{89}	GSI values determined from RMR_{89}	GSI range field estimation
Right abutment	Highly weathered aphanitic basalt	48	43	30 – 45 (38)[a]
Right reservoir	Moderately weathered aphanitic basalt	55	50	40 – 55 (48)[a]
Left abutment	Highly weathered aphanitic basalt	44	39	25 – 35 (30)[a]
Where **RMR** = rock mass rating and **GSI** = geological strength index, a = Average value				

5.2.1. Estimation of Rock Mass Strength and Deformation parameters

RocData software were used to estimate various geomechanical parameters of rock mass in this investigation. The Geological Strength Index (GSI), Uniaxial Compressive Strength of intact rocks, material constant of intact rocks (mi), Disturbance factor (D), slope height and unit weight of rock (γ) are all input parameters of the RocData software.

In this study, the GSI value was computed using equation 7 from the obtained RMR value and the last form of the quantitative GSI chart based on field observation. However, the GSI determined in the field was employed in the slope stability analysis. According to Hussian et al. (2020) GSI from field was used as the visual impression of the rock structure including block and surface condition of the discontinuities represented by joint characteristics (roughness and alteration) and providing reliable data in the form of rock mass strength properties which are used as input parameters.

The input parameters for RocData can be derived via laboratory tests, field data, and pre-built databases in software. The Uniaxial Compressive Strength of Intact Rocks (UCS) and unit weight of rock (γ) were obtained from laboratory tests. Since the dam abutment slope was excavated mechanically, the disturbance (D) value of 0.7 was considered, while mi value of 25 was considered for basalt from pre-built databases in RocData software (Table 5.7).

Table 5. 7 Values of input parameter for RocData

Location	Rock unit	Input parameters for RocData					
		σci (MPa)	GSI	mi	D	γ(MN/m^3)	H (m)
RAS1	Moderately weathered basalt	107.41	38	25	0.7	0.02580	65
	Highly weathered Basalt	69.46	38	25	0.7	0.02403	65
RAS2	Moderately weathered Basalt	102.58	38	25	0.7	0.02678	65
Where σci is the uniaxial compressive strength of intact rock, mi is rock material constant, GSI is Geological Strength Index, D is Disturbance factors, γ is unit weight and H is slope height. RAS1 and RAS2 right abutment slope section 1 and 2 respectively.							

The geomechanical parameters of rock mass, such as compressive strength, cohesion, friction angle, and deformation modulus, were determined using RocData software according to Hoek-Brown failure criteria (Table 5. 8 and Appendix 6). The results demonstrated that the strength of rock mass, cohesion, and friction angle are all affected by the degree of weathering.

Table 5. 8 Geo-mechanical properties of rock mass of Gololcha dam site

Slope section	Geo-mechanical properties of the rock mass (Output Parameters of RocData)						
	Mohr-Columb Fit		Hoek-Brown Constant			Rock mass parameters	
	C(MPa)	$\Phi(^0)$	mb	s	a	Em(GPa)	UCS(MPa)
RAS1	0.541	48.49	0.829	0.0001	0.513	3.257	1.069
	0.439	45.85	0.829	0.0001	0.513	2.715	0.691
RAS2	0.534	48.10	0.829	0.0001	0.513	3.257	1.021
Where C is Cohesion, ϕ is Friction angle, mb, s, and a are rock mass material constants, Em is the modulus of deformation, & UCS is Uniaxial compressive strength of rock mass.							

Since the cohesion value of the rock is ranging from 0.439MPa to 0.541MPa, the rock is classified as high strength according to Bieniawski (1989).

5.3. Characterization of Subsurface Rock Mass

Boreholes and geophysical survey results were used to determine the geotechnical properties of the subsurface rock mass and to conduct subsurface exploration at the Gololcha dam site. OWWDSE (2021) drilled a total of 4 boreholes at the main dam site, and along the proposed spillway to assess the condition of subsurface geology, groundwater level. The boreholes were used to verify the foundation conditions and conduct lugeon or water pressure tests, which determine the permeability of the subsurface rock masses, and they were located along the main dam axis and at both abutments. As a result, each borehole's geological state, rock-quality designation (RQD) values, and permeability of rock mass have been calculated.

5.3.1. Borehole logs

According to the drilled borehole, the lithological unit is uniform, with variations due to weathering and jointing. From left abutment there are two boreholes (GDBH-A01 and GDBH-A02), whereas from right abutment there also two boreholes (GDBH-A03 and GDBH-A04). Data logging for boreholes was developed as shown in Figure 5. 2&Figure 5. 3. The borehole log from GDBH-A04 reveals highly weathered aphanitic basalt up to 11 meters deep and moderately weathered basalt between 2 and 5 meters deep. Moderately weathered and highly fractured aphanitic basalt extends up to 30m depth. Furthermore, from 16m to 21m depth, highly weathered vesicular basalt transitions between moderately weathered aphanitic basalt (Figure 5. 2). Gravel, boulder, cobble, and blocks with fine material (soil) extend up to 13 meters from borehole GDBH-A03, moderately to highly weathered aphanitic basalt extends to 19 meters, and moderately weathered aphanitic basalt extends to 30 meters. Furthermore, aphanitic basalt that is fresh to slightly weathered and moderately fractured appears deeper than 30m depth of borehole (Figure 5. 2).

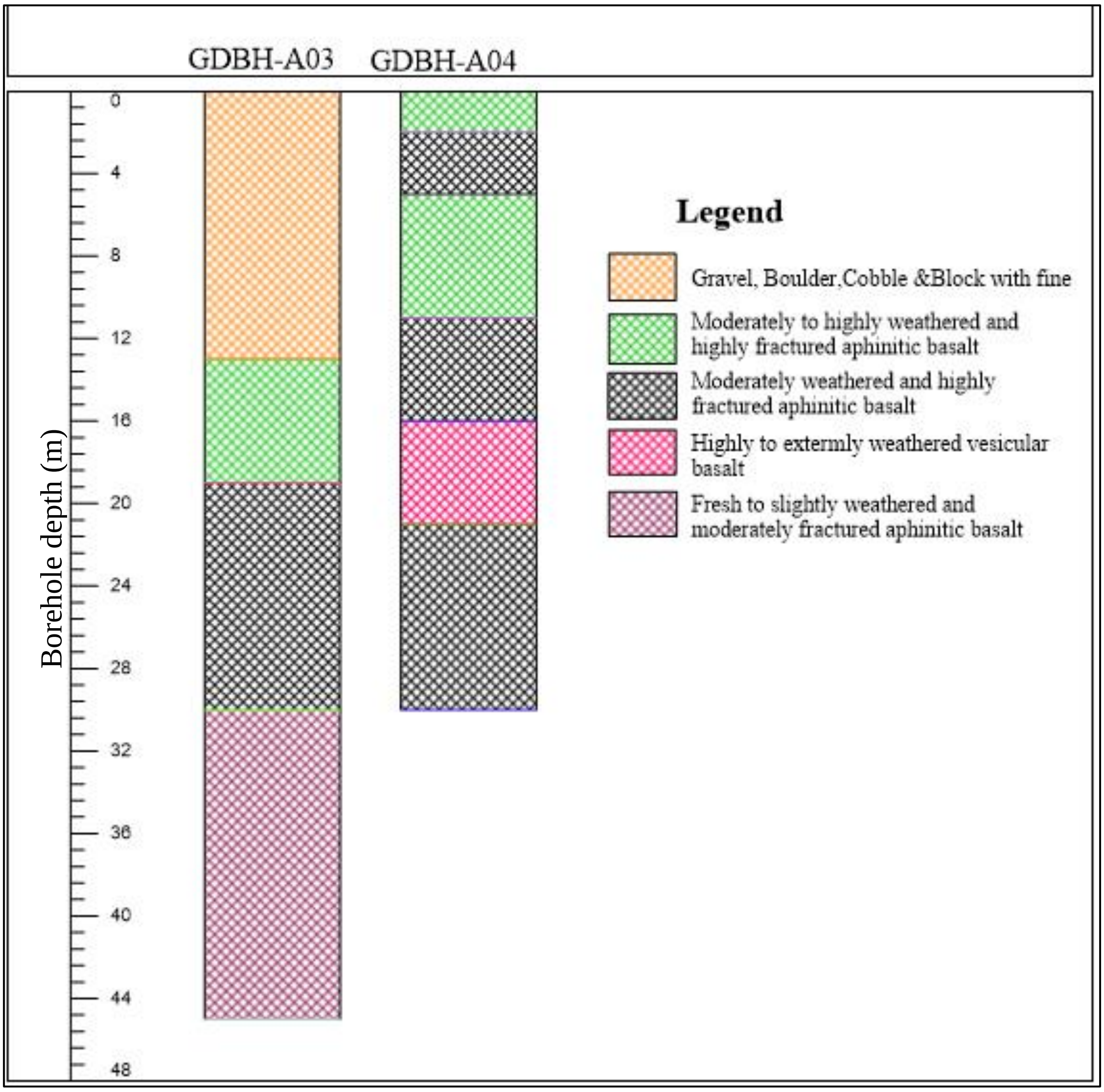

Figure 5. 2 Borehole log from A03 and A04 borehole at right abutment

At left abutment the area is mostly covered by soil containing gravel, cobble, boulders, and blocks that extends to a depth of 30m from borehole GDBH-A02. Gravel, boulder, cobble, and block with soil extend to a depth of 14m in the other borehole (GDBH-A01), and deeper of 14m, the lithology is moderately weathered and highly fractured aphanitic basalt (Figure 5. 3).

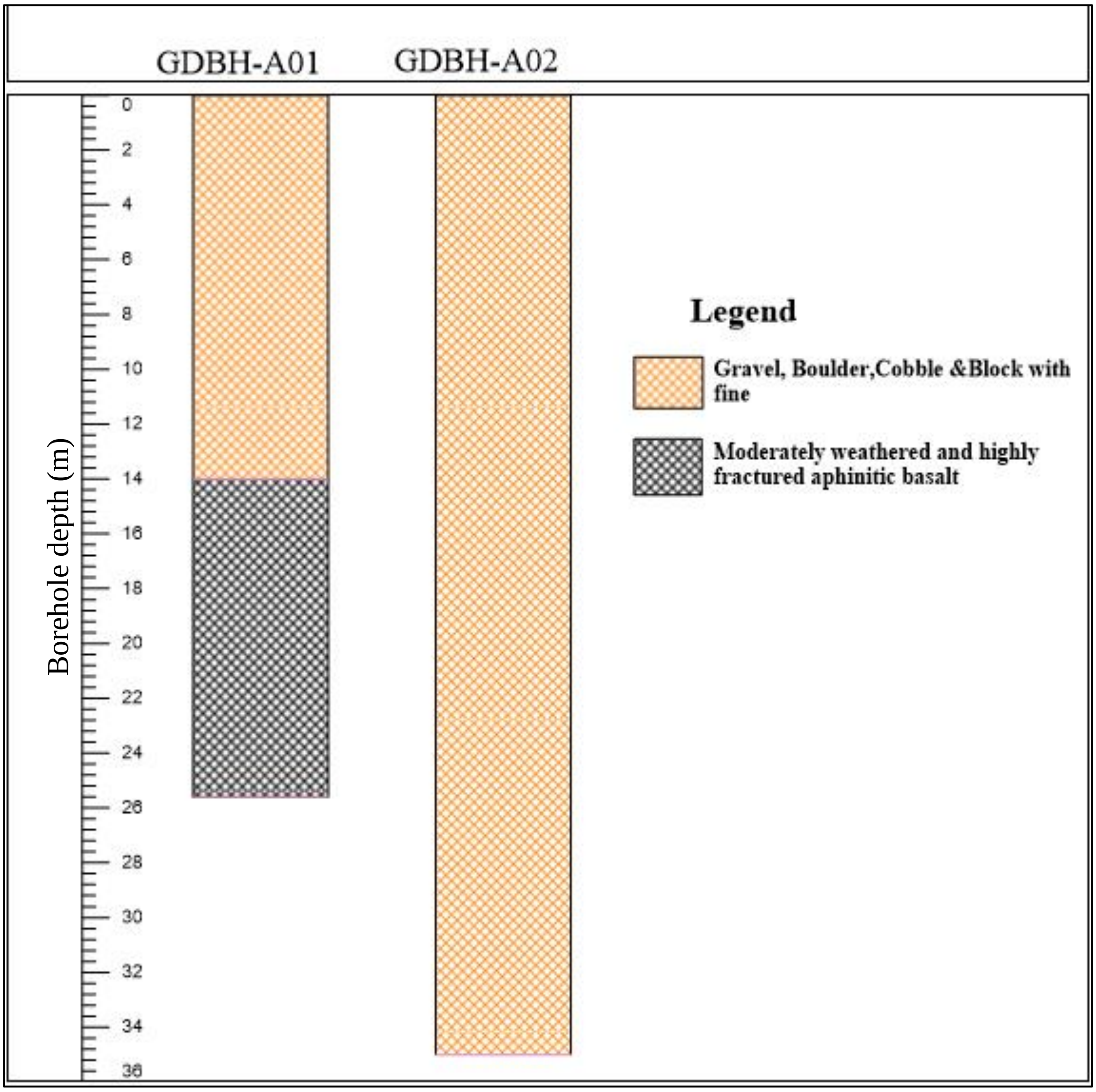

Figure 5. 3 Borehole log from A01 and A02 borehole at left abutment

The presence of highly fractured characteristics of the rock beneath the foundation of the dam increases hydraulic conductivity after impoundment of water to reservoir of the dam. Therefore, it might very favorable to excessive leakage problem and foundation issue.

5.3.2. Rock Quality Designation (RQD)

One of the parameters used to determine the quality of rock mass is RQD. The investigation of RQD with depth was done via borehole drilling. Each borehole's RQD classification was determined according to Deere's (1968). Accordingly, the drilled borehole revealed the result of RQD from both abutments for each borehole with respect to depth interval (Figure 5.4).

As a result shows, from left abutment of dam axis, RQD value for borehole GDBH-A01 is ranging from 0 to 20% (RQD value 0 up to the depth of 14m and 20% from 14 -25.6m depth) (Figure 5. 4*A*), the rock falls under very poor rock class and also for borehole GDBH –A02 is 0%, which is generally rock mass classify in very poor rock class according to Deere's (1968). From right abutment also shows that RQD value for borehole GDBH –A03 ranging from 0 to 70% classifying as very poor to good rock class (Figure 5. 4C), whereas for borehole GDBH- A04 RQD value range from 0 to 50% which classify as very poor to fair rock class (Figure 5. 4B).

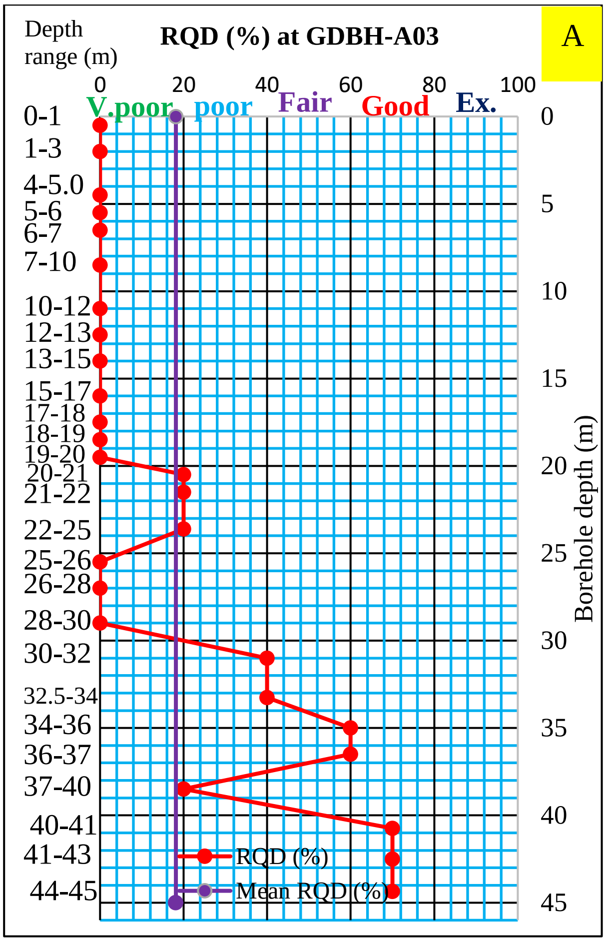

A
RQD (%) at GDBH-A03
Depth
range (m)
0
20
40
60
80
100
V.poor
poor
Fair
Good
Ex.
0-1
1-3
4-5.0
5-6
6-7
7-10
10-12
12-13
13-15
15-17
17-18
18-19
19-20
20-21
21-22
22-25
25-26
26-28
28-30
30-32
32.5-34
34-36
36-37
37-40
40-41
41-43
44-45
RQD (%)
Mean RQD (%)
Borehole depth (m)
0
5
10
15
20
25
30
35
40
45

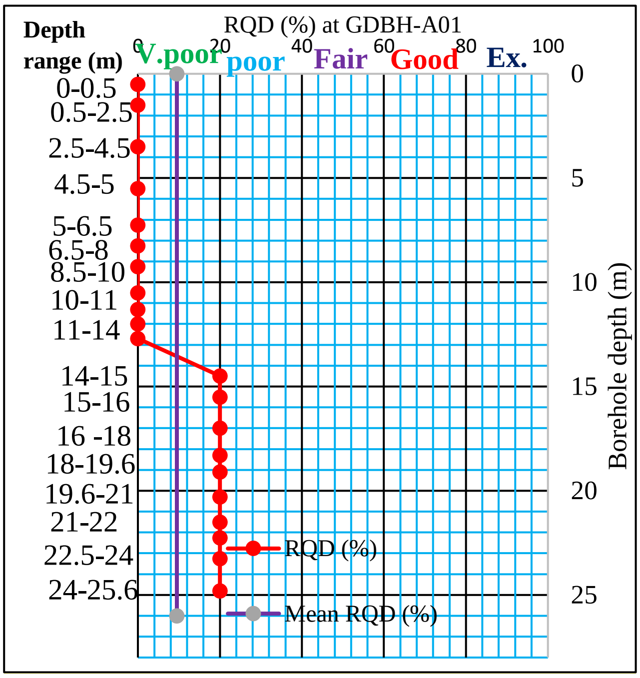

RQD (%) at GDBH-A01
Depth
range (m)
0
20
40
60
80
100
V.poor
poor
Fair
Good
Ex.
0-0.5
0.5-2.5
2.5-4.5
4.5-5
5-6.5
6.5-8
8.5-10
10-11
11-14
14-15
15-16
16 -18
18-19.6
19.6-21
21-22
22.5-24
24-25.6
RQD (%)
Mean RQD (%)
Borehole depth (m)
0
5
10
15
20
25

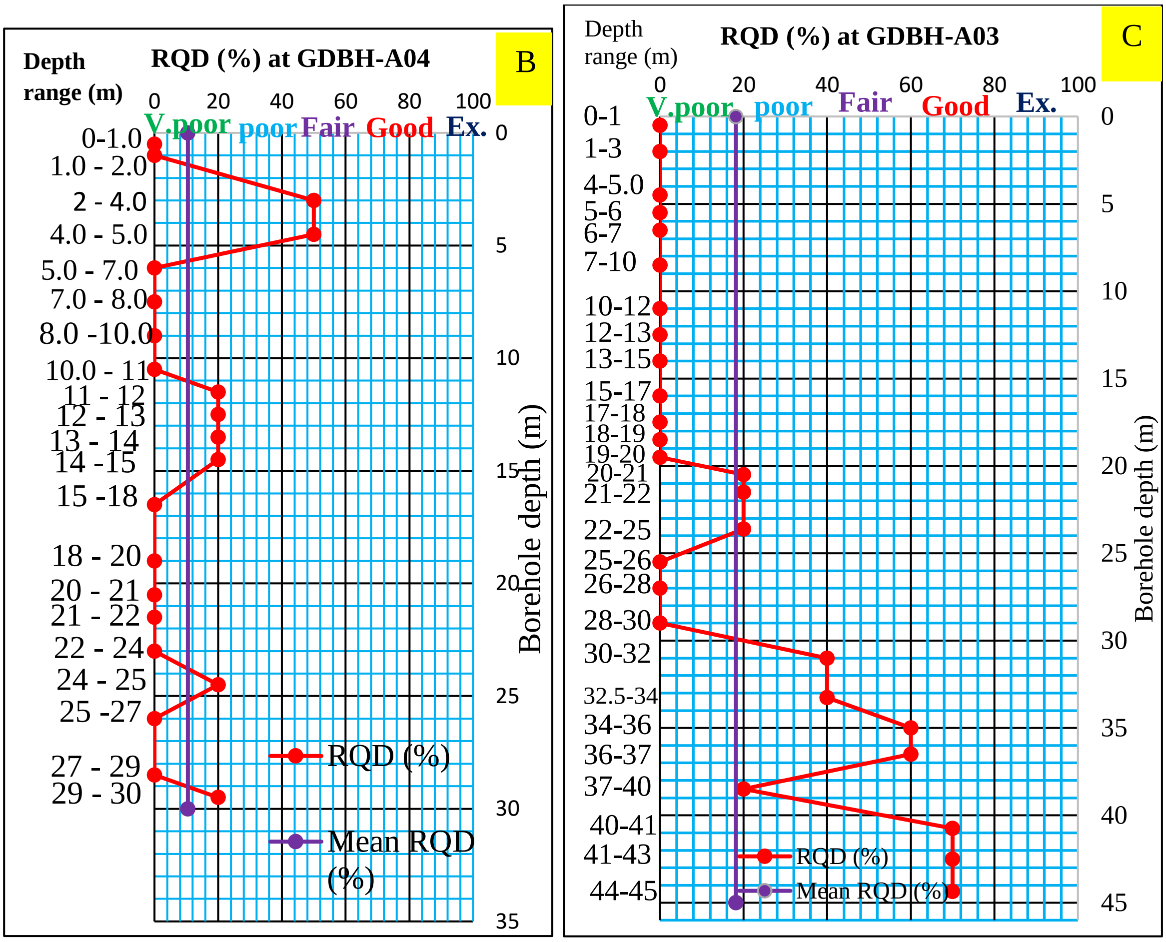

Figure 5. 4 Variation of RQD with depth

In general, the study area's RQD value ranges from very poor to good rock classification. RQD value from two boreholes (GDBH-A01 and GDBH-A02) which is very poor classification indicates the thickness of soil and highly weathered & fractured rock is very thick. So there is excessive seepage problem expected in this specifics. This result indicates that the area is characterized by extensively fractured to fragmented rock up to a particular depth. GDBH-A03 borehole indicates that the rock mass of the area is strongly jointed and fragmented until it reaches a depth of 40 meters. This highly fractured rock mass can lead to excessive seepage as well as deformation of foundation.

5.3.3. Geophysical Investigation

Geophysical approaches are used to characterize the subsurface in an indirect manner. It provides a picture of the conditions beneath the surface. The most prevalent geophysical tool for investigating foundation issues at dam sites is seismic refraction. Overburden formation, bedrock depths, and areas of bedrock weathering are all described via refraction study. To evaluate foundation conditions at the Gololcha dam site, five seismic lines were explored (Figure 5. 5).

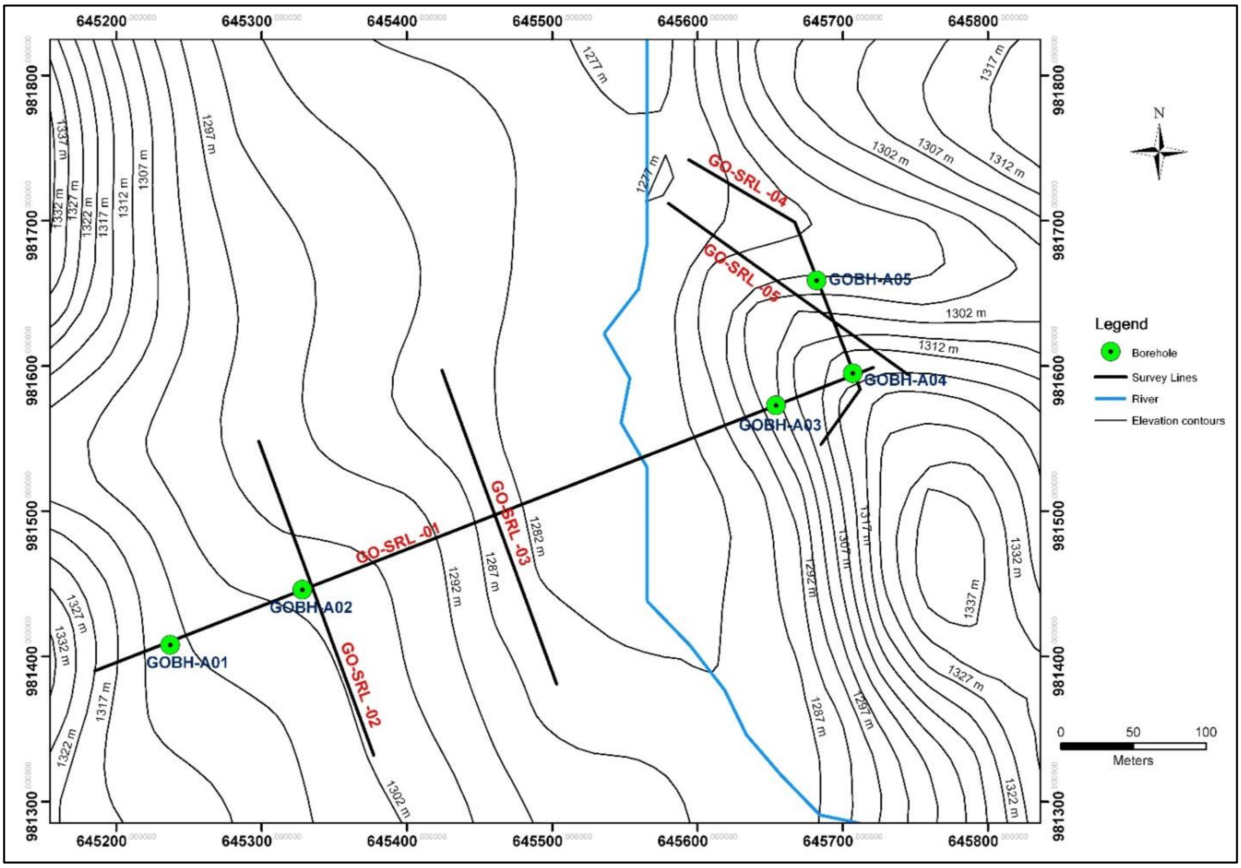

Figure 5. 5 Layout of Survey Lines (OWWDSE, 2021)

Line GO-SRL-1: This line, which is 575 meters long, is surveyed along the dam axis. It runs from the left to the right abutment. The obtained data was processed and evaluated using the tomography inversion approach, as shown in Figure 5. 6.

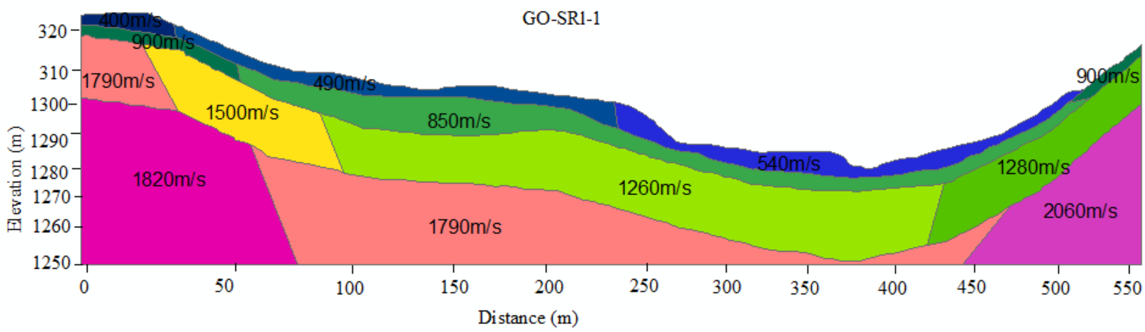

Figure 5. 6 Geoseismic section along Line GO-SRL-1, Layer-section

The very low velocity formation (350-600m/s) in the upper part of the segment is attributable to loose top soil. Seismic velocity of around 900m/s indicates the second stratum, which could be heavily weathered basalt. Between 100 and 200 m, these upper two layers of low velocity appear to have a depth of more than 10 m and become thinner as the segment progresses. Weathered and fractured basalt extending to about 35 m depth from 100 m to 400 m distance and appearing up to 20 m and 25 m depth on the left and right abutments, respectively, is the third layer with a velocity value of 1150-1760 m/s, whereas the bottom layer with a velocity of about 2000 m/s could be low fractured volcanic rock. The velocity value revealed that the upper three layers are characterized as loose soil to highly fractured and weathered rocks from surface to depth, respectively, which is the potential area of leakage problem. At the center of the dam the velocity becomes low than two abutments in respective layers this indicates the fractured and weathered of basaltic rock is deep at the center of the dam axis.

Line GO-SRL-2: This survey line was conducted at left abutment, along proposed conduit, which is perpendicular to dam axis. A four-layer model is deduced from the layer section (Figure 5. 7).

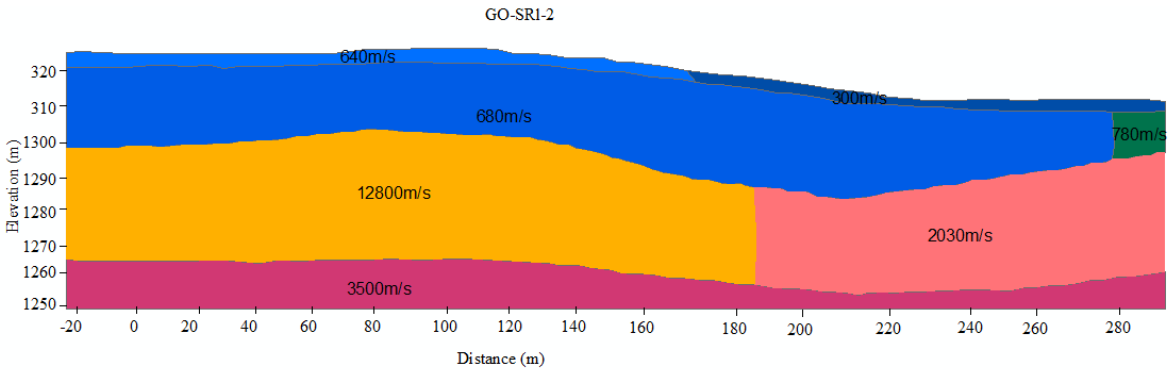

Figure 5. 7 Geoseismic section along Line GO-SRL-2 - Layer section

The upper layer with relatively low velocity (300-520 m/s) corresponds to loose soil, while the second strata of 640- 780 m/s corresponds to heavily weathered basalt. Between 0 and 100 m distance (upstream), the upper and second low resistivity layer extends to around 15 m depth, and less than 10 m on the downstream side. Weathered/fractured volcanic rock could be responsible for the third layer's seismic velocity (1280-2000 m/s), the lower velocity from upstream revealed that the rock is highly fractured and weathered at upstream than downstream. It appears to be approximately 30 meters deep. Seismic velocity (2300-3500 m/s) in the bottom layer reveals a fractured volcanic rock formation. This specific line is coincide with borehole GDBH-A02, in this area there is very thick soil deposit and highly weathered rock, which is very favorable for leakage problem.

Line GO-SRL-3: This line was conducted perpendicular to the dam axis, start from upstream and runs toward downstream. The layered model is described as a four-layer section (Figure 5. 8).

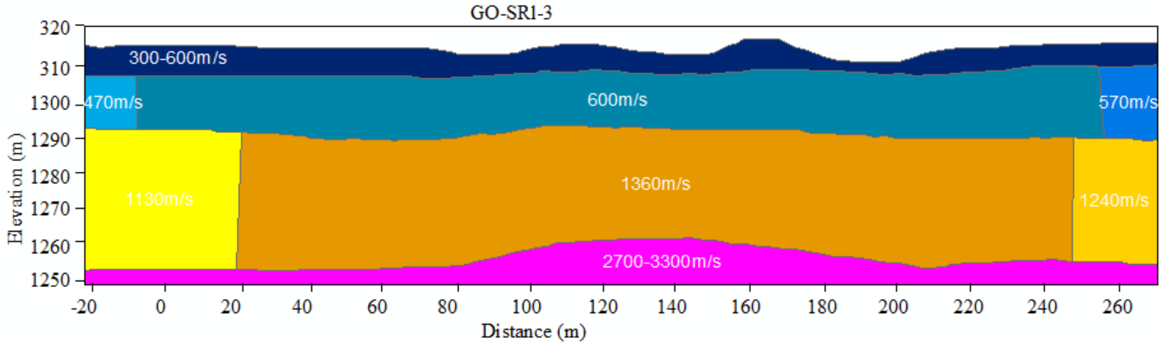

Figure 5. 8 Geoseismic section along Line GO-SRL-3- Layer section

The top layer of low velocity (300-600 m/s) revealing around 5 m of loose soil or heavily weathered basalt and also from upstream to downstream the layer is almost the same, that means alluvial soil deposit. The second stratum, which has a velocity of 470- 600 m/s, contains heavily weathered volcanic rock that extends to a depth of more than 10 m and the weathering degree is high at upstream and downstream. The third layer velocity (1130-1360 m/s) extends to more than 30 m depth, indicating weathered/fractured volcanic rock formation with the degree of weathering high from upstream and downstream than the dam axis, whereas the fourth layer velocity (2750-3300 m/s) may indicate substantially fractured volcanic rock occurrence. Soil deposit and highly weathered rock extends to more than 30m depth, which is the potential leakage problem of the area.

Line GO-SRL-4: This line was conducted perpendicular to the dam axis, start from upstream and runs toward downstream. The layered model is described as a four-layer section (Figure 5. 9).

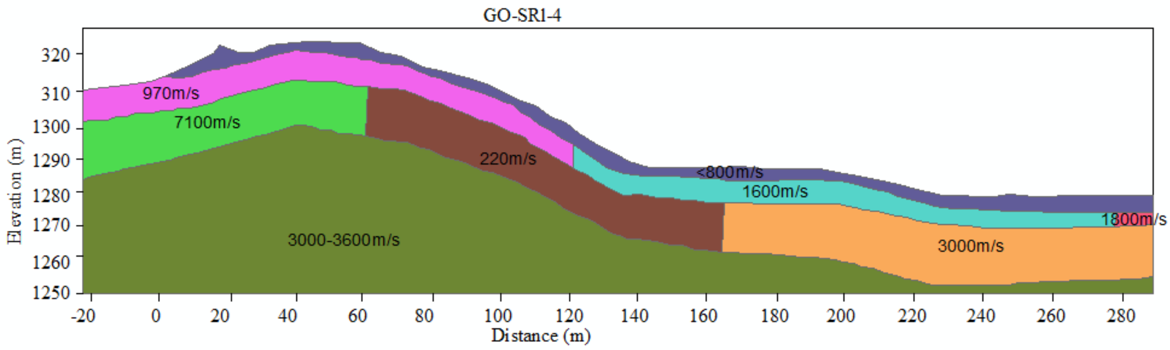

Figure 5. 9 Geoseismic section along Line GO-SRL-4, - Layer section

The velocity values in the tomographic section gradually rise with depth, from less than 800 m/s in the upper region to more than 2900 m/s at nearly 30 m depth. There are four layers in the layer section. The upper layer velocity (<800 m/s) indicates loose soil, while the second layer velocity (870- 1900 m/s) indicates heavily weathered basalt as shown in figure above the degree of weathering also degrease from upstream to downstream. The third layer velocity (2200-3000 m/s) indicates the presence of fractured rocks, whereas the bottom layer velocity (3000m/s-3600m/s) indicates as less fractured/fragmented rock formation.

Generally the variation of velocity is due to the variation of degree of fracturing and weathering. Hence the degree of fracturing and weathering is decrease from surface to depth and also from upstream to downstream.

Line GO-SRL-5: The line connects the upstream and downstream sides of the river. The layered model is described as a three-layer section (Figure 5. 10).

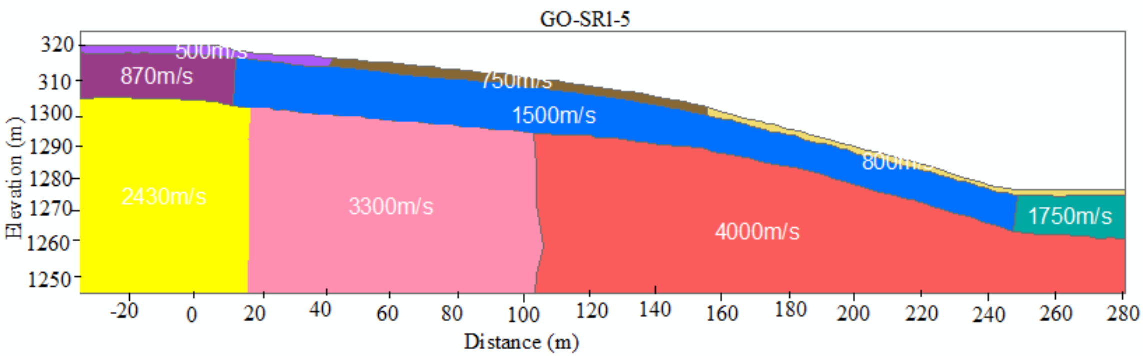

Figure 5. 10 Geoseismic section along Line GO-SRL-5- Layer section

On the upper part of both sections, low velocity formations of500- 800 m/s and 870-1500 m/s may be seen. The upper layer, which has a velocity of less than 800 m/s, and the second layer, which has a velocity of around 870-1500 m/s, stretch to about 15 m depth on the upstream side and about 10 m depth on the downstream side. On the downstream side, high velocity rocks usually occur at a shallower depth than on the upstream side. And also the rock from upstream is highly fractured than downstream since the velocity is gradually increase from upstream to downstream.

5.3.4. Correlation between geophysical results and sub-surface RQD (%)

The result from geophysical method's shows that velocity increases gradually as depth increases. The RQD of subsurface rock increases with depth as well. Figure 5. 11 shows the correlation between RQD values from boreholes and GO-SRL-1 and GO-SRL-2 geophysical seismic refraction results. The GO-SRL-1 line coincides with the dam's axis, which is connected with all boreholes. The velocity from refraction and RQD from boreholes increases with depth. RQD from GDBH-A01 borehole and velocity at this specific point is agree since the velocity very low until 25m depth and also RQD value is 0 to 20% which is very poor classification. At the GDBH-A02 borehole, GO-SRL-2 crosses the dam axis from upstream to downstream. The RQD value from the GDBH-A02 borehole is 0%, and seismic refraction reveals that low velocity layer is highly thick layer (upper and second layers), indicating highly weathered and fractured rocks with soil deposits, which is agreed with each other. The RQD value from GDBH-A04 borehole and velocity at this specific location is dis agree since the velocity at 30m depth is high but RQD value at this depth is classified as very poor classification. This disagreement was due to infilling material of fractured rock which is increase the velocity of seismic refraction but RQD remains in very poor classification.

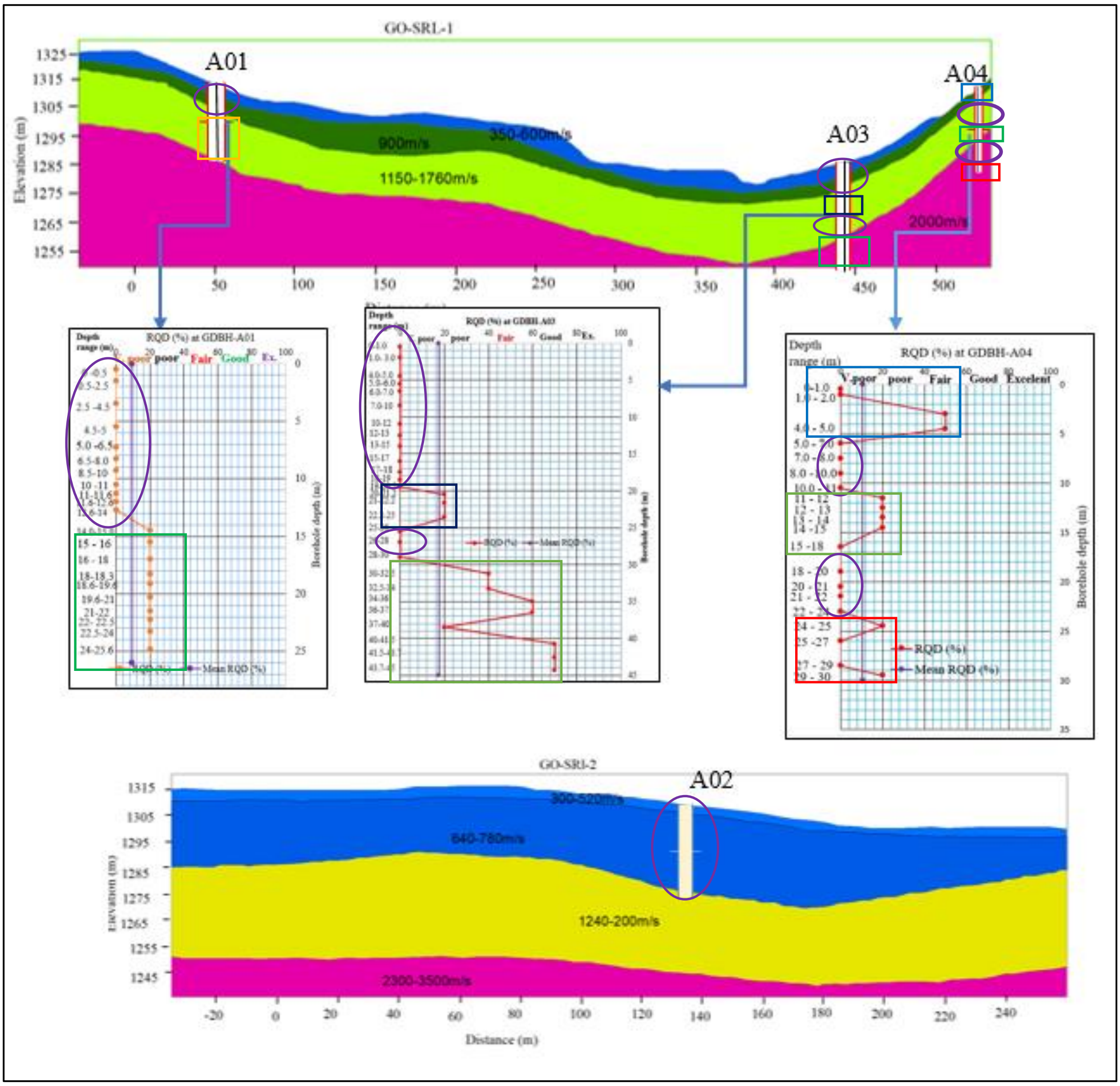

Figure 5. 11 Correlation between RQD and Seismic refraction

5.4. Engineering Characterization of Soils

Representative soil samples from the test pit were obtained for laboratory testing of soil index properties such as particle size distribution (sieve and hydrometer analysis), Atterberg limits (liquid and plastic limit), natural moisture content (NMC), and specific gravity. To measure the permeability of the soil in the reservoir area, a permeability test is also performed. The test pits are between 1 and 2.5 meters deep. The detail of each is discussed in next section.

5.4.1. Natural moisture content

The test was carried out in accordance with ASTM D2216. The purpose of determining a soil's moisture content is to figure out how much water or moisture is contained in a particular quantity of soil in terms of dry weight. At the left riverbank in the reservoir region, the natural moisture content of the soils ranges from 10.65% to 22.37%, according to the results. As the result shows the natural moisture content is low in the study area.

5.4.2. Specific Gravity Test

0The test was carried out in accordance with ASTM D854 (1998) standard by using a pycnometer. The result of specific gravity is used for calculation of void ratio, degree of saturation, porosity, and other soil parameters. Its result from representative soil sample of study area is range from 2.60 to 2.7.

5.4.3. Atterberg Limit Test

The moisture content with in the soil is affect the consistency of the soil. The state of soil changes from one state to other as the water content with in it is varies. At very high moisture content, soil behaves like liquid states and as water content decrease gradually the state of soil change to other. The moisture content correspond to these change of state is known as Atterberg limit or consistency limit. The purpose of an Atterberg limit test is to determine the liquid limit, plastic limit and plasticity index of fine-grained soil and to classify soil according to the Unified Soil Classification System. The result of Atterberg limits test are presented in (Table 5. 9). According to the result from the test, liquid limit (LL) ranges from 29.93% to 53.38% (appendix 8), Plastic limit (PL) ranges from 20.21% to 32.43% (appendix 9) and plastic index ranges from 9.72% to 20.95%.

Table 5. 9 Summaries of Atterberg limit results

Atterberg limits	Sample Id			
	TP -1	TP-2	TP-3	TP-4
LL (%)	41.33	53.38	44.50	29.93
PL (%)	27.44	32.43	29.78	20.21
PI (%)	13.89	20.95	14.72	9.72

5.4.4. Particle Size Analysis

Particle size analysis has been done to determine the percentage of different grain size containing with in the soil. Particle size analysis has been conducted into two categories, one is sieve analysis in which the percentage of soil particle size coarser than 0.075mm and the other category is Hydrometer analysis used for the percentage of soil particle size finer than 0.075mm. The analysis were done on disturbed soil sample obtained from test pits. Particle size distribution curve or gradation curve were plotted (Figure 5. 12 and Appendix 7) based on the result of particle size analysis. Depending on the curve, it is possible to determine the distribution of soil particles and also the curve gives the idea for the gradation of the soil which means weather the soil is well graded or poorly graded. From the result of particle size analysis and Atterberg limits the soil can be classified into different groups according to Unified Soil Classification System (USCS) as presented in Table 5. 10.

Table 5. 10 Particle size analysis and Atterberg limit result

Sample Id	**Particle size analysis**				**Atterberg limit**			**USCS**	**Plasticity Class** (Ramana, 1993)
	Gravel	Sand	Silt	Clay	LL	PL	PI		
TP-1	36.5	55.73	6.98	0.79	41.33	27.44	13.89	SW	Low plasticity
TP-2	7.24	32.1	51.71	8.96	53.38	32.43	20.95	MH/OH	High plasticity
TP-3	0.00	5.94	78.64	15.43	44.50	29.78	14.72	ML/OL	low plasticity
TP-4	0.76	51.37	38.85	9.12	29.93	20.21	9.72	SW	Low plasticity

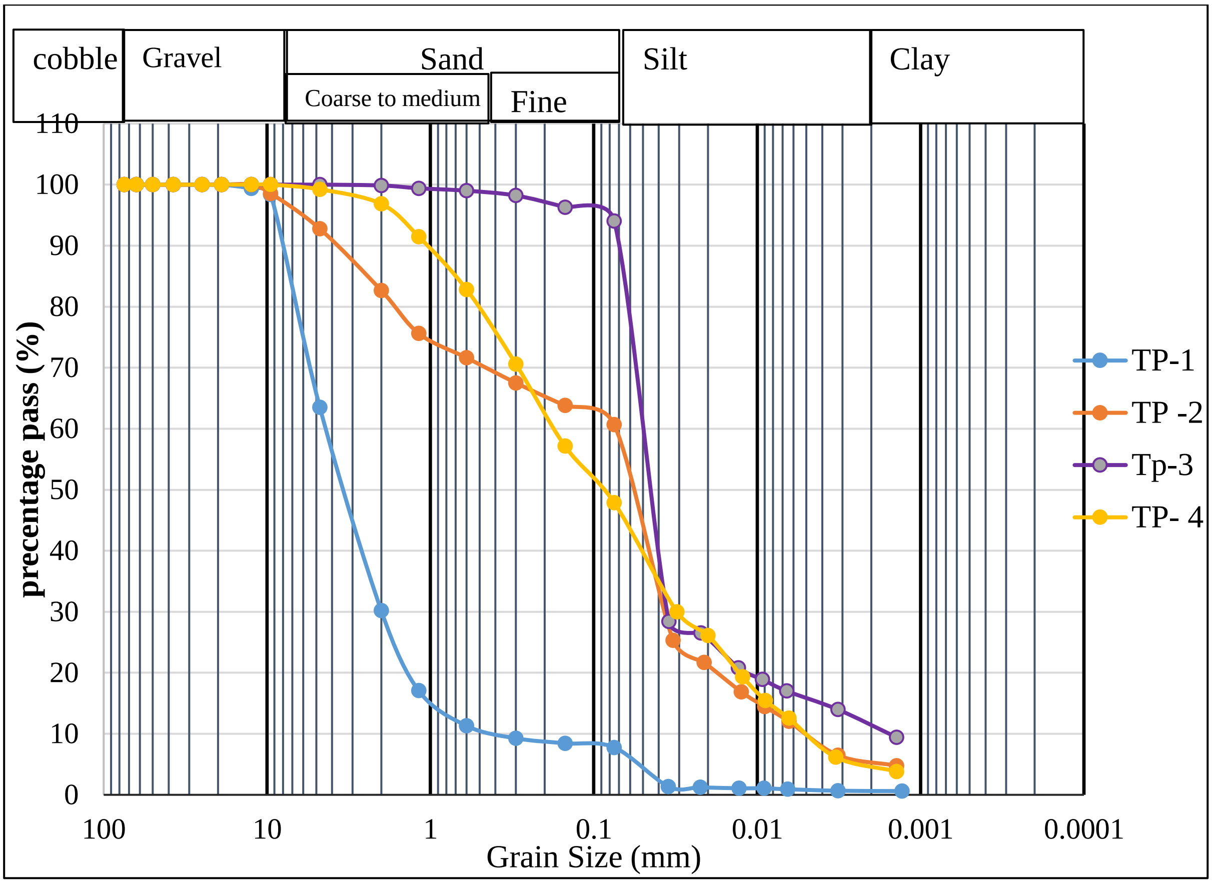

Figure 5. 12 Grain size distribution curve of soil sample

5.4.5. Soil Classification by USC systems

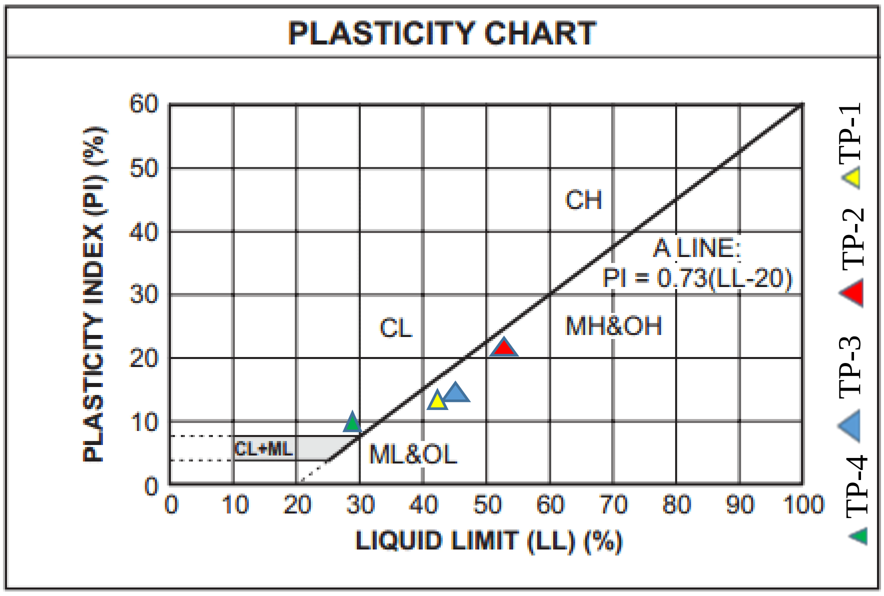

Figure 5. 13 Plasticity chart that shows some of the soil in the study area

For engineering application the most used classification method of soil is Unified Soil Classification System (USCS). The classification is based on the percentage of grain size constituents, coefficient of uniformity, gradation, liquid limit and plasticity index. From the particle size analysis the soil sample is mainly dominated sand and silt, 55.73% of sand at the TP-1, 51.71% of silt from TP-2, 78.64% of silt from TP-3 and 51.37% of sand from TP-4(Table 5.10). As a result the soil from TP-2 and TP-3 contains more than 50% passing 0.075mm and classified as fine soil. According to USC, the soil sample from TP-1 falls under SW (Well graded sand), whereas from TP-2 falls under MH or OH which implies high plastic silt (Figure 5. 13). And also the soil from TP-3 falls under ML which is low plastic silt, whereas TP-4 falls under well graded Sand (SW).

The soil and rock that found at the study area according to engineering classification shown in the Figure 5. 14 & its cross sectional view also shown in Figure 5.15

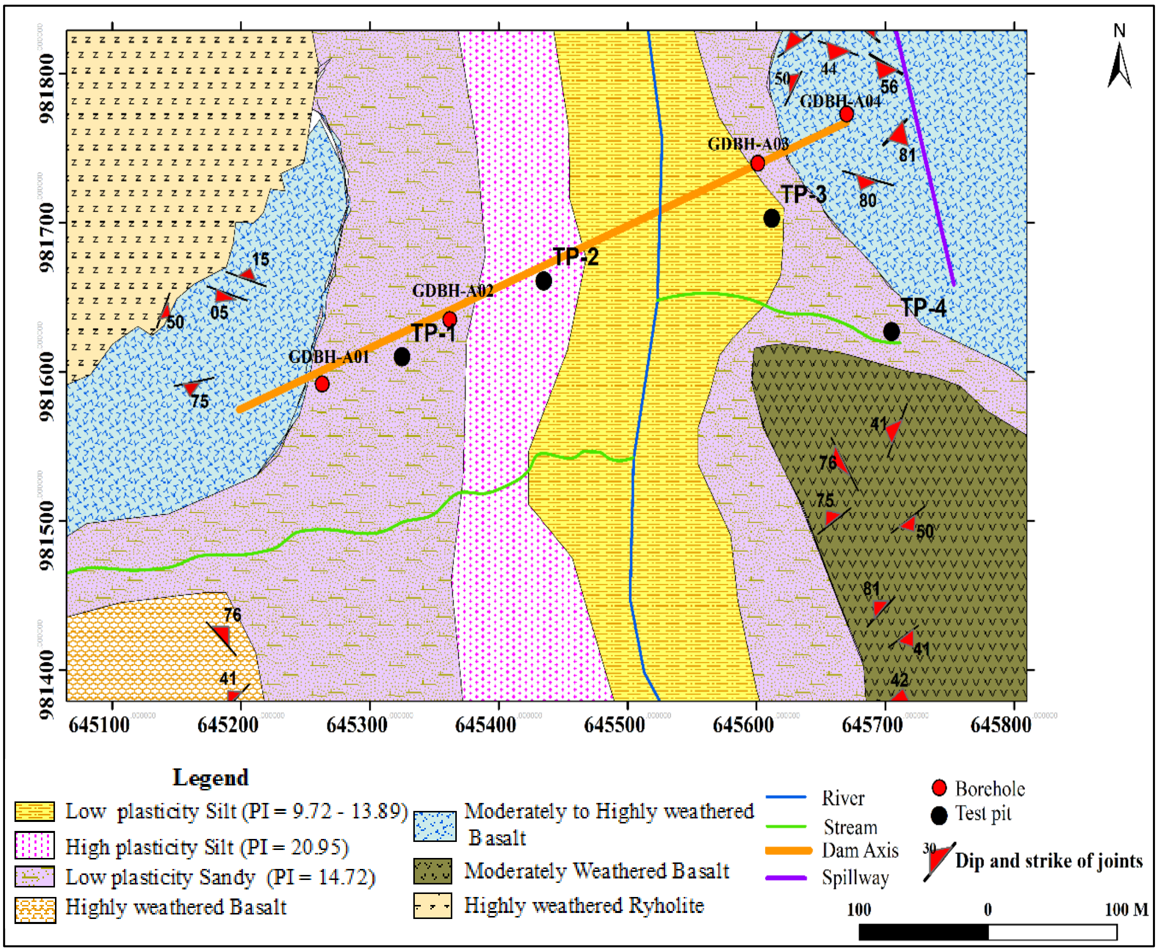

Figure 5. 14 Engineering geological map of the dam site at scale of 1:3,000

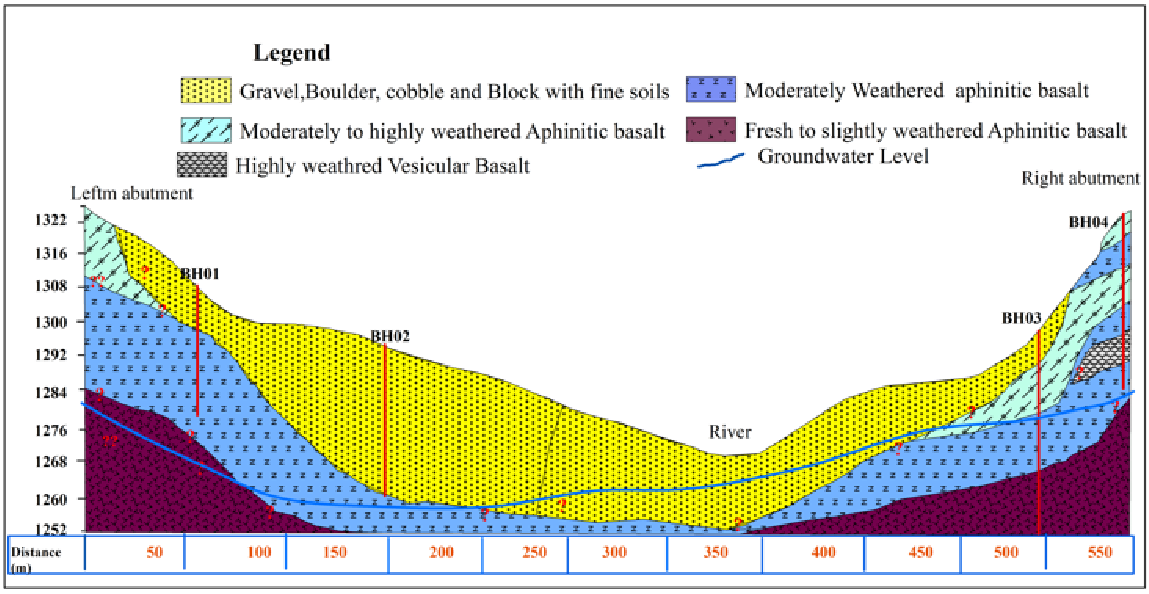

Figure 5. 15 Cross section of engineering geological map

5.5. Abutment and Reservoir Water Tightness Analysis

The permeability of both rock and soil was conducted in the present study. The permeability of soil was determined by laboratory test, whereas rock's permeability was evaluated by surface discontinuity survey and also falling head permeability test and few depth of packer test in the borehole. Various factor affect the water tightness of the dam, which include; permeability of underlying material, geological structure, the extent of the submerged valley in the area, position of the water table in the reservoir area, the lengths and gradients of potential leakage paths and the instability of the river valley sides (Fell et al., 2005).

At Gololcha dam site the permeability of underlying soil and rock and other factors that affect the water tightness were evaluated and the detail were discussed below.

5.5.1. Permeability of soil

To determine the coefficient of permeability of the soil deposits in the study area, a laboratory permeability test was performed on representative soil samples collected from the test pits. From the lab test particle size distribution and Atterberg limit are also used to estimate the permeability of the soil at the study area. As a result from the particle size distribution and Atterberg limit analysis indicate the soil at the Gololcha dam site contains significant fine material (clay and silt soil), which indicates the soil is semi permeable. In addition the coefficient of permeability was evaluated from the representative soil. Table 5. 11 shows the results of coefficient of permeability analyses performed on representative soil samples. From the result the coefficient of permeability is almost the same for all sample;

with the minimum value of $1.71*10^{-6}$cm/s at TP-3 from the right side of the river and maximum value of $2.39*10^{-6}$cm/s at TP-2 from left side of the river. From the result all soil sample permeability classified into semi-permeable (Table 5. 11 and Appendix 2).

Table 5. 11 Permeability result from laboratory test

Location	Sample Id	Depth (m)	Sample type	Coefficient of permeability, K(cm/s)	Classification of permeability according to USBR (1987).
Left side	TP-1	2	Disturbed	$2.17*10^{-6}$	Semi-pervious
	TP-2	2.5	Disturbed	$2.39*10^{-6}$	Semi-pervious
Right side	TP-3	1	Disturbed	$1.71*10^{-6}$	Semi-pervious
	TP-4	1	Disturbed	$2.05*10^{-6}$	Semi-pervious

5.5.2. Surface rock mass permeability

Discontinuity within the rock mass and its geometrical properties (such as orientation, aperture, spacing, roughness and infilling) are important parameters affecting the permeability (Gurocak & Alemdag, 2012; Öge, 2017). The permeability value is affected by the discontinuity orientation as the water in the rock mass travels along discontinuity surface and also compactness/opening and roughness, as well as the type of infilling also affect the permeability (Gurocak & Alemdag, 2012). Many equations based on experimental studies have been developed to estimate the hydraulic conductivity of individual fractures that intersect the rock mass. In the present study, the relationship between the hydraulic conductivity (k) and fracture characteristics (spacing, S and aperture, e) is given by equation 10 which is derived by Snow (1965) and Louis (1974) used to estimate the hydraulic conductivity of the rock mass that is exposed on the dam abutments and reservoir area. The result of hydraulic conductivity from the surface discontinuity survey were showed in Table 5. 12 and Appendix 4. The result revealed that $1.64*10^{-3}$m/s to 1.05 m/s at right abutment, which falls under moderately to highly permeable rock mass and $2.13*10^{-2}$m/s to $1.09*10^{-1}$m/s at left abutment, which falls under permeable rock mass according Bell (2007). Whereas the result from reservoir area is ranging from $3.94*10^{-3}$m/s to $8.1*10^{-1}$m/s which also falls under moderately to highly permeable rock mass.

Table 5. 12 Permeability result from surface discontinuity survey

Location	No	K(m/s)	Classification according to Bell (2007)
Right abutment	1	$1.64*10^{-3}$	Moderately permeable
	2	$1.1*10^{-3}$	Moderately permeable
	3	1.05	Highly permeable
	4	$8.3*10^{-1}$	Highly permeable
	5	$5.3*10^{-1}$	Highly permeable
	6	$3.27*10^{-2}$	Highly permeable
	7	$1.308*10^{-2}$	Highly permeable
	8	$7.610*10^{-1}$	Highly permeable
Left abutment	9	$2.13*10^{-2}$	Highly permeable
	10	$1.84*10^{-2}$	Highly permeable
	11	$8.1*10^{-1}$	Highly permeable
	12	$1.09*10^{-1}$	Highly permeable
Right reservoir rim	13	$1.31*10^{-2}$	Highly permeable
	14	$3.67*10^{-2}$	Highly permeable
	15	$3.94*10^{-3}$	Moderately permeable
	16	$4.08*10^{-3}$	Moderately permeable
	17	$2.73*10^{-3}$	Moderately permeable
	18	$2.34*10^{-3}$	Moderately permeable
	19	1.05	Highly permeable
	20	$3.27*10^{-3}$	Moderately permeable
Left reservoir rim	21	$1.77*10^{-1}$	Highly permeable
	22	$5.52*10^{-2}$	Highly permeable
	23	$1.7*10^{-1}$	Highly permeable
	24	$7.34*10^{-2}$	Highly permeable
	25	$1.64*10^{-2}$	Highly permeable

5.5.3. Sub surface permeability

Hydraulic conductivity test is the most common and important method in order to determine the permeability of the dam foundation. In the study area the permeability was tested by falling head test and with combination of packer test in two borehole. During the investigation, falling head permeability experiments were performed on soil and heavily fragmented rocks. Totally twenty (20) falling head field permeability tests, with the test interval of 5m were performed. The packer tests were conducted for 15m in each boreholes (GDBH-A03 and GDBH-A03). Hydraulic conductivity result from falling head and packer test were given in Table 5. 13 below. From the result foundation of the dam is permeable up to 30m depth. Therefore, ground treatment (e.g. grout curtain) has to be carried out to the depths of the base of permeable formation to avoid excessive leakage. Hydraulic conductivity result from falling head and packer test were given in Table 5.13 below.

Table 5. 13 Falling head and packer test result from borehole after OWWDSE 2021

Borehole Id	Test interval (m)	Hydraulic conductivity(cm/s)	Classification according to USBR (1987)
GDBH-A01	0.00 -10.00	(2.67 - 7.09) $*10^{-4}$	High permeable
	10.00 -25.00	$4.68*10^{-4}$ - 3.16 $*10^{-5}$	Semi-permeable
GDBH-A02	0.0 - 11.00	7.2 - $8.0*10^{-4}$	Semi-permeable
	10.50 – 35.00	3.11 - $7.11*10^{-3}$	High permeable
GDBH-A03	0.00 – 10.00	1.9 – 9.99 * 10^{-4}	Semi-permeable
	10.00 – 15.00	8.25E-03	High permeable
	15.00 – 25.00	4.38 - 6.78 $*10^{-4}$	Semi-permeable
	25.00 – 30.00	1.29E-02	High permeable
GDBH-A04	5.00 – 10.00	3.49 $*10^{-4-}$ - $4.68*10^{-5}$	Semi-permeable
	Depth interval for Lugeon test	Lugeon value (Lu)	Classification according to Fell et.al. (2005)
GDBH-A03	30.00 -45.00	1.2 – 5.0	Low/moderate permeable
GDBH-A04	15.00 – 25.00	1.8 - 2.0	Low/moderate permeable
	25.00 – 30.00	0.3	Low permeable

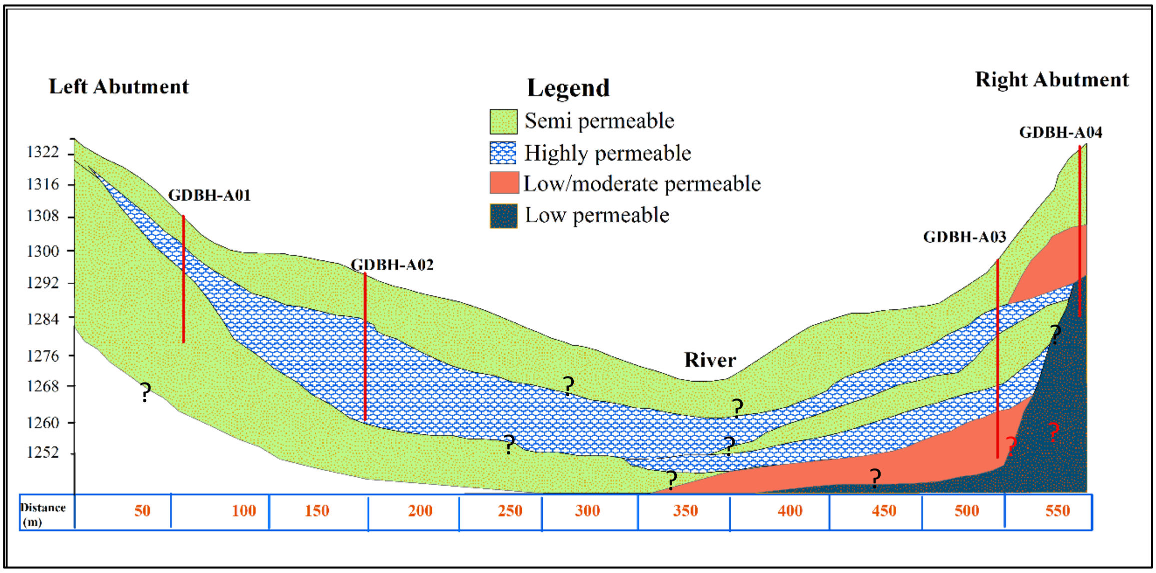

Figure 5. 16 Permeability cross-section along dam axis

From the result foundation of the dam is characterized as permeable to semi-permeable according to Figure 5.16. These permeability area of the dam is the potential area for the excessive leakage problem. Therefore, ground treatment (e.g. grout curtain) has to be carried out to the depths of the base of permeable formation to avoid excessive leakage.

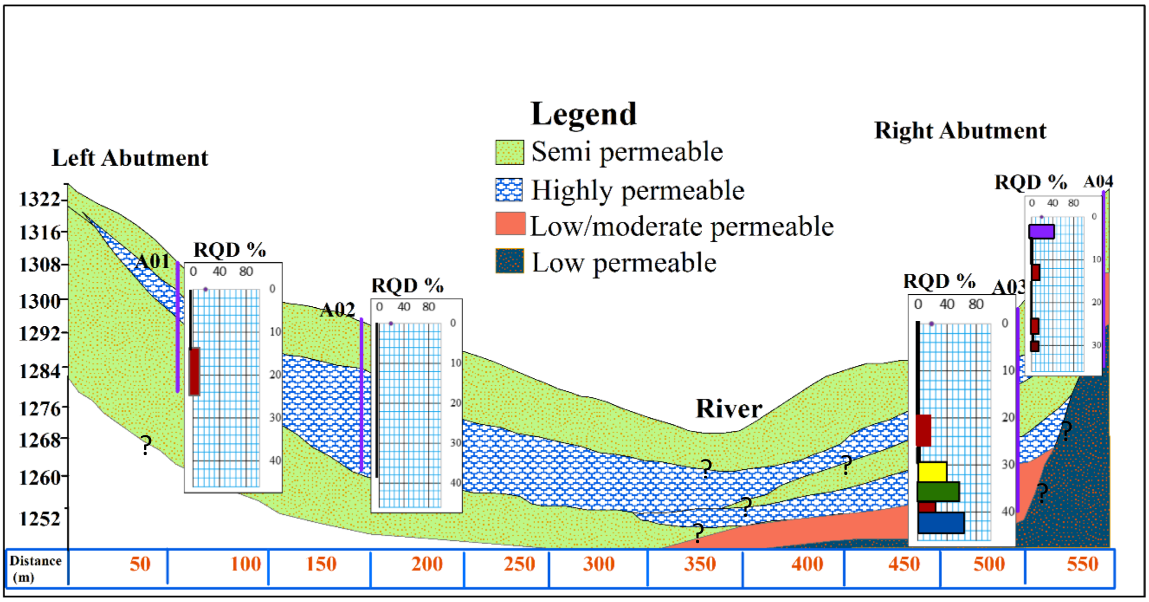

Figure 5. 17 Correlation between RQD% and permeability

The correlation between RQD and permeability is generally agreed upon, since the RQD value for medium and high permeability is 0 to 20%, and as the permeability decreases to low, the RQD value increases at right abutment (GDBH-A03) to 70% Figure 5. 17. As a result, at the right abutment, leakage was predicted to reach a depth of 40m, while at the left abutment, the exact depth to which semi-permeable ended remains unknown.

5.5.4. Ground Water Condition

The Gololcha dam is located in the lower awash basin in the eastern Ethiopian rift escarpment. The severely fractured and weathered volcanic rocks observed in the research area are ideal for a possible groundwater storage and flow zone. Groundwater levels were tested in boreholes by OWWDSE (2021). Accordingly, the groundwater level from GDBH-A01 is 18 meters, , but the groundwater level from the other boreholes was not observed up to the depth of drilled borehole, i.e. 25.6 meters, 35 meters, and 30 meters from GDBH-A01, GDBH-A02, and GDBH-A04, respectively (Table 5. 14). As a result, the groundwater level is very deep, and the rock is severely fractured and weathered, making flow of water inside the rock mass very favorable, because hydraulic conductivity of rock exposed is moderately to highly permeable.

Table 5. 14 Summary of groundwater level from borehole (after OWWDSE 2021)

Location	Borehole ID	Elevation	Depth (m)	Groundwater level (m)
Left abutment	GDBH-A01	1302	25.60	Null
	GDBH-A02	1298	35	Null
Right abutment	GDBH-A03	1285	45	18
	GDBH-A04	1319	30	Null

5.5.5. Water Tightness Analysis Based on Water Tightness Model

The water tightness model is the most reliable tool for assessing and confirming probable reservoir leakage after water impoundment(Fell et al., 2005). Topography, geology, groundwater condition, rainfall/climatic condition, hydraulic conductivity of the lithological units, and design of the reservoir's maximum Full Supply Level (FSL) were all elements considered in determining the water-tightness for portions of non-soluble rocks. As a result, according to Fell et al. (2005), the Gololcha dam abutments and reservoir area are evaluated using the following assumptions and parameters. The Gololcha dam site and its surrounding environment are characterized by a wide valley with a minor crest, extensively fractured rocks, and strong hydraulic conductivity. The project area consists of a wide reservoir valley with gentle slopes. The dam site and surrounding reservoir region were separated into two distinct segments based on topographical, geological, and hydrogeological parameters, as well as the resemblance and fit of the water-tightness model, and a cross-section line was drawn as shown Figure 5. 18, and each section was explained briefly as follows.

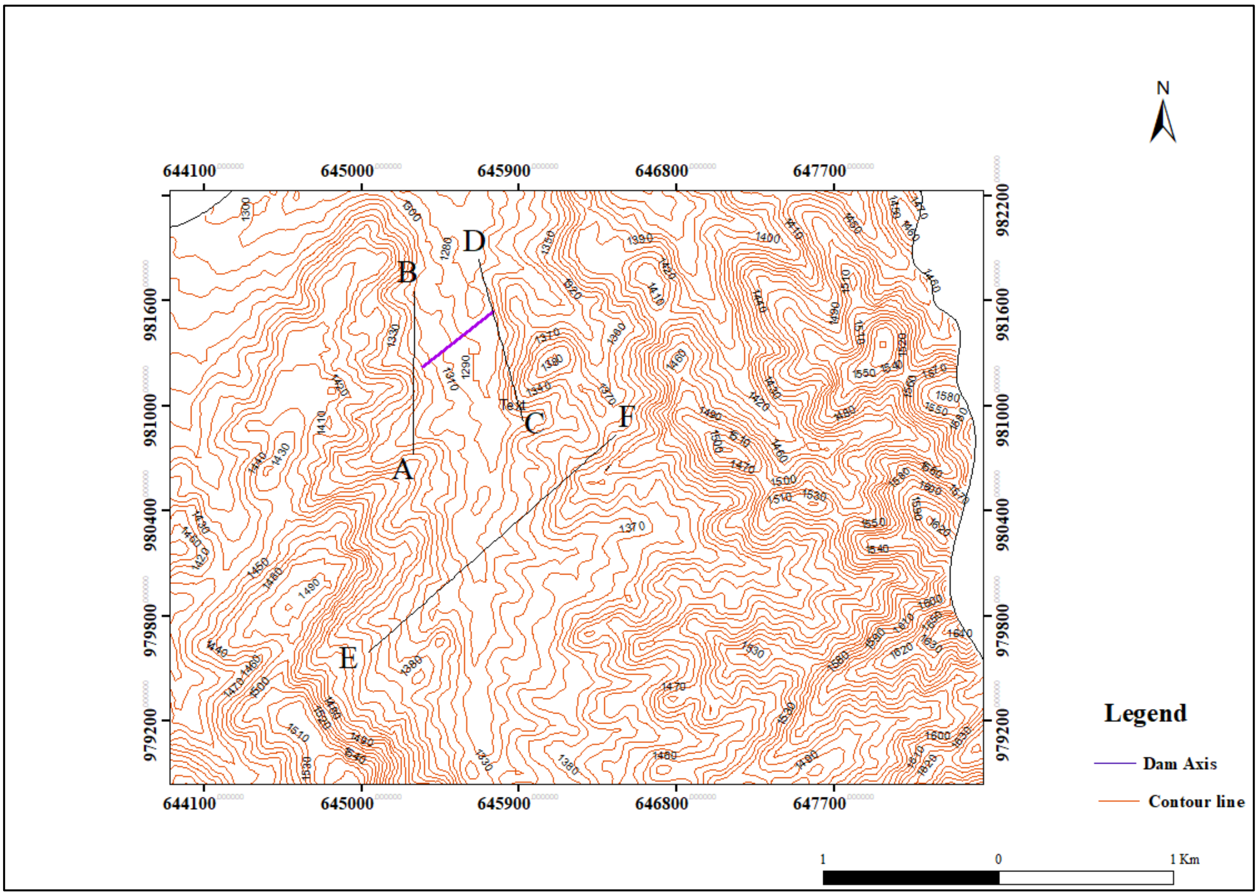

Figure 5. 18 contour of the study area used for cross-section to water tightness model.

1. Narrow valley and nearly gently sloped ridge that creates the dam's two abutments, as illustrated in Figure 5. 18 by A-B and C-D cross section lines at the left and right abutments, respectively. The ridge that forms the valley's rim for storage is thought to be low. As a result, the stress release is expected to affect the rock that forms the ridge and below FSL. The dam's abutments were built by heavily weathered, jointed, and fractured rocks, with soil covering the base. Because the leaking path traversed the dam axis in a roughly parallel direction to the river flow, the majority of the joint set orientations are advantageous to the leakage path. The surface hydraulic conductivity of rock masses and the in-situ permeability packer test results at both abutments revealed that the hydraulic conductivity ranged from moderately permeable to highly permeable. The depth to the ground water level along the abutments is below full reservoir levels, and groundwater is unlikely to rise significantly to achieve FSL. As a result of the porous rocks stated above and the considerable hydraulic gradient between the FSL and the actual groundwater table, significant leakage is expected. This area resembles and corresponds to the model E seen in Figure 2. 2 as shown Figure 5. 19 A&B.

2. Very wide river valley surrounded by following extensive high ground that represents a substantial part of the reservoir area. The valley that forms the rim of the reservoir and gradually increasing the topographic elevation that result the flow direction of water to north direction as shown in Figure 5. 18 by E – F cross section line. In this section the surface hydraulic conductivity assessment of rock masses revealed that the hydraulic conductivity of rock masses ranges from moderately permeable to highly permeable, with these characteristics resulting in potential high water leakage from the reservoir through the fractured rock after the water is impounded in the reservoir. The groundwater table in this part of the reservoir basin is assumed to be deep (>20m) as the study area falls in the low rain fall region (Figure1.3). Furthermore, there is no any surface manifestations of wetland occurrence and seasonal springs in the inner slopes of the reservoir area, which indicates a deep water table. At first stage of reservoir impoundment, a substantial volume of water is predicted to be lost from the storage to fill cavities in the valley side rocks. The inferred water table is below FSL (Figure 5. 19C), the potential leakage is expected.

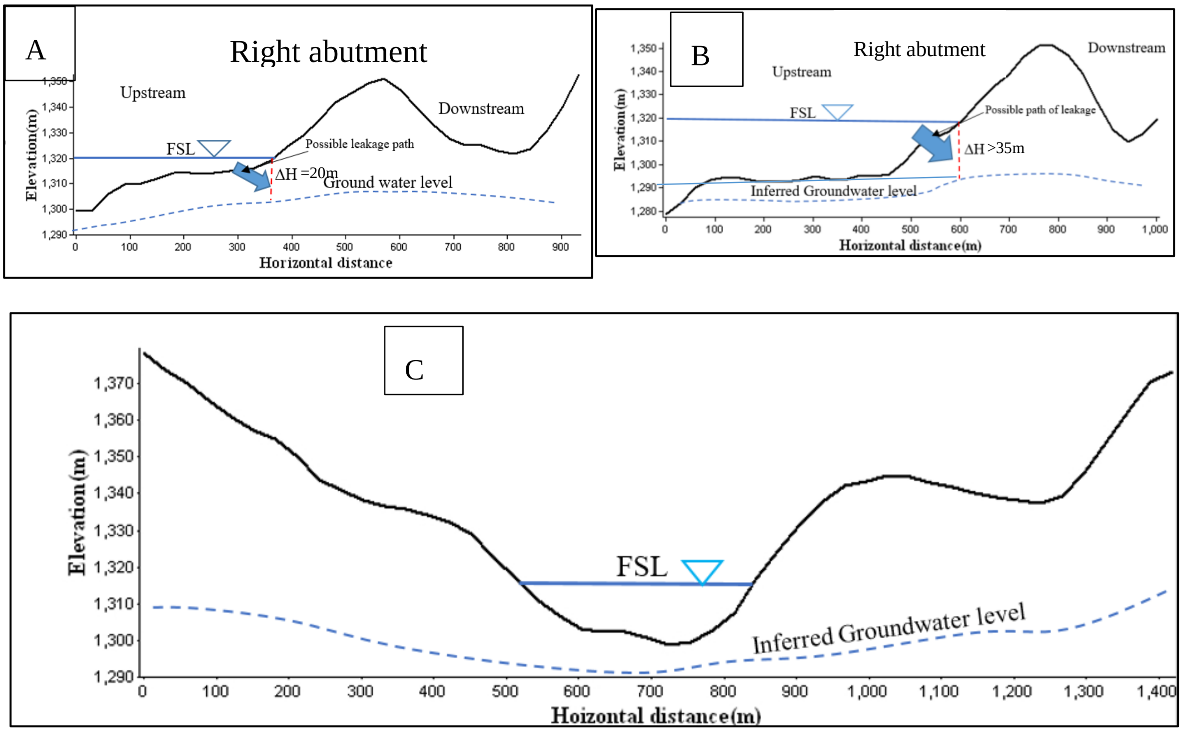

Figure 5. 19 Water tightness model for the study area (a) Right abutment, (b) Left abutment and (c) reservoir area

5.6. Slope stability analysis

During field work, the slope of the dam abutment was studied using a discontinuity survey and rock sample to determine the slope section that would be unstable during construction as well as after construction and impounded water to the reservoir. As seen in the field, there are two slope sections from the dam's right abutment (RAS1 and RAS2) that may be unstable due to their geometry (Figure 5. 20).The slope section (RAS1) is covered by soil deposit and highly fractured rocks, while the slope section (RAS2) is covered by weathered and severely fractured basaltic rock. Since the slope sections are covered by soil deposit and highly fractured and weathered rock, the expected mode of failure is non-structural controlled circular mode of failure for slope section RAS1 and structural controlled mode of failure for slope section RAS2. As a result, the stability analysis of RAS2 was performed first by kinematic method by using Dip software (Rocscience,2004) and then performed by Deterministic method using Rocplane and Sewedge software (Rocscience, 2004) for planner mode of failure and wedge mode of failure respectively. Whereas, RAS1 was performed utilizing a deterministic approach conducted by the spencer method using slide software, since it is non- structural controlled mode of failure.

Kinematic method employed the dip amount and dip direction to identify the possible mode of failure. The deterministic approach employed the geometry of the slope and shear strength parameters (cohesion, friction angle) and the unit weight of material, to determine slope stability in terms of the safety factor. From fieldwork slope geometry was measured, whereas the shear strength parameters (cohesion and friction angle) of rock used in the analysis were estimated from Hoek-Brown failure criteria using RocData software and the unit weight was determined from lab test. In addition, the slope geometry (height and slope angle) and material parameters during the stability analysis, external loads such as horizontal seismic acceleration and groundwater conditions were also taken into account. The study area is found in high seismic risk zone and horizontal seismic load coefficient with a magnitude (α) = 0.1 was considered for the analysis under dynamic condition (Ayele, 2017).

Figure 5. 20 Slope section from right abutment (A & B) RAS 2 and (C) RAS 1

5.6.1 Stability Analysis for Structurally Controlled Slope Sections

5.6.1.1 Kinematic Analysis

Kinematical analyses was done for the structurally controlled slope failure i.e. RAS2 slope sections found at the right abutment respectively were analyzed using Dips 6 software (Rocscience, 2004) and possible mode of failures was identified. The input parameters for Dip software are given table below (Table 5.20). Accordingly, one planner (JS3) and two wedge failure (JS1 &JS3 and JS2 & JS3) (Figure 5.20).

Table 5. 15 Input parameters used in Dips software for kinematic analysis.

Slope section	Joint orientation (Dip/dip direction				Friction cone	Possible mode of failure
	JS1	JS2	JS3	Slope face		
RAS2	75/345	50/140 DD	25/172 DD	59/88 DD	25	
D= Dip Amount, DD= Dip Direction						

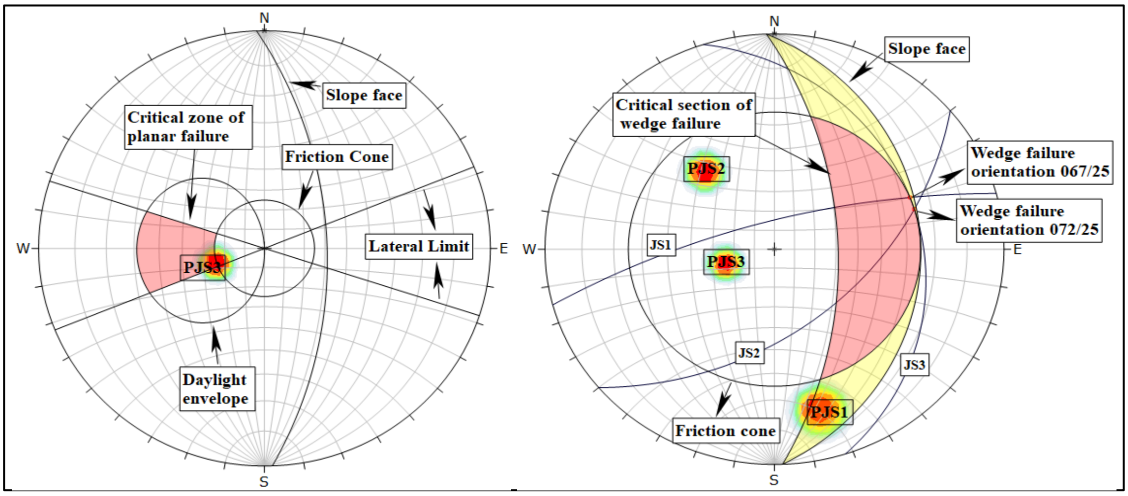

Figure 5. 21 Result from kinematical analysis A) Planner mode of failure, B) Wedge mode of failure

Accordingly, at the right abutment, RAS2 slope section were kinematically analyzed for the planar mode of failure**.** The obtained analysis result indicate that at this slope section planar mode of failure occurred due to joint set 3 (JS3) and wedge failure also obtained due to intersection of joint set 1 and joint set 3 (JS1 & JS3) and joint set 2 and joint set 3 (JS2 & JS3). Furthermore, the stability analysis of the planar mode of failure was done using the deterministic method by using RocPlane software to determine the factor of safety andwedge mode of failure was analyzed by using Swedge software to determine the factor of safety.

5.6.1.2 Stability Analysis of planner mode of failure

Analysis was conducted for JS3 which is planner mode of failure from the result of kinematic analysis. The input parameters were given in Table 5.16.

Table 5. 16 input parameters for Rocplane software

Slope section	Input parameters for RocPlane V. 2.0									
	JS	Slope geometry						Strength		αs
RAS2	JS	Sa (^{0})	Sh (m)	γ_d/ γ_s(t/m^3)	Fpa (^{0})	W (^{0})	Ufa (^{0})	C (t/m^2)	Φ (^{0})	0.1
	JS3	59	60	2.23/2.72	25	2	18	1.835	31.56	

JS= Joint set, Sa= slope angle, Sh= slope height, γ_d= dry unit weight, γ_s = saturated unit weight Fpa= failure plane angle, W= waviness, Ufa=upper face angle, c= cohesion, Φ= friction angle, γw= unit weight of water, αs = seismic coefficient.

FOS was calculated under static condition (dry and saturated) and dynamic condition (dry and saturated) with the help of Rocplane software. And the interpretation of FOS was made according to Norrish & Wyllie (1996). As they stated that FOS > 1 is indicates that the slope is stable, whereas FOS < 1 suggests that the slope is unstable. The result of analysis was given in Figure 5.22 and Table 5.17).

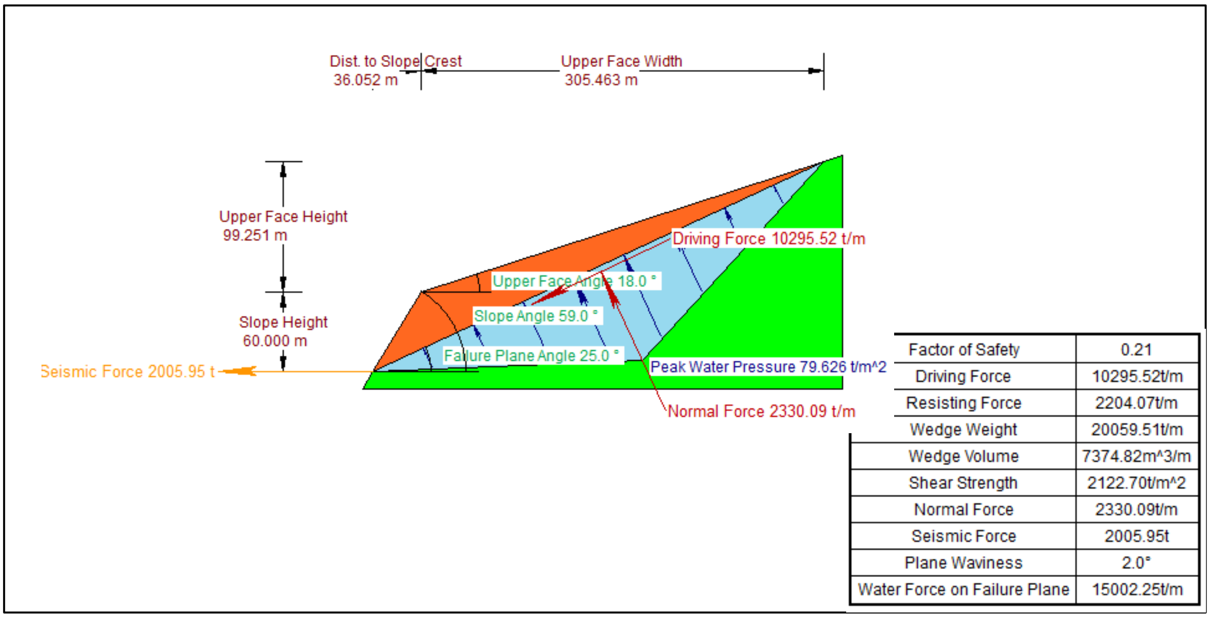

Figure 5. 22 Result of slope stability analysis from Rocplane software under dynamic saturate condition.

Table 5. 17 Summary of FOS for planar mode of failure

Slope section	JS	FOS result under different anticipated conditions			
		Static dry	Dynamic dry	Static saturated	Dynamic saturated
RAS2	JS3	1.49	1.175	0.325	0.21

From the analysis result the slope is unstable under saturated condition with the FOS=0.325 which is less than 1 and as the figure 5.22 shows that under dynamic saturate condition which is the worst condition, Resisting force is 2204.07t/m and driving force is 10295.52t/m. This indicates the resisting force is less than driving force, therefore the slope is unstable in worst condition (dynamic saturate condition). Furthermore, the slope is stable under dry condition (static and dynamic). This indicates the pore water pressure is the main significant to destabilize the slope.

5.6.1.3 Slope stability analysis for Wedge mode of failure

Analysis was conducted for wedge mode of failure (JS1&JS3) and (JS2 & JS3) from the result of kinematic analysis (Figure 5.20). The input parameters were given in Table 5.18. Analysis was conducted with the help of sewedge V. 4.0 software.

Table 5. 18 Input parameters for Swedge

Slope section	Input parameters for Swedge V. 4.0									
	JS	Slope geometry					Strength		Force	
		JS D/DD(^{0})	Sh (m)	γ_d/ γ_s(t/m^3)	SF (D/DD^0)	UF (D/DD^0)	C (t/m^2)	Φ (^{0})	γw (t/m^3)	αs
RAS2	JS1	75/345	60	2.23/2.72	59/88	18/95	2.55	39.97	1	0.1
	JS2	50/140					2.447	39.80		
	JS3	25/72					1.835	31.56		
JS= joint set, Sh=slope height, γ=unit weight, s/d=saturated/dry, SF=slope face, UF=upper face, c=cohesion, Φ=friction angle, γw= unit weight of water, αs= seismic coefficient.										

FOS was calculated under different anticipated condition (static dry, dynamic dry, static saturated and dynamic saturated). Analysis result is shown below Figure 5.23 and Figure 5.24. From the analysis the effect of pore water pressure is the main cause to unstable the slope as the water fill increases the value of FOS is become decrease (Table 5.19). This indicates the slope is unstable under saturated condition and stable under dry condition either under dynamic or static condition.

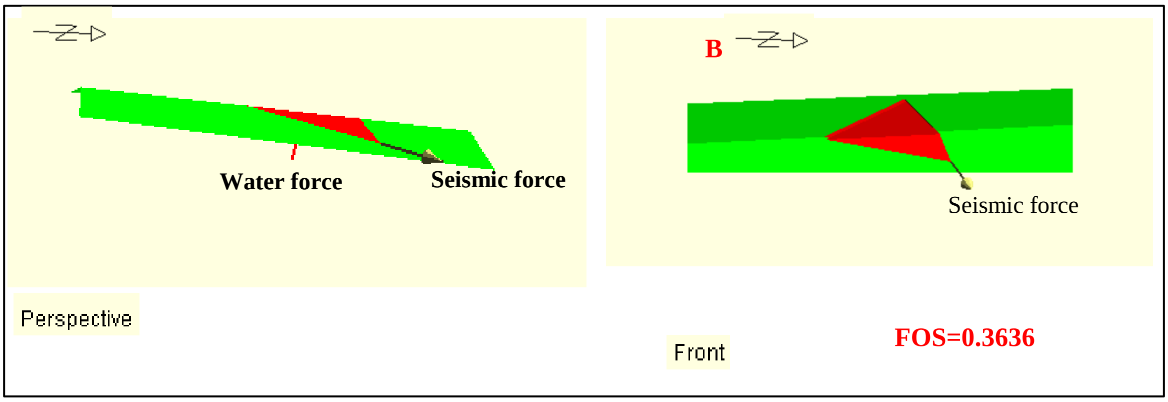

Figure 5. 23 Result of stability analysis of JS1&JS3 from Swedge software under dynamic saturated condition.

Table 5. 19 Summary of FOS for wedge mode of failure

Slope section	JS	FOS result under different anticipated conditions					
		Static dry	Dynamic dry	Static saturated	Dynamic partially saturated		Dynamic saturated
					(50%)	75%	
RAS2	JS1 &JS3	1.447	1.171	0.4424	1.07	0.8283	0.3636
	JS2& JS3	1.473	1.91	0.4625	1.057	0.8226	0.377

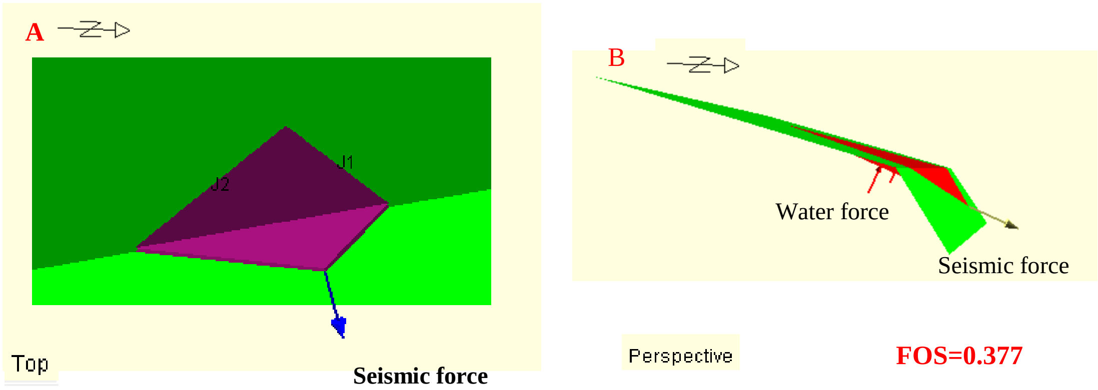

Figure 5. 24 Result of stability analysis of JS1&JS3 from Swedge software under dynamic saturated condition; A) 3D top view of slope section and B) 3D perspective view of slope section.

5.6.2 Stability Analysis for Non-Structurally Controlled Slope Sections

5.6.2.1 Stability analysis by Deterministic Method

The analysis was conducted for slope section RAS1 which is covered by soil deposit and highly weathered basaltic rock with the help of slide software. Input parameters used for analysis were given in Table 5.20.

Table 5. 20 Input parameters for deterministic slope stability analysis

Slope section	Slope geometry		Lithological unit	Parameters (From RocData and lab result)			α (g)
	Angle (^{0})	Height(m)		C (MPa)	ϕ (°)	γ (KN/m3)	
RAS1	47 at upper layer	16	Sandy	0.04345	35.41	13.537	0.1
	31 at base of slope	49	HWD	0.439	45.85	24.03	
			MWB	0.541	48.49	25.80	
Where C is Cohesion, ϕ is Friction angle, γ is unit weight of rock, α is Horizontal seismic acceleration HWB is highly weathered basalt and MWB is moderately weathered basalt.							

The analyses result for slope section 1 (RAS1) during static dry condition revealed a minimum FOS of 2.045 with resisting and driving moments of $1.37*10^6$KN-m and 672754KN-m, respectively and resisting and driving horizontal force of 12122kN and 5928kN, respectively, whereas during dynamic dry condition the minimum factor of safety is 1.711 with resisting and driving moments of $1.33*10^6$KN-m and 779887KN-m, respectively and resisting and driving horizontal force of 11818kN and 6905kN, respectively, (Table 5. 21 and Figure 5. 25 A&B). When the slope is assumed to be saturated and no earthquake occurs (i.e. static saturated condition), the minimum FOS is 0.85, with corresponding resisting and driving moment of 633388KN-m and 745296KN-m, respectively and resisting and driving horizontal force of 5794kN and 6818kN, respectively (Table 5. 21 and Figure 5. 25C). Furthermore, the lowest FOS is 0.707 when the slope is assumed to be saturated and exposed to horizontal seismic acceleration (dynamic saturated condition), and the resistive and driving moment corresponding to this factor of safety are 610514KN-m and 863981KN-m, respectively resisting and driving horizontal force of 5662kN and 8013kN, respectively, (Table 5. 21 and Figure 5. 25D).

Table 5. 21 Factor of safety and other output of the slope under various condition from slide software

Slope section	Description	Analysis condition			
		Static dry	Dynamic dry	Static saturate	Dynamic saturate
RAS1	Factor of safety (FOS)	2.045	1.711	0.85	0.707
	Resisting moment(KN-m)	$1.37*10^6$	$1.33*10^6$	633388	610514
	Driving moment(KN-m)	672754	779887	745296	863981
	Resisting horizontal force(kN)	12122	11818	5794	5662
	Driving horizontal force (kN)	5928	6905	6818	8013

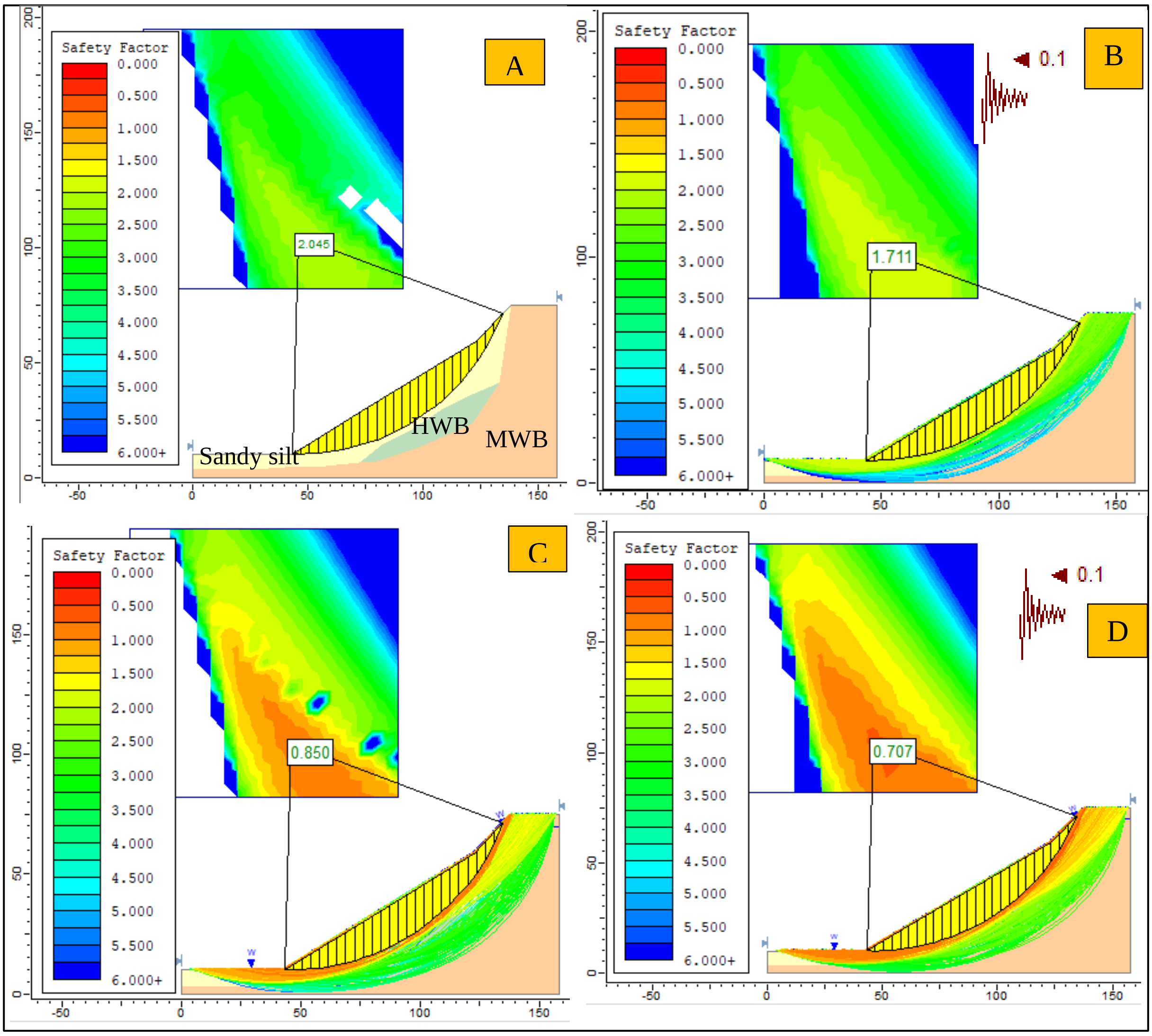

Figure 5. 25 Slope stability analysis for the right abutment slope 1 (RAS 1) utilizing the limit equilibrium method using slide software under A) static dry condition B) dynamic dry condition, C) static saturated condition and D) Dynamic saturated condition.

Generally, at RAS1 slope sections, the analysis result showed that the slope was found to be unstable during saturated conditions and stable under dry conditions. This indicated that the pore water pressure significantly contributed in destabilizing these particular slope sections as compared to horizontal seismic acceleration. Whereas, at RAS 2 slope section the analysis result revealed that the slope was found to be stable under all condition, since the factor of safety is greater than 1.

5.7 Stabilization of unstable slope section

One of remedial measures for unstable slope section is removing weak materials on slope area to reduce its angle which means “flattening slope”. In other hand remedial is modifying the slope geometry is often done by reducing the slope angle, reducing the weight at the head of the slope. The slope section RAS1 was found to be unstable in saturated conditions in this study, hence it was modified and analyzed (Figure 5. 26).

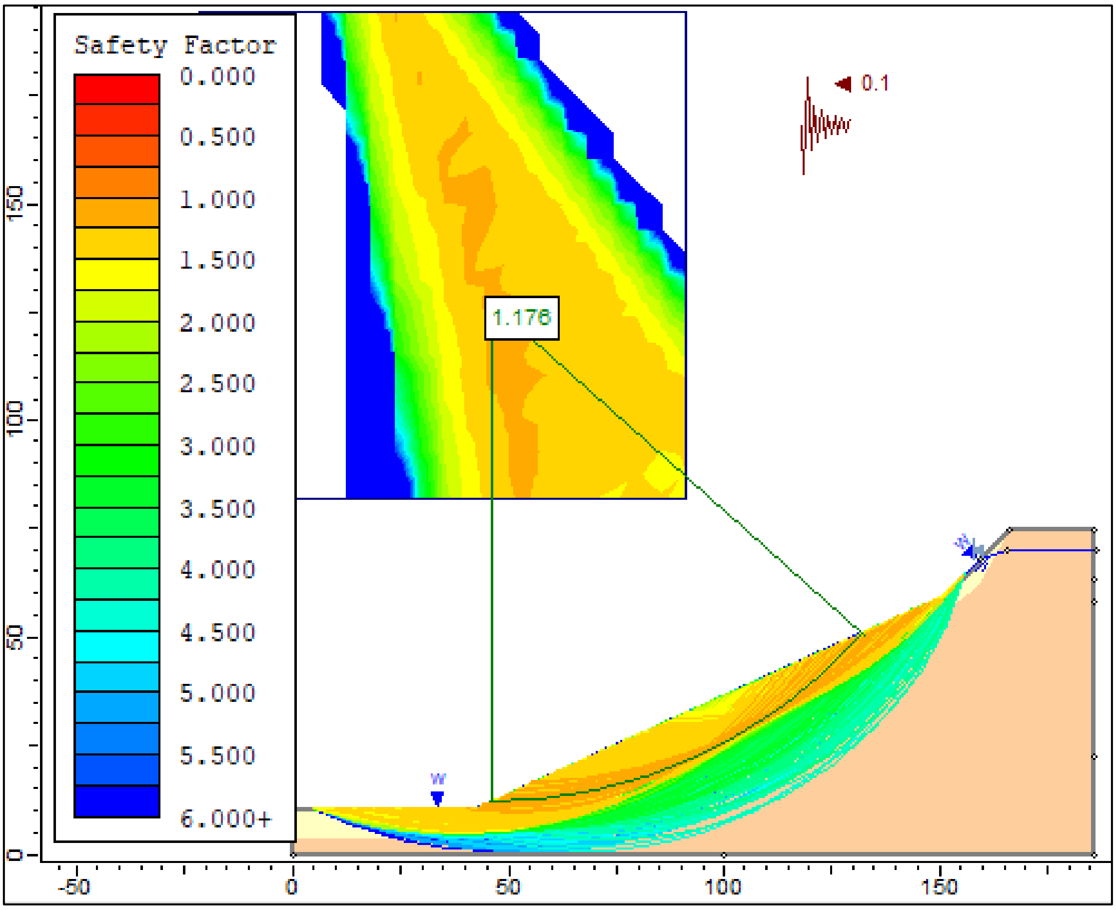

Figure 5. 26 Slope analysis of RAS 1 after reduced its angle.

Before the modification, the slope angle was 31^0 (1.6H: 1V), with FOS < 1.00 in saturated conditions. However, after flattening the geometry, the slope angle was reduced to 24^0 and the slope stability was analyzed under the dynamic saturate condition, which is the worst condition in slope stability analysis. The result of FOS = 1.176. (Figure 5. 26). As a result, reducing the slope angle to 24^0 makes the slope stable under all conditions.

6. CONCLUSIONS AND RECOMMENDATIONS

6.1 Conclusions

This research focuses on engineering geological studies, particularly slope stability and water tightness analyses. Geological and engineering geological mapping, discontinuity surveys, laboratory experiments, and secondary data from OWWDSE were used to attain this goal. The result from field, laboratory and borehole data from OWWDSE was evaluated and discussed in terms of slope stability and water tightness. Based on this finding, the following conclusion are drawn:

- ✓ In the study area, the main lithological units are alluvial and residual soils, which are dominated by silt and sandy soils, and basaltic rocks that form small ridge from left and right side of the river.
- ✓ The rock masses that make up both abutments are weathered to moderately weathered, extensively fractured, and jointed basaltic rocks.
- ✓ From discontinuity survey revealed that the rock of the area is intersected by nearly three to four joint sets. Some of discontinuity orientations are parallel and nearly parallel to the direction of water flow that intersect dam axis which is very favorable to leakage paths. There are also random fractures with low persistence, but interconnected, which can increases hydraulic conductivity.
- ✓ RQD from surface rock exposure (from joint volumetric count) at the study area ranges from 30.5% to 45.22%, which falls into poor qualities of rock classification. Poor quality of rock mass related to high weathering and fracturing. Similarly the RQD value from subsurface data (borehole) revealed that the rock with extensive fracturing extends to the depth of 40m.
- ✓ The intact rock strength from point load test range from 69.46MPa to 146.97MPa. As a result the rock that forms dam abutment and reservoir rim of the study area has medium to high strength.
- ✓ The RMR rock classification from study area falls into fairs and GSI rock classification revealed disintegrated to blocky/disturbed/seamy rock structure.
- ✓ Correlation between subsurface RQD and velocity from seismic refraction revealed that the subsurface unit is highly fractured, jointed and weathered up to 30-35m depth. Furthermore, the thickness of the deposit of soil with gravel, cobble and block near to the center of dam axis extends to 35m depth.

- ✓ Stability analysis was performed using Kinematic method for RAS2 since it is structural controlled and deterministic method (Limit Equilibrium Method) for RAS1 and RAS2 slope section by considering different condition at right abutment. Result of analyses revealed that slope section RAS1 is unstable under saturate condition and stable during dry dynamic condition. Hence, the effect of pore water pressure plays a great role in destabilizing this slope section.
- ✓ Deterministic stability analysis using RocPlane and Swedge software revealed that RAS2 slope sections was found to be unstable during saturated conditions and stable under dry conditions. Thus, pore water pressure significantly contributed in destabilizing these particular slope sections as compared to seismic activity.
- ✓ The hydraulic conductivity analysis of surface discontinuity spacing and aperture data revealed that the rock mass had moderate to high permeability values at both the dam abutments and in the reservoir area. As a result, considerable leakage is expected after the reservoir's impoundment, particularly through both dam abutments.
- ✓ The permeability of the soils from laboratory test is relatively low, indicating that water can be retained in the reservoir area following impoundment. As a result, the reservoir site is nearly watertight, with just minor seepage
- ✓ Water tightness analysis results based on the water tightness model revealed that significant potential leakage from the reservoir is expected through both the left and right abutments.

6.2 Recommendations

The following recommendations can be made based on the findings of geological, geotechnical, and geophysical investigations.

- ✓ Soil deposit (residual and alluvial soil) should be removed from the dam axis before construction of the dam.
- ✓ At RAS 1 slope section is unstable mainly during saturate condition and stable under dry static condition. Therefore, this study recommended that in this slope sections the failed material should first be removed in order to reduce the slope angles and then shotcrete were recommended to increase the stability of the slope. As the effect of pore water pressure is a great role for destabilizing slope, it is essential to provide sufficient drain hole to remove pore water pressure that building up underneath.

- ✓ The slope stability become stable when the angle of slope of is reduced to 24^0. Therefore this study recommended to remove the soil material until the slope angle becomes 24^0.
- ✓ At the slope section RAS2, the planar and wedge mode of failure was identified. Therefore, to prevent the sliding and stabilize those slope sections, rock bolt and anchors are recommended as remedial measures.
- ✓ The results of the water tightness analysis, which included surface discontinuity data, permeability testing, and a water tightness model, revealed a potential leakage in the dam's left and right abutments. As a result, curtain grouting is recommended at the right and left abutments. At the right abutment the grouting is recommended to the depth of 45m.
- ✓ The study also recommended that as reservoir rim which is highly hydraulic conductive area is wider clay blanketing should provide to prevent potential leakage through reservoir rim of the dam area.
- ✓ As the subsurface investigation data is not sufficient to know the exact depth to which the grouting extends. Hence, this study recommends drilling of additional boreholes at left abutment and river center to greater depth and corresponding water pressure tests to decide depth of curtain grouting.

Research Fund Acknowledgment

This research project is funded by Adama Science and Technology University Under the grant number ASTU/SM-R/391/22, Adama, Ethiopia.

REFERENCE

Abdulkadir, M. (2009). Assessment of micro-dam irrigation projects and runoff predictions for ungauged catchments in northern Ethiopia. *Unpublished PhD Dissertation, Universität Münster, Münster*.

Abramson, L. W., Lee, T. S., Sharma, S., & Boyce, G. M. (2002). Slope stability concepts. Slope stabilisation and stabilisation methods. *Published by John Willey &Sons, Inc*, 329–461.

Ajalloeian, R., & Azimian, A. (2013). *Geotechnical Engineering Assessment of the Nargesi*. 1369–1392. https://doi.org/10.1007/s10706-013-9661-3

Aladejare, A. E., Alofe, E. D., Onifade, M., Lawal, A. I., Ozoji, T. M., & Zhang, Z. X. (2021). Empirical Estimation of Uniaxial Compressive Strength of Rock: Database of Simple, Multiple, and Artificial Intelligence-Based Regressions. *Geotechnical and Geological Engineering*, *39*(6), 4427–4455. https://doi.org/10.1007/s10706-021-01772-5

Aladejare, A. E., & Idris, M. A. (2020). Performance analysis of empirical models for predicting rock mass deformation modulus using regression and Bayesian methods. *Journal of Rock Mechanics and Geotechnical Engineering*, *12*(6), 1263–1271.

Arora, K. R. (2003). Soil Mechanics in Foundation Engineering. In *Engineering Geology* (Six Editio, Vol. 7, Issue 2).

ASTM. (1998). Standard test method for laboratory determination of water (moisture) content of soil and rock by mass. *Annual Book of ASTM Standards, Water and Environmental Technology*, 218–222.

ASTM D 2434 (1994). Standard test method for permeability of granular soil. ASTM Stand. Philadelphia, PA; 19103.

ASTM D 3080 (1998). Standard test method for direct shear test of soils under consolidated drained conditions. ASTM Stand. Conshohocken, PA, Vol. 04.08, pp.339-344.

ASTM D 422-63 (1998). Standard test method for particle-size analysis of soils. ASTM Stand. Conshohocken, PA; 19428.

ASTM D 4318 (1998). Standard test method for liquid limit, plastic limit and plasticity index of soils. ASTM Stand. Conshohocken, PA; 19428.

ASTM D 5731 (1995). ASTM standard test method for determination of point load strength index of rocks. ASTM Stand. Conshohocken, Vol.04.08, PA; 142-148

ASTM D 698 (1998). Standard test method for laboratory compaction characteristics of soils. ASTM Stand. Conshohocken, PA 19428.

ASTM, D. (1992). *Standard test method for specific gravity of soils*.

Avella, S. (1993). *An analysis of a worldwide status for monitoring and analysis of dam deformation*.

Aydin, A., & Basu, A. (2005). The Schmidt hammer in rock material characterization. *Engineering Geology, 81*(1), 1–14. https://doi.org/10.1016/j.enggeo.2005.06.006

Aydin, Adnan. (2015). *ISRM Suggested Method for Determination of the Schmidt Hammer Rebound Hardness: Revised Version BT - The ISRM Suggested Methods for Rock Characterization, Testing and Monitoring: 2007-2014* (R. Ulusay (ed.); pp. 25–33). Springer International Publishing. https://doi.org/10.1007/978-3-319-07713-0_2

Ayele, A. (2017). Probabilistic seismic hazard analysis (PSHA) for Ethiopia and the neighboring region. *Journal of African Earth Sciences*, *134*, 257–264. https://doi.org/10.1016/j.jafrearsci.2017.06.016

Barton, N., & Choubey, V. (1977). The shear strength of rock joints in theory and practice. *Rock Mechanics Felsmechanik Mécanique Des Roches*, *10*(1–2), 1–54. https://doi.org/10.1007/BF01261801

Barton, Nicholas, Lien, R., & Lunde, J. (1974). Engineering classification of rock masses for the design of tunnel support. *Rock Mechanics, 6*(4), 189–236.

Basahel, H., & Mitri, H. (2017). Journal of Rock Mechanics and Geotechnical Engineering Application of rock mass classi fi cation systems to rock slope stability assessment : A case study. *Journal of Rock Mechanics and Geotechnical Engineering*. https://doi.org/10.1016/j.jrmge.2017.07.007

Beiranvand, B., & Komasi, M. (2021). An investigation on dam settlement during and end of construction using instrumentation data and numerical analysis. *SN Applied Sciences*, *3*(3), 1–10. https://doi.org/10.1007/s42452-021-04306-z

Bieniawski, Z. (1988). The rock mass rating (RMR) system (geomechanics classification) in engineering practice. In *Rock Classification Systems for Engineering Purposes*. ASTM International.

Bieniawski, Z T. (1968). Note on in situ testing of the strength of coal pillars. *Journal of the Southern African Institute of Mining and Metallurgy*, *68*(10), 455–465.

Bieniawski, Z T. (1973). Engineering classification of jointed rock masses. *Civil Engineering= Siviele Ingenieurswese*, *1973*(12), 335–343.

Bieniawski, Z T. (1993). Classification of rock masses for engineering: the RMR system and future trends. In *Rock Testing and Site Characterization* (pp. 553–573). Elsevier.

Bieniawski, Zdzisław Tadeusz. (1989). *Engineering rock mass classifications: a complete manual for engineers and geologists in mining, civil, and petroleum engineering*. John Wiley & Sons.

Broch, E., & Franklin, J. A. (1972). The point-load strength test. *International Journal of Rock Mechanics and Mining Sciences & Geomechanics Abstracts*, *9*(6), 669–676.

Chala, E. T., & Rao, K. S. (2017). *Influence of Weathering on the Engineering Behaviour of Rocks under Triaxial Confining Conditions*. 570–578. https://doi.org/10.1061/9780784480472.060

Christian, J. T. (2004). Geotechnical engineering reliability: How well do we know what we are doing? *Journal of Geotechnical and Geoenvironmental Engineering*, *130*(10), 985–1003.

Deere, D. U., Hendron, A. J., Patton, F. D., & Cording, E. J. (1966). Design of surface and near-surface construction in rock. *8th U.S. Symposium on Rock Mechanics, USRMS 1966*, 237–302.

Eberhardt, E. (2013). *Rock Slope Stability Analysis-Utilization of Advanced Numerical Techniques*. *December*.

Ehsan, S., Afzal, S., Usman, M., Rasheed, M., & Jamil, W. (2016). *Dam Break Modeling by using HEC-RAS*. *04*, 26–31. https://doi.org/10.24081/nijesr.2016.1.0006

El-Naqa, A. (2001). The hydraulic conductivity of the fractures intersecting Cambrian sandstone rock masses, central Jordan. *Environmental Geology*, *40*(8), 973–982. https://doi.org/10.1007/s002540100266

Fell, R., MacGregor, P., Stapledon, D., & Bell, G. (2005). *Geotechnical engineering of* *dams*. CRC press.

Fookes, P. G. (1966). British practice American practice. *Engineering Geology*, *2*(2), 81–106.

Foyo, A., Sánchez, M. A., & Tomillo, C. (2005). A proposal for a Secondary Permeability Index obtained from water pressure tests in dam foundations. *Engineering Geology*, *77*(1–2), 69–82. https://doi.org/10.1016/j.enggeo.2004.08.007

Ge, W., Wang, X., Li, Z., Zhang, H., Guo, X., Wang, T., Gao, W., Lin, C., & Gelder, P. Van. (2021). *Interval Analysis of the Loss of Life Caused by Dam Failure*. *147*(1), 1–7. https://doi.org/10.1061/(ASCE)WR.1943-5452.0001311

Goodman, R E. (1976). Methods of geological engineering in discontinuities of rocks: west, St. *Paul, Minn*.

Goodman, Richard E. (1989). *Introduction to rock mechanics.pdf*. John Wiley & Sons.

Griffiths, D. V., & Marquez, R. M. (2007). Three-dimensional slope stability analysis by elasto-plastic finite elements. *Geotechnique*, *57*(6), 537–546. https://doi.org/10.1680/geot.2007.57.6.537

Gurocak, Z., & Alemdag, S. (2012). Assessment of permeability and injection depth at the Atasu dam site (Turkey) based on experimental and numerical analyses. *Bulletin of Engineering Geology and the Environment*, *71*(2), 221–229. https://doi.org/10.1007/s10064-011-0400-9

Gurocak, Z., Alemdag, S., & Zaman, M. M. (2008). Rock slope stability and excavatability assessment of rocks at the Kapikaya dam site, Turkey. *Engineering Geology*, *96*(1–2), 17–27. https://doi.org/10.1016/j.enggeo.2007.08.005

Hamm, S. Y., Kim, M. S., Cheong, J. Y., Kim, J. Y., Son, M., & Kim, T. W. (2007). Relationship between hydraulic conductivity and fracture properties estimated from packer tests and borehole data in a fractured granite. *Engineering Geology*, *92*(1–2), 73–87. https://doi.org/10.1016/j.enggeo.2007.03.010

Hammah, R. E., Yacoub, T. E., Corkum, B. C., & Curran, J. H. (2005). The shear strength reduction method for the generalized Hoek-Brown criterion. *Alaska Rocks 2005, The 40th US Symposium on Rock Mechanics (USRMS)*.

Haregeweyn, N., Poesen, J., Nyssen, J., De Wit, J., Haile, M., Govers, G., & Deckers, S.

(2006). Reservoirs in Tigray (Northern Ethiopia): Characteristics and sediment deposition problems. *Land Degradation and Development*, *17*(2), 211–230. https://doi.org/10.1002/ldr.698

Hobst, L., & Zajíc, J. (1983). Stabilization of Rock and Soil Slopes by Anchoring. In L. HOBST & J. B. T.-D. in G. E. ZAJÍC (Eds.), *Anchoring in Rock and Soil* (Vol. 33, pp. 359–406). Elsevier. https://doi.org/https://doi.org/10.1016/B978-0-444-99689-3.50026-1

Hoek, E, & Brown, E. T. (1997). Practical estimates of rock mass strength. International Journal of Rock Mechanics and Mining Sciences. *34 (8): 1 165-1*, 186.

Hoek, E, Carter, T. G., & Diederichs, M. S. (2013). Quantification of the geological strength index chart. *47th US Rock Mechanics/Geomechanics Symposium*.

Hoek, Evert. (2007). Practical Rock Engineering: RocScience. *Available from the Publisher at Http://Www. Rocscience. Com/Hoek/PracticalRockEngineering. Asp*.

Hoek, Evert, & Bray, J. D. (1981). *Rock slope engineering*. CRC Press.

Houlsby, A. C. (1991). *Construction and design of cement grouting: a guide to grouting in rock foundations* (Vol. 67). John Wiley & Sons.

Hudson, J. A., & Harrison, J. P. (1997). *Engineering rock mechanics; An Introduction to the principles*.

Hussian, S., Mohammad, N., Ur Rehman, Z., Khan, N. M., Shahzada, K., Ali, S., Tahir, M., Raza, S., & Sherin, S. (2020). Review of the geological strength index (GSI) as an empirical classification and rock mass property estimation tool: Origination, modifications, applications, and limitations. *Advances in Civil Engineering*, *2020*. https://doi.org/10.1155/2020/6471837

ICOLD, Ic. (1974). *Lessons from dam incidents*. Complete ed ed.

ISRM. (1978). Suggested Methods for Determining Tensile Strength of Rock Materials - 1. Suggested Method for Determining Direct Tensile Strength. *International Journal of Rock Mechanics and Mining Sciences*, *15*(3), 99–103.

Jaeger, J. C. (1971). Friction of Rocks and Stability of Rock Slopes. *Geotechnique*, *21*(2), 97–134. https://doi.org/10.1680/geot.1971.21.2.97

Karagüzel, R., & Kilic, R. (2000). The effect of the alteration degree of ophiolitic melange on permeability and grouting. *Engineering Geology*, *57*(1–2), 1–12.

Karaman, K., & Kesimal, A. (2015). A comparative study of Schmidt hammer test methods for estimating the uniaxial compressive strength of rocks. *Bulletin of Engineering Geology and the Environment*, *74*(2), 507–520. https://doi.org/10.1007/s10064-014-0617-5

Kazmin, V. (1975). The Precambrian of Ethiopia and some aspects of the geology of the Mozambique Belt. *Geophysical Observatory Bulletin*, *1*.

Kazmin, V., & Seifemichael, B. (1978). Geology and development of the Nazareth area, Northern Ethiopia Rift. *Geol. Surv. of Ethiopia*.

Kliche, C. A. (1999). Rock slope stability SME. *Littleton, Co*.

Kutter, H. K. (1972). Analytical methods for rock slope analysis. In *Rock Mechanics* (pp. 197–211). Springer.

Lin, H., Zhong, W., Xiong, W., & Tang, W. (2014). Slope Stability Analysis Using Limit Equilibrium Method in Nonlinear Criterion. *The Scientific World Journal*, *2014*, 206062. https://doi.org/10.1155/2014/206062

Louis, C. (1967). *Strömungsvorgänge in klüftigen Medien und ihre Wirkung auf die Standsicherheit von Bauwerken und Böschungen im Fels* (Vol. 30). Universität Fridericiana, Inst. f. Bodenmechanik u. Felsmechanik.

Marinos, V., Marinos, P., & Hoek, E. (2005). The geological strength index: Applications and limitations. *Bulletin of Engineering Geology and the Environment*, *64*(1), 55–65. https://doi.org/10.1007/s10064-004-0270-5

Markland, J. T. (1972). *A useful technique for estimating the stability of rock slopes when the rigid wedge slide type of failure is expected*. Interdepartmental Rock Mechanics Project, Imperial College of Science and ….

Memon, Y. (2018). A comparison between limit equilibrium and finite element methods for slope stability analysis. *Missouri University of Science & Technology, Rolla, Missouri*, *December*, 1–18. https://doi.org/10.13140/RG.2.2.16932.53124

MOA. (2011). *Ministry of Agriculture Natural Resources Small-Scale Irrigation Situation Analysis and*. *October*.

Moges, B., & Meten, M. (2019). Engineering geological characterization of rocks in gullele botanic garden dam site, addis ababa, central ethiopia. *International Journal of Scientific and Technology Research*, *8*(10), 3504–3522.

Mozafari, M., Raeisi, E., & Zare, M. (2012). Water leakage paths in the Doosti Dam, Turkmenistan and Iran. *Environmental Earth Sciences*, *65*(1), 103–117. https://doi.org/10.1007/s12665-011-1069-x

National Research Council. (1983). *Safety of existing dams: Evaluation and improvement*. National Academies Press. https://doi.org/10.17226/289

Norrish, N. I., & Wyllie, D. C. (1996). Landslides: Investigation and Mitigation. Chapter 15-Rock slope stability analysis. *Transportation Research Board Special Report*, *247*.

Nusier, O. K., Alawneh, A. S., & Malkawi, A. I. H. (2002). Remedial measures to control seepage problems in the Kafrein dam, Jordan. *Bulletin of Engineering Geology and the Environment*, *61*(2), 145–152. https://doi.org/10.1007/s100640100131

Öge, I. F. (2017). Assessing Rock Mass Permeability Using Discontinuity Properties. In *ISRM European Rock Mechanics Symposium - EUROCK 2017*.

OWWDSE. (2021). *GEOTECHNICAL INVESTIGATION OF GOLOLCHA DAM PROJECT MAIN DAM SITE*.

Özsan, A., Öcal, A., Akin, M., & Başarir, H. (2007). Engineering geological appraisal of the Sulakyurt dam site, Turkey. *Bulletin of Engineering Geology and the Environment*, *66*(4), 483–492. https://doi.org/10.1007/s10064-007-0092-3

Palmstrom, A. (1982). The volumetric joint count—a useful and simple measure of the degree of rock mass jointing. *International Association of Engineering Geology. International Congress. 4*, 221–228.

Palmstrom, Arild. (2005). Measurements of and correlations between block size and rock quality designation (RQD). *Tunnelling and Underground Space Technology*, *20*(4), 362–377. https://doi.org/10.1016/j.tust.2005.01.005

Panet, M., Vormeringer, R., Vigier, G., & Goodman, R. E. (1969). Discussion of "Graphical Stability Analysis of Slopes in Jointed Rock." *Journal of the Soil Mechanics and Foundations Division*, *95*(2), 685–702.

Pantelidis, L. (2009). Rock slope stability assessment through rock mass classification systems. *International Journal of Rock Mechanics and Mining Sciences*, *46*(2), 315–

325. https://doi.org/10.1016/j.ijrmms.2008.06.003

Park, H., & West, T. R. (2001). Development of a probabilistic approach for rock wedge failure. *Engineering Geology*, *59*(3–4), 233–251. https://doi.org/10.1016/S0013-7952(00)00076-4

Quiñones-Rozo, C. (2010). Lugeon test interpretation, revisited. *Collaborative Management of Integrated Watersheds, US Society of Dams, 30th Annual Conference*, 405–414.

Ramana, K. V. (1993). Humid tropical expansive soils of Trinidad: Their geotechnical properties and areal distribution. *Engineering Geology*, *34*(1–2), 27–44. https://doi.org/10.1016/0013-7952(93)90041-A

Rocscience. (2004). *Rocscience software products: Dips, Slide, Phase2*. Rocscience Toronto.

Şen, Z., & Eissa, E. A. (1991). Volumetric rock quality designation. *Journal of Geotechnical Engineering*, *117*(9), 1331–1346. https://doi.org/10.1061/(ASCE)0733-9410(1991)117:9(1331)

Shehata, A. K. (2006). Design of downstream blanket for overflow spillway founded on complex formation. *J. Appl. Sci. Res*, *2*(12), 1217–1227.

Sherard, J. L. (1968). Some considerations concerning underseepage control for earth dams. *Proceedings of the Symposium on Earth and Rockfill Dams, India*, *1*, 204–214.

Snow, D. T. (1965). *A parallel plate model of fractured permeable media*. University of California, Berkeley.

Steffen, O. K. H., Contreras, L. F., Terbrugge, P. J., & Venter, J. (2008). A risk evaluation approach for pit slope design. *The 42nd US Rock Mechanics Symposium (USRMS)*.

Terzaghi, K., Peck, R. B., & Mesri, G. (1996). *Soil mechanics in engineering practice*. John Wiley & Sons.

Tesema, F. W., & Ekmekci, M. (2019). Use of Packer Test Results in Hydrogeological Characterization : A Comparison of Calculation Methods for a Representative Value. *Momona Ethiopian Journal of Science*, *11*(1), 52–69. https://doi.org/http://dx.doi.org/10.4314/mejs.v11i1.4

Turkmen, S. (2003). Treatment of the seepage problems at the Kalecik Dam (Turkey).

Engineering Geology, *68*(3–4), 159–169. https://doi.org/10.1016/S0013-7952(02)00225-9

U.S. Department of the Interior, B. of R. (1987). Design of small dams. *A Water Resources Technical Publication*, 904.

Ulusay, R., Türeli, K., & Ider, M. H. (1994). Prediction of engineering properties of a selected litharenite sandstone from its petrographic characteristics using correlation and multivariate statistical techniques. *Engineering Geology*, *38*(1–2), 135–157.

Ureel, S., & Momayez, M. (2014). An Investigation of the Limit Equilibrium Method and Numerical Modeling for Rock Slope Stability Analysis. *Geotechnical Special Publication*, *237*(GSP), 126–135. https://doi.org/https://doi.org/10.1061/9780784413395.025

Uromeihy, A., & Barzegari, G. (2007). *Evaluation and treatment of seepage problems at Chapar-Abad Dam , Iran*. *91*, 219–228. https://doi.org/10.1016/j.enggeo.2007.01.012

Warner, J. (2004). *Practical handbook of grouting: soil, rock, and structures*. John Wiley & Sons.

Wickham, G. E., Tiedemann, Hr., & Skinner, E. H. (1972). Support determinations based on geologic predictions. *N Am Rapid Excav & Tunnelling Conf Proc*, *1*.

Wyllie, D. C., & Mah, C. (2004). *Rock slope engineering*. CRC Press.

Yoon, W. S., Jeong, U. J., & Kim, J. H. (2002). Kinematic analysis for sliding failure of multi-faced rock slopes. *Engineering Geology*, *67*(1–2), 51–61. https://doi.org/10.1016/S0013-7952(02)00144-8

Zewdu, A. (2020). Modeling the slope of embankment dam during static and dynamic stability analysis: a case study of Koga dam, Ethiopia. *Modeling Earth Systems and Environment*, *6*(4), 1963–1979. https://doi.org/10.1007/s40808-020-00832-8

Zumrawi, M. M. E. (2015). *Failure Investigation of Tawila Dam in North*. *May*.

APPENDICES

Appendix 1: Samples of soil and rock with respect to location

No	Rock sample				Soil sample		
	Sample ID	Easting	Northing	Location	Sample Id	Easting	Northing
1	RDA1	645777	981788	Right abutment	TP-1	645325	981610
2	RDA2	64568	981713	Right abutment	TP-2	645435	981661
3	LDA1	645110	981645	Left abutment	TP-3	645705	981627
4	RRA1	645768	981061	Right reservoir rim	TP-4	645705	981627
5	RRA2	645800	981407	Right reservoir rim			
6	RRA3	645277	981190	Right reservoir rim			

Appendix 2: Coefficient of Permeability of soils according to (USBR, 1987)

Coefficient of permeability(mm/sec)	Classification
Greater than 10^{-3}	Permeable
10^{-5} to 10^{-3}	Semi-permeable
Less than 10^{-5}	Impermeable

Appendix 3: Hydraulic conductivity of rock mass descriptions according to (Bell,

Spacing Interval(m)	Description	Coefficient of permeability K (m/sec)	Permeability description
<0.2	Very close to extremely close spacing discontinuity.	$10^{-2} – 1$	Highly permeable
0.2 – 0.6	Closely to moderately spaced discontinuity	$10^{-5} – 10^{-2}$	Moderately permeable
0.6 -2.0	Widely to extremely wide spaced discontinuity	$10^{-9} – 10^{-5}$	Slightly permeable
>2.0	No discontinuity	$<10^{-9}$	Effectively impermeable

Appendix 4: Discontinuity survey and hydraulic conductivity

	No	Average aperture, e,(m)	Spacing, S,(m)	K(m/s) K = $\frac{ge^3}{12\mu S}$
Right abutment	1	0.001	0.5	0.001635
	2	0.001	0.74	0.00110
	3	0.0075	0.33	1.05
	4	0.008	0.5	$8.3*10^{-1}$
	5	0.005	0.19	$5.3*10^{-1}$
	6	0.002	0.2	0.0327
	7	0.002	0.5	0.01308
	8	0.008	0.55	0.7610
Left abutment	9	0.0025	0.6	0.02128
	10	0.0015	0.15	0.01839
	11	0.0075	0.42	0.8211
	12	0.0038	0.41	0.1094
Right reservoir rim	13	0.002	0.5	0.01308
	14	0.003	0.6	0.0367
	15	0.0015	0.7	0.003941
	16	0.001	0.2	0.0040875
	17	0.001	0.3	0.002725
	18	0.001	0.35	0.002335
	19	0.008	0.4	1.0464
	20	0.001	0.25	0.00327
Left reservoir rim	21	0.007	0.2	0.1769
	22	0.003	0.4	0.05518
	23	0.005	0.6	0.1703
	24	0.003	0.3	0.073575
	25	0.002	0.4	0.01635

Appendix 5: Classification of UCS of rock according to Deere and Miller (1966)

Unconfined Compressive Strength (UCS) (MPa)	Description of Strength
Over 224	Very high strength
112- 224	High strength
56 - 112	Medium strength
28 - 56	Low strength

<28	Very low strength

Appendix 6: Output of shear parameters from RocData software

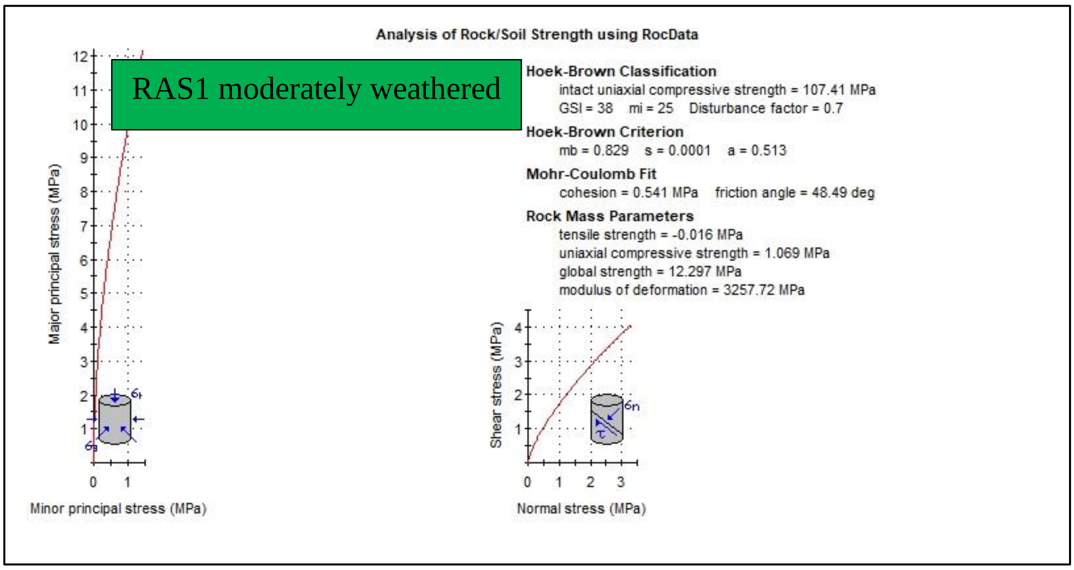

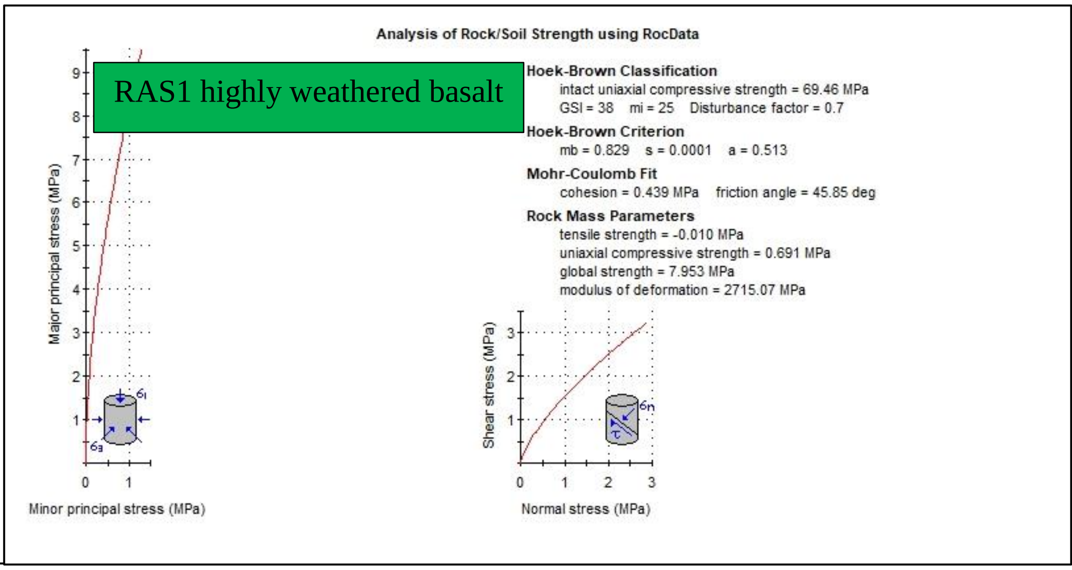

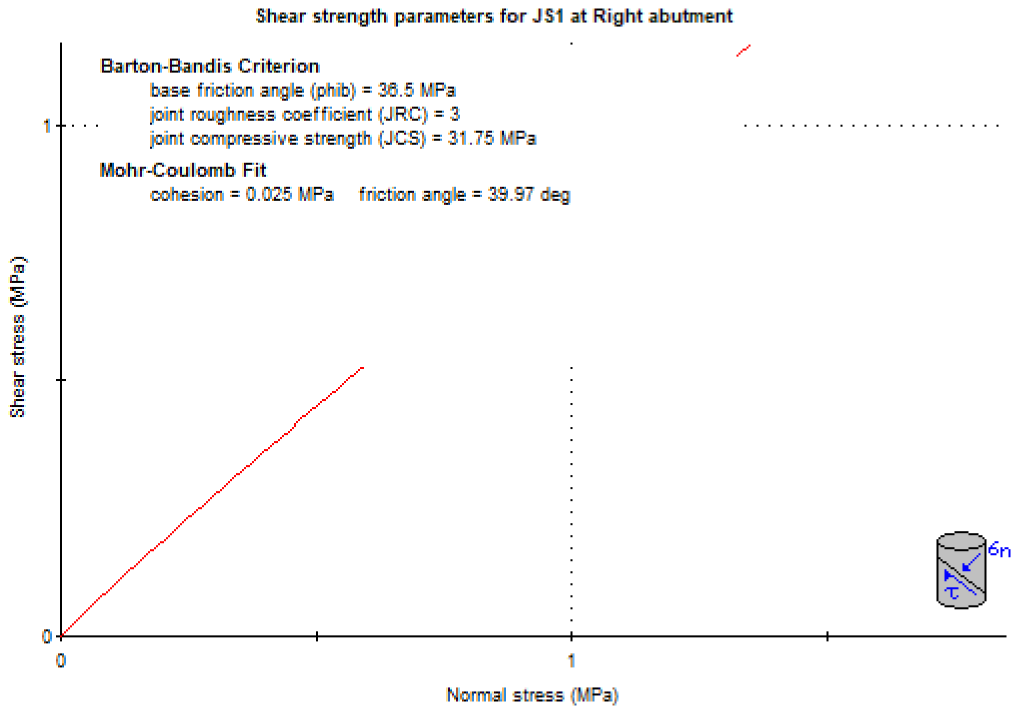
Shear strength parameters for JS1 at Right abutment
Barton-Bandis Criterion
base friction angle (phib) = 36.5 MPa
joint roughness coefficient (JRC) = 3
joint compressive strength (JCS) = 31.75 MPa
Mohr-Coulomb Fit
cohesion = 0.025 MPa friction angle = 39.97 deg
Shear stress (MPa)
Normal stress (MPa)
0
1
0
1

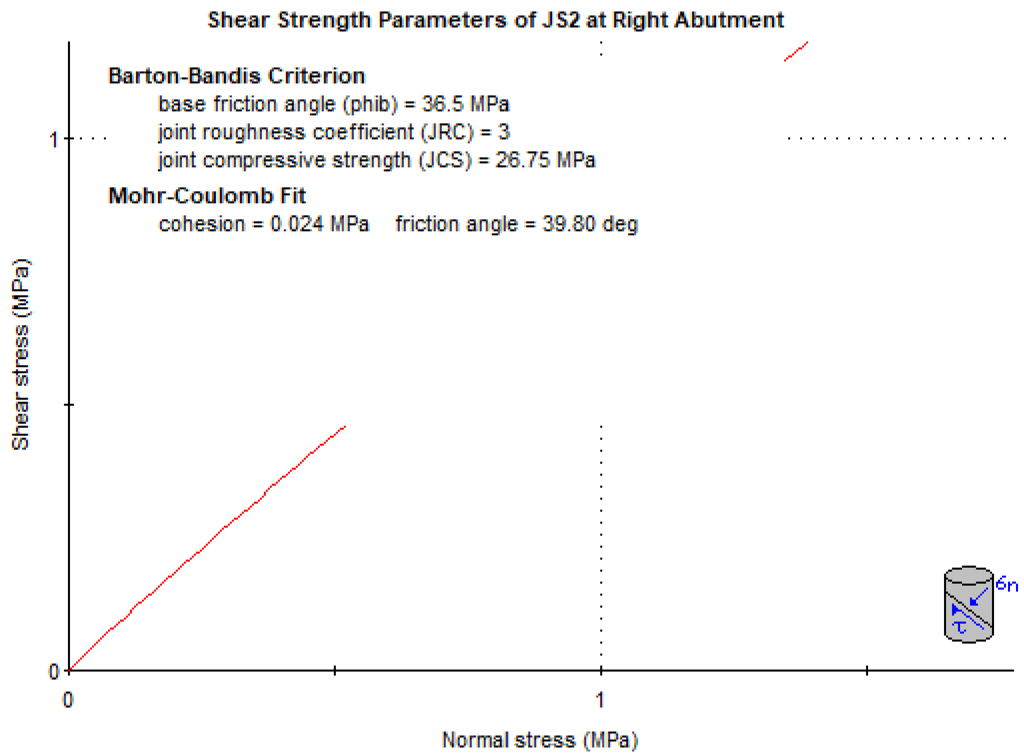
Shear Strength Parameters of JS2 at Right Abutment
Barton-Bandis Criterion
base friction angle (phib) = 36.5 MPa
joint roughness coefficient (JRC) = 3
joint compressive strength (JCS) = 26.75 MPa
Mohr-Coulomb Fit
cohesion = 0.024 MPa friction angle = 39.80 deg
Shear stress (MPa)
Normal stress (MPa)
0
1
0
1

Appendix 7: Result from sieve analysis and hydrometer

Test type	Sieve size	Opening diameter (mm)	Percentage pass (%)			
			TP-1	**TP- 2**	**TP-3**	**TP-4**
Sieve analysis	3″	**75**	100	100	100	100
	21/2″	**63**	100	100	100	100
	2″	**50**	100	100	100	100
	11/2″	**37.5**	100	100	100	100
	1″	**25**	100	100	100	100
	3/4″	**19**	100	100	100	100
	1/2″	**12.5**	99.38	100	100	100
	3/8″	**9.5**	98.38	98.57	100	100
	N^0 4	**4.75**	63.5	92.76	100	99.24
	N^0 10	**2**	30.18	82.67	99.87	96.85
	N^0 16	**1.18**	17.07	75.62	99.41	91.49
	N^0 30	**0.6**	11.3	71.62	99.01	82.8
	N^0 50	**0.3**	9.26	67.52	98.22	70.61
	N^0 100	**0.15**	8.45	63.81	96.31	57.14
	N^0 200	**0.075**	7.77	60.67	94.06	47.87
Hydrometer		**0.035**	1.37	25.32	28.41	29.99
		0.0223	1.22	21.69	26.51	26.12
		0.0129	1.07	16.86	20.81	19.34
		0.0091	1.07	14.45	18.91	15.46
		0.0065	0.91	12.03	17.01	12.55
		0.0032	0.67	6.47	13.97	6.16
		0.0013	0.61	4.78	9.42	3.84

Appendix 8: Result of liquid limit from Atterberg limit chart

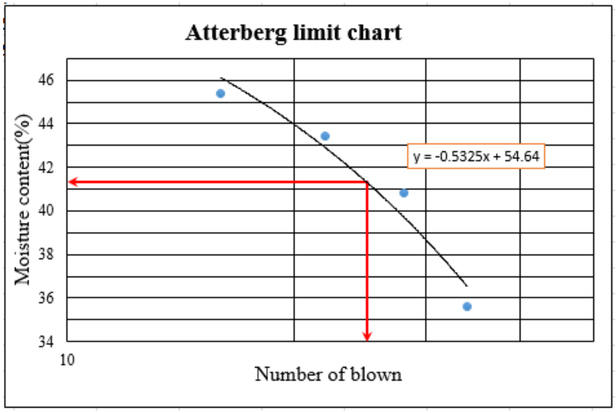

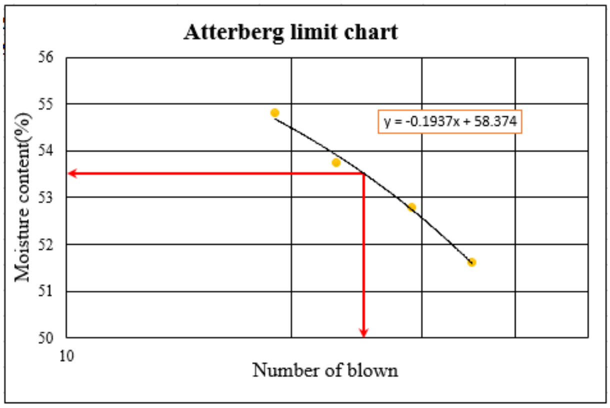

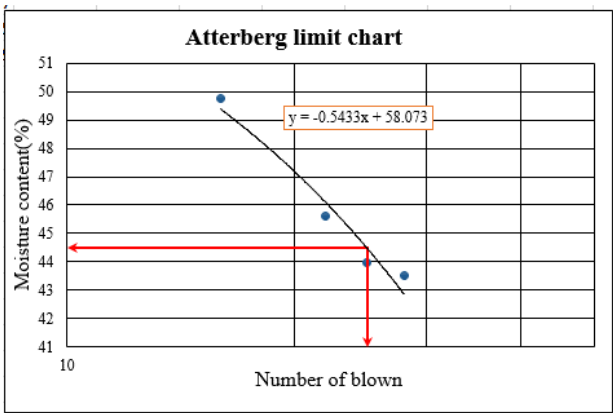

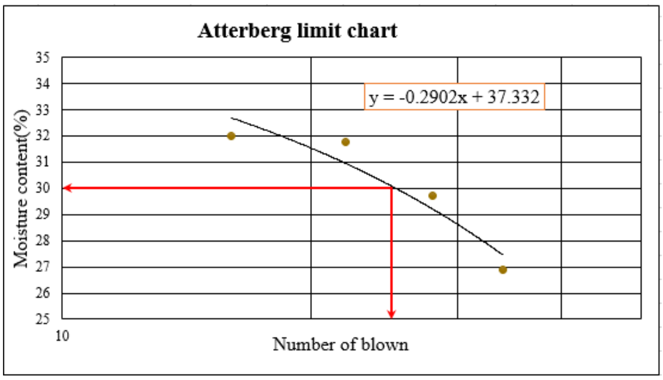

Appendix 9: plastic limit result

Test type	Plastic limit test							
Sample ID	TP-1		TP-2		TP-3		TP-4	
No. Trial	1	2	1	2	1	2	1	2
Mass of moist sample + Can (M_1)	30.63	30.2	24.73	24.93	26.44	26.49	26.46	26.46
Mass of dried sample + Can (M_2)	27.23	26.86	22.20	22.52	23.79	23.75	24.65	24.56
Mass of Can (M_c)	14.73	14.79	14.43	15.06	14.89	14.55	15.67	15.18
Mass of moist $M_m = M_1 - M_2$	3.40	3.34	2.53	2.41	2.65	2.74	1.81	1.90
Mass of dried soil $M_d = M_2 - M_c$	12.5	12.07	7.77	7.46	8.90	9.20	8.98	9.38
Moisture content $W = M_m/M_d x100\%$	27.20	27.67	32.56	32.31	29.78	29.78	20.16	20.26
PL	27.44		32.43		29.78		20.21	

Appendix 10: direct shear test result

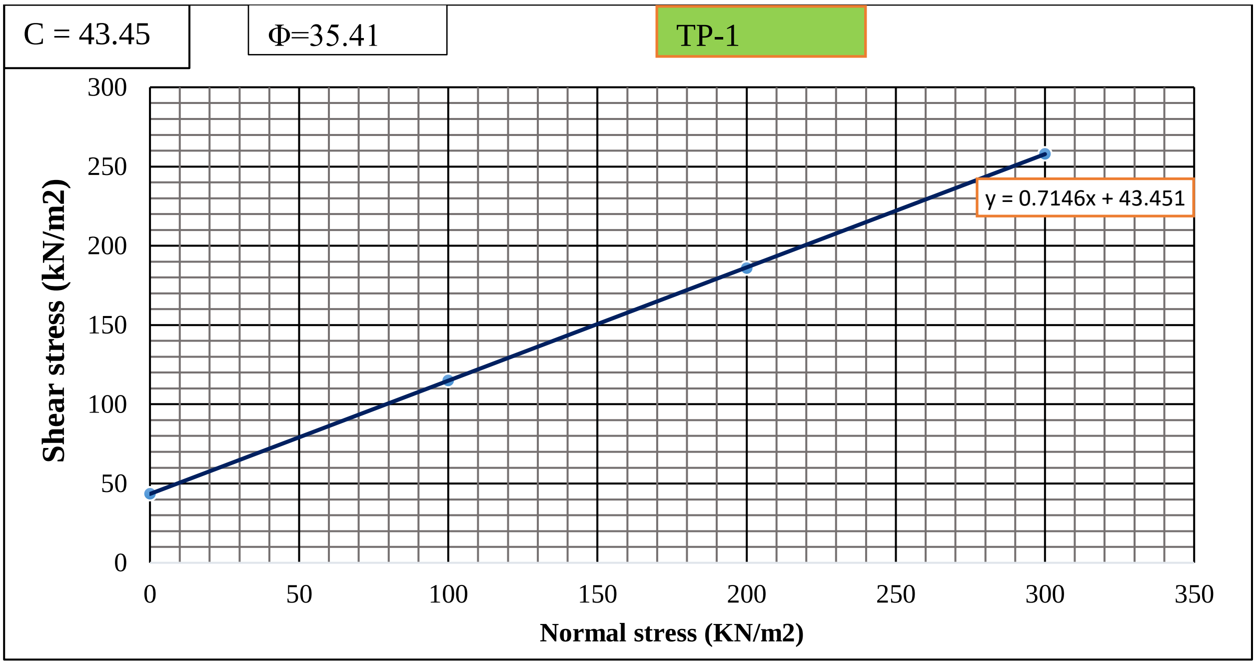

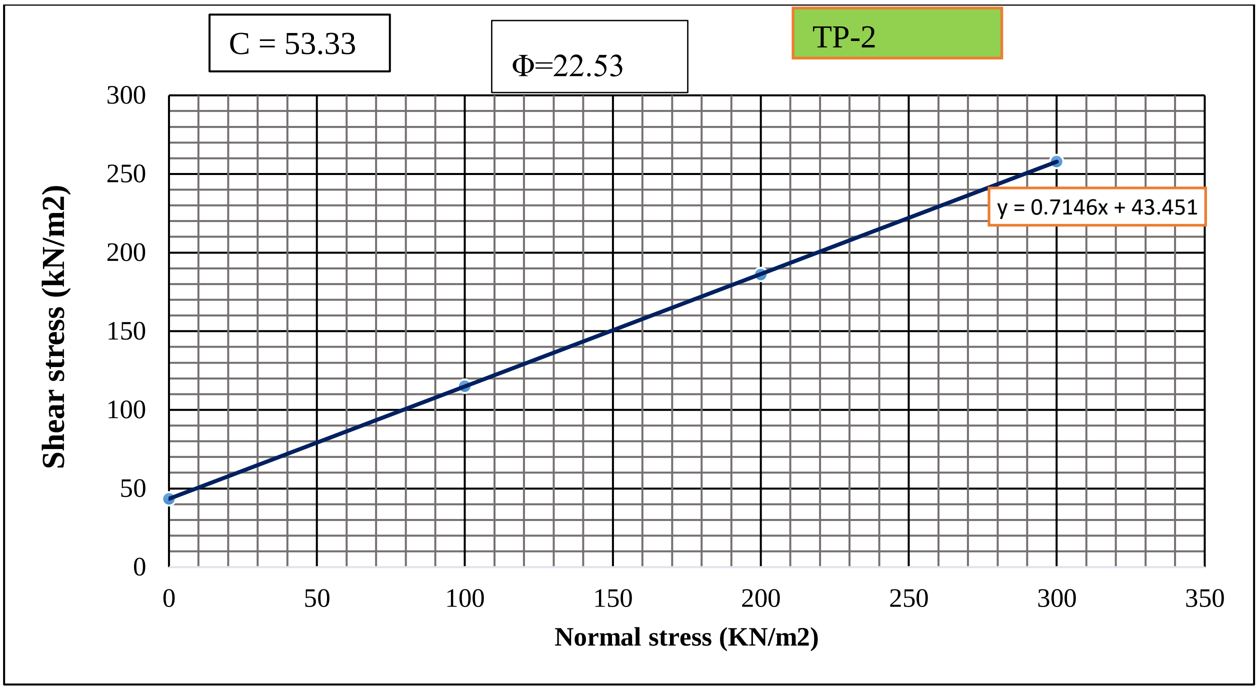
C = 53.33
Φ=22.53
TP-2
y = 0.7146x + 43.451
Shear stress (kN/m2)
Normal stress (KN/m2)
0
50
100
150
200
250
300
350